Journal of

ELECTROANALYTICAL CHEMISTRY

International Journal Dealing with all Aspects of Electroanalytical Chemistry, Including Fundamental Electrochemistry

E L S E V I E R

GENERAL INFORMATION

Types of contributions

(a) Original research work not previously published in other periodicals.
(b) Reviews on recent developments in various fields.
(c) Short communications.
(d) Bibliographical notes and book reviews.

Languages

Papers will be published in English, French or German.

Submission of papers

Papers should be sent to one of the following Editors:

Professor J. O'M. Bockris, John Harrison Laboratory of Chemistry, University of Pennsylvania, Philadelphia 4, Pa., U.S.A.
Dr. R. Parsons, Department of Chemistry, The University, Bristol 8, England.
Professor C. N. Reilley, Department of Chemistry, University of North Carolina, Chapel Hill, N.C., U.S.A.

Authors should preferably submit two copies in double-spaced typing on pages of uniform size. Legends for figures should be typed on a separate page. The figures should be in a form suitable for reproduction, drawn in Indian ink on drawing paper or tracing paper, with lettering etc. in thin pencil. The sheets of drawing or tracing paper should preferably be of the same dimensions as those on which the article is typed. Photographs should be submitted as clear black and white prints on glossy paper.
All references should be given at the end of the paper. They should be numbered and the numbers should appear in the text at the appropriate places.
A summary of 50 to 200 words should be included.

Reprints

Twenty-five reprints will be supplied free of charge. Additional reprints can be ordered at quoted prices. They must be ordered on order forms which are sent together with the proofs.

Publication

The *Journal of Electroanalytical Chemistry* appears monthly and has six issues per volume. and two volumes per year, each of approx. 500 pages.

Subscription price (post free): £ 10.15.0 or $ 30.00 or Dfl. 108.00 per year; £ 5.7.6 or $ 15.00 or Dfl. 54.00 per volume.

Additional cost for copies by air mail available on request.
For advertising rates apply to the publishers.

Subscriptions

Subscriptions should be sent to:

ELSEVIER PUBLISHING COMPANY, P.O. Box 211, Spuistraat 110-112, Amsterdam-C., The Netherlands.

JOURNAL OF ELECTROANALYTICAL CHEMISTRY

VOL. 5 (1963)

JOURNAL
of
ELECTROANALYTICAL CHEMISTRY

INTERNATIONAL JOURNAL DEALING WITH ALL ASPECTS OF ELECTROANALYTICAL CHEMISTRY, INCLUDING FUNDAMENTAL ELECTROCHEMISTRY

Vol. 5 1963

ELSEVIER PUBLISHING COMPANY

AMSTERDAM

ELSEVIER PUBLISHING COMPANY, AMSTERDAM

Printed in The Netherlands by

NEDERLANDSE BOEKDRUK INRICHTING N.V., 'S-HERTOGENBOSCH

PUBLISHERS NOTE

We regret to announce that, taking effect from January 1963, Professor MILAZZO has given up his position as editor of the *Journal of Electroanalytical Chemistry*. We wish to use this opportunity to express our appreciation and our particular thanks to him for everything he did to benefit the Journal, which developed during the period of his editorship in a most gratifying way.

His place on the Editorial Board is to be taken by Dr. R. PARSONS of the University of Bristol, whom we are delighted to welcome.

After careful consideration it has been decided to discontinue publication of the Abstracts Section of the Journal. An important factor contributing to this decision was that readers can now find the information published in this section from other sources, for instance the "Electrochemistry" section of *Chemical Abstracts*. We prefer to use the space formerly occupied by the Abstracts Section to publish original papers.

We would also like to record our particular thanks to all the abstractors, whose valuable co-operation was always much appreciated.

ELSEVIER PUBLISHING COMPANY

POLAROGRAPHIC STUDY OF THE MOLYBDENUM CATALYZED REDUCTION OF CHLORATE, PERCHLORATE AND NITRATE

I. M. KOLTHOFF AND I. HODARA*

School of Chemistry, University of Minnesota, Minneapolis, Minn. (U.S.A.)

(Received January 19th, 1962)

INTRODUCTION

OSTWALD[1] mentioned more than seventy years ago that molybdenum(VI) catalyzes the reduction of bromate by iodide. KOLTHOFF[2] used molybdate as a catalyst in the reaction between chlorate and iodide. More recently, HAIGHT[3] described a method for the chemical reduction of chlorate and perchlorate with tin(II) salts or zinc amalgam, with molybdate as catalyst. The effect of molybdenum(VI) on the polarographic reduction of perchlorate was first observed by HÖLTJE AND GEYER[4], who reported that the molybdenum wave is much greater in perchloric acid than in sulfuric or hydrochloric acid media. HAIGHT published a systematic study of the polarographic reduction of perchlorate in the presence of molybdenum and made use of the catalytic waves in the estimation of molybdenum in steel[5]. Other workers have also applied the same technique to the determination of molybdenum in various substances[6,7,8]. HAIGHT did not report the value of $m^{1/2}t^{1/2}$ of his capillary, but states that $m^{2/3}t^{1/6}$ was 1.38, as compared to a value 1.79 of our capillary. An exact comparison of HAIGHT's data with ours is not possible since this should be done at the same $m^{1/2}t^{1/2}$ value. Under identical experimental conditions, we observed limiting values of the catalytic currents which were of the order of 7% smaller than those reported by HAIGHT. We studied the effect of sulfuric acid and molybdenum(VI) concentrations on the limiting currents and found results in general agreement with those reported by HAIGHT[5]. Since it is of interest to have a record of the catalytic currents at a given $m^{1/2}t^{1/2}$ value of the capillary, some of our data are tabulated in the experimental part.

JOHNSON AND ROBINSON[9] reported that molybdenum in acid medium catalyzes the reduction of nitrate, and made use of this effect in the determination of traces of molybdenum and of concentrations of nitrate between 0.001 and 0.075 M. They used a solution which was 0.1 M in sulfuric acid and 0.2 M in sodium sulfate as supporting electrolyte. They report a value of 1.30 for $m^{2/3}t^{1/6}$, but do not give the values of m and t separately. Therefore, a strict comparison of their and our results is not possible; under identical experimental conditions our values of the catalytic currents are about 30% smaller than those reported by JOHNSON AND ROBINSON. In the experimental part, the effects on catalytic nitrate and perchlorate waves of variation of sulfuric

* On leave from the Israel Atomic Energy Commission Laboratories.

acid concentration at different molybdenum concentrations are tabulated. The effects of mercury height in the reservoir and of phosphoric acid on various catalytic waves are also reported.

The main purpose of this paper is to describe the characteristics of reduction waves of chlorate catalyzed by molybdenum. These catalytic waves are not mentioned in the literature and differ in many respects from those of perchlorate and nitrate.

EXPERIMENTAL

Chemicals

Ammonium molybdate, $(NH_4)_6Mo_7O_{24}.4H_2O$, was a reagent grade product from Baker. A stock solution was prepared and its molybdenum content was determined as reported previously[10].

All other chemicals were reagent quality. Using recrystallized sodium chlorate, perchlorate and nitrate, respectively, yielded the same results as were obtained with original products.

Unless otherwise stated, the characteristics of the capillary were, at a given mercury column height (86.8 cm), $m = 1.610$ mg sec^{-1}, and $t = 4.96$ sec in 0.1 M sulfuric acid at an applied potential of —0.8 V *vs.* S.C.E.

All reported currents are the average currents corrected for the residual current, obtained from separate blank curves, except in Figs. 1 and 3, where polarograms uncorrected for residual currents are reproduced. Potentials are corrected for the "*iR*-drop" and refer to the S.C.E.

All experiments were carried out at 25 $\pm$ 0.1°; other conditions were the same as reported previously[10].

RESULTS

Catalytic waves of perchlorate and nitrate

Effect of sulfuric acid. In solutions 0.01 to 5 M in sulfuric acid and 0.5 M in sodium perchlorate or 0.5 M in sodium nitrate, 0.1 mM molybdenum(VI) gives two waves. The height of the first wave is very small as compared to that of the second wave and

TABLE I

EFFECT OF SULFURIC ACID CONCENTRATION ON THE CATALYTIC WAVES OF PERCHLORATE AND NITRATE IN THE PRESENCE OF 0.102 mM MOLYBDENUM(VI)

$C_{H_2SO_4}$ M	$(i_d)_{tot}$ (μA)	0.5 M $NaClO_4$			0.5 M $NaNO_3$		
		i_1 (μA)	i_c (μA)	i_c/i_c in 0.05 M H_2SO_4	i_1 (μA)	i_c (μA)	i_c/i_c in 0.05 M H_2SO_4
0.01	0.76	6.20	5.44	1.08	—	—	—
0.02	0.76	—	—	—	17.1	16.3	1.03
0.05	0.78	5.80	5.02	1.00	16.6	15.8	1.00
0.1	0.77	5.45	4.68	0.93	16.1	15.3	0.97
0.25	0.75	5.15	4.40	0.88	15.4	14.6	0.92
0.5	0.72	5.00	4.28	0.85	14.7[a]	14.0	0.89
1	0.70	4.63	3.93	0.78	14.4[a]	13.7	0.87
2	0.63	3.65	3.02	0.60	13.9	13.3	0.84
5	0.54	1.60	1.06	0.21	11.9[b]	11.4	0.72

[a] Current by tangent method.
[b] Peak current.

its half-wave potential of + 0.05 V and its height correspond to the normal reduction of molybdenum(VI) to molybdenum(V)[10]. Table I presents data of the catalytic currents i_c of perchlorate and of nitrate in a solution 0.102 mM in molybdenum(VI) and 0.5 M in sodium perchlorate or sodium nitrate, at various sulfuric acid concentrations. The limiting current i_l is taken equal to the total limiting current i_t minus the residual current of the supporting electrolyte in the absence of molybdenum: $i_l = i_t - i_r$. The catalytic current i_c is taken equal to $i_l - i_d$, in which i_d denotes the diffusion current of molybdenum in the absence of nitrate or perchlorate at the potential at which i_t is measured. The characteristics of the polarograms obtained with nitrate are illustrated in Fig. 1. The polarograms with perchlorate at various concentrations of sulfuric acid are similar to those in Fig. 1.

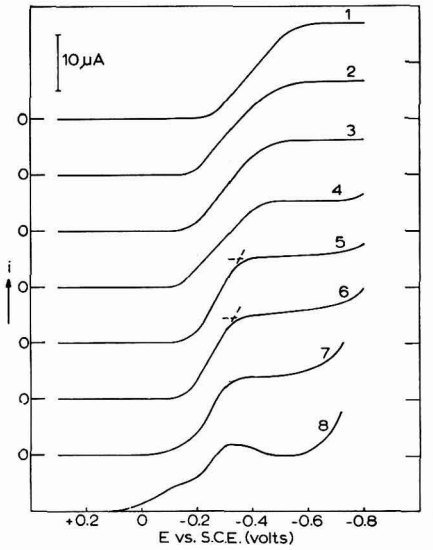

Fig. 1. Effect of sulfuric acid concentration on catalytic nitrate waves in the presence of 0.102 mM molybdenum(VI) and 0.5 M sodium nitrate. Molar concentration of sulfuric acid: (1), 0.02; (2), 0.05; (3), 0.1; (4), 0.25; (5), 0.5; (6), 1; (7), 2; (8), 5.

The limiting current (i_l) of the catalytic wave of perchlorate was measured at —0.8 V and that of nitrate at —0.65 V at low sulfuric acid concentrations, and by the tangent method in solutions more acidic than 0.25 M sulfuric acid. Between 0.02 and 2 M sulfuric acid concentration the limiting currents of the catalytic waves are well-defined both for perchlorate and nitrate, but in 5 M sulfuric acid that of perchlorate is ill-defined, while that of nitrate exhibits a maximum, after which it attains a constant value between —0.5 and —0.6 V. The relative decrease of the catalytic current of nitrate with increasing sulfuric acid concentration is considerably less than that of perchlorate. As a matter of fact, the product of $i_c \cdot \eta^{1/2}$ (η being the relative viscosity of sulfuric acid with respect to water at a given sulfuric acid concentration[11]) for nitrate remains practically constant between 0.02 and 5 M sulfuric acid.

Experiments have been made in 1 *M* perchloric and in 1 *M* nitric acid in the absence of sulfuric acid. The characteristics of the waves are the same as in mixtures being 1 *M* in sulfuric acid and 1 *M* in sodium perchlorate or 1 *M* in sodium nitrate, respectively. The catalytic currents in the absence of sulfuric acid are about 25% larger than those in the mixtures.

The half-wave potential of the catalytic wave of perchlorate changes from —0.45 to —0.20 V, and of nitrate from —0.40 to —0.24 V when the sulfuric acid concentration is increased from 0.01 to 5 *M*.

Effect of concentration of perchlorate or nitrate. In Table II are listed the catalytic currents of perchlorate and of nitrate in 0.102 m*M* molybdenum(VI) and 1 *M* sulfuric acid at various perchlorate or nitrate concentrations. The half-wave potentials of +0.07 V for the first and —0.26 V for the second waves are independent of either perchlorate or nitrate concentrations and practically equal to those of the normal reduction waves of molybdenum(VI) in 1 *M* sulfuric acid[10].

TABLE II

EFFECT OF PERCHLORATE OR NITRATE CONCENTRATION (C_{A^-}) ON THE CATALYTIC WAVES OF PERCHLORATE AND OF NITRATE IN THE PRESENCE OF 0.102 m*M* MOLYBDENUM IN 1 *M* SULFURIC ACID
i_d of Mo(VI) to Mo(III) is 0.7 μA at —0.8 V

C_{A^-} *M*	*NaClO₄*			*NaNO₃*		
	i_l (μA)	i_c (μA)	$i_c/C_{ClO_4^-}$ (μA/*M*)	i_l (μA)	i_c (μA)	$i_c/C_{NO_3^-}$ (μA/*M*)
0.1	2.23	1.53	15.3	5.5[a]	4.8	48.0
0.2	3.05	2.35	11.8	8.1[a]	7.4	37.0
0.5	4.63	3.93	7.9	14.4[a]	13.7	27.4
1	6.40	5.70	5.7	20.9	20.2	20.2
1.5	8.00	7.30	4.9	24.2[a]	23.5	15.7

[a] Tangent method.

TABLE III

CATALYTIC CURRENTS OF PERCHLORATE AND NITRATE IN 1 *M* SULFURIC ACID AT VARIOUS MOLYBDENUM(VI) CONCENTRATIONS

$C_{Mo(VI)}$ $M \cdot 10^5$	0.5 *M NaClO₄*		0.5 *M NaNO₃*	
	i_l (μA)	$i_l/C_{Mo(VI)}$ (μA/*mM* l^{-1})	i_l (μA)[a]	$i_l/C_{Mo(VI)}$ (μA/*mM* l^{-1})
2.04	1.06	52.0	3.15	155
4.08	1.98	48.4	6.10	150
6.12	2.96	48.4	9.30	151
8.16	3.78	46.3	11.9	146
10.2	4.63	45.3	14.4	141
12.2	5.43	44.6	16.1	132
14.3	6.23	43.6	19.2	134

[a] At tangent potential.

Effect of molybdenum(VI) concentration. Values of the limiting currents in 1 *M* sulfuric acid are presented in Table III. The half-wave potential of the catalytic wave with either perchlorate or nitrate was —0.26 V and independent of molybdenum(VI) concentration.

Effect of height of mercury column (h_{Hg}). The catalytic current of perchlorate and of nitrate is practically independent of the height of the mercury column above the capillary, as is evident from the data in Table IV. The diffusion currents (i_d for Mo(VI) to Mo(III)) corresponding to various heights of mercury have been estimated from the determined value of 0.70 μA at a mercury column height of 86.8 cm using the relation $i_d/h_{Hg}^{1/2}$ = constant.

TABLE IV

EFFECT OF HEIGHT OF MERCURY (h_{Hg}) ON LIMITING CURRENTS IN THE PRESENCE OF 0.102 mM MOLYBDENUM(VI) IN 1 M SULFURIC ACID

h_{Hg} (cm)	$(i_d)_{tot}$ (μA)	0.5 M $NaClO_4$		0.5 M $NaNO_3$	
		i_l (μA)	i_c (μA)	i_l (μA)	i_c (μA)
116.8	0.8	4.8	4.0	14.6	13.8
99.0	0.8	4.7	3.9	14.1	13.3
86.8	0.7	4.6	3.9	14.4	13.7
71.5	0.6	4.4	3.8	14.1	13.5
59.1	0.6	4.3	3.7	13.7	13.1

TABLE V

EFFECT OF PHOSPHORIC ACID CONCENTRATION ON CATALYTIC WAVES OF NITRATE IN THE PRESENCE OF 0.102 mM MOLYBDENUM(VI), 0.5 M SODIUM NITRATE AND 1 M SULFURIC ACID
i_d of Mo(VI) to Mo(III) is 0.7 μA at —0.8 V

$C_{H_3PO_4}$ (M)	$-(E_{1/2})_2$ (V)	i_c (μA)
0	0.26	13.7
0.01	0.26	12.6
0.05	0.26	9.2
0.1	0.27	6.7
0.3	0.28	2.4
0.5	0.30	1.2

Effect of phosphoric acid on catalytic waves of nitrate. Phosphoric acid hardly affects the half-wave potential but causes a decrease in the catalytic nitrate current. In 0.5 M phosphoric acid the catalytic wave height is only 9% of that in the absence of the acid. Results are presented in Table V.

Catalytic waves of chlorate

The characteristics of catalytic chlorate waves obtained in acid medium in the presence of molybdenum(VI) differ in many respects from those observed with nitrate or perchlorate. As an example, Fig. 2 gives polarograms obtained in a solution 0.05 mM in molybdenum(VI) and 0.5 M in sodium chlorate at different concentrations of sulfuric acid. From the difference between the measured currents (dotted lines) and those corrected for the residual current of the supporting electrolyte (drawn curves) it is evident that the residual current becomes appreciable at potentials more negative

than —0.1 V and increases with increasing sulfuric acid concentration. Chlorate in acid media is highly irreversibly and incompletely reduced, yielding drawn-out current–potential curves, the currents increasing gradually with increasing negative potential and with increasing sulfuric acid concentration. As an illustration some values at —0.4 V are given in Table VI.

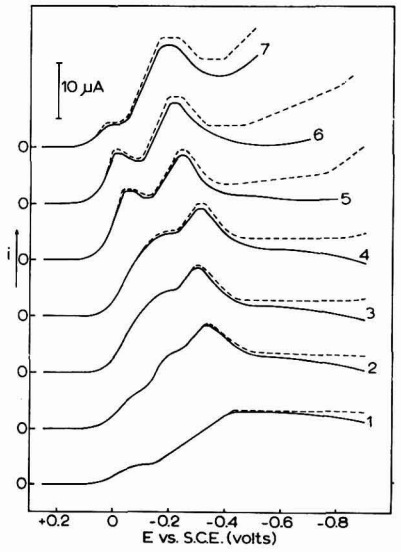

Fig. 2. Catalytic chlorate waves in 0.5 *M* sodium chlorate and 0.05 m*M* molybdenum(VI) solution at varying sulfuric acid concentrations. Dotted lines are currents uncorrected for residual currents, drawn lines are corrected. Molar concentration of sulfuric acid: (1), 0.01; (2), 0.05; (3), 0.1; (4), 0.2; (5), 0.5; (6), 1; (7), 2.

TABLE VI

CURRENT IN 0.5 *M* SODIUM CHLORATE AT —0.4 V AT VARIOUS SULFURIC ACID CONCENTRATIONS

$C_{H_2SO_4}$ (*M*)	*i* (*μA*)
0.01	0.3
0.05	0.6
0.10	0.8
0.2	1.1
0.5	1.9
1	2.8
2	3.6

Chlorate yields two catalytic currents in the presence of molybdenum(VI), the first one being poorly defined at sulfuric acid concentrations less than 0.5 *M* and yielding a maximum (peak) in 0.5 and 1 *M* sulfuric acid, (Fig. 2). The half-wave potential at the higher acidities varies between —0.01 V in 0.5 *M* acid and +0.06 V in 2 *M* acid. The second catalytic current does not yield a well-defined limiting current, but exhib-

its a rounded maximum (peak) at sulfuric acid concentrations equal to or greater than 0.05 M. Table VII lists half-wave potentials $(E_{1/2})_2$, peak potentials $(E_{peak})_2$ and also values of the peak currents $(i_p)_2$ (corrected for i_r). For comparison, half-wave potentials of wave B_1 in a solution 0.51 mM in molybdenum(VI) in the absence of chlorate[10] are added.

TABLE VII

CHARACTERISTICS OF CATALYTIC CHLORATE CURRENTS (2nd PEAK) IN 0.5 M SODIUM CHLORATE AND 0.05 mM MOLYBDENUM(VI) AT VARIOUS SULFURIC ACID CONCENTRATIONS

$C_{H_2SO_4}$ (M)	$-(E_{1/2})_2$ (V)	$-(E_{1/2})_{B_1}$ 0.5 mM Mo(VI) (V)	$-(E_{peak})_2$ (V)	$(i_p)_2$ (μA)	$(i_p)_2/(i_p)_2$ in 0.05 M H_2SO_4
0.01	0.28	0.36	0.45	12.9	0.72
0.05	0.29	0.31	0.35	18.0	1.00
0.1	0.26	0.29	0.30	18.4	1.02
0.2	0.27	—	0.31	19.2	1.07
0.5	0.19	0.36	0.25	18.3	1.02
1	0.15	0.32	0.22	17.5	0.97
2	0.09	0.29	0.19	17.8	0.99

The second peak current is practically independent of sulfuric acid concentration when the acid concentration is increased from 0.05 to 2 M, even though the viscosity of the medium increases markedly.

Effect of chlorate concentration. Polarograms were run in 0.05 M sulfuric acid being 0.5 mM in molybdenum(VI) at chlorate concentrations between 0.0005 and 0.05 M. Figure 3 gives current–potential curves at very small chlorate concen-

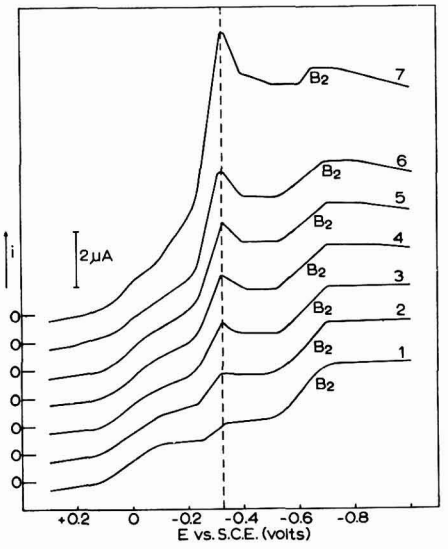

Fig. 3. Effect of small concentrations of sodium chlorate using 0.51 mM molybdenum(VI) in 0.05 M sulfuric acid. Chlorate concentration: (1), 0; (2), 0.5; (3), 1; (4), 1.5; (5), 2.0; (6), 2.5; (7), 5 mM.

trations. In the absence of chlorate, the second molybdenum wave B corresponding to the overall reduction of molybdenum(V) to molybdenum(III) is split into two waves B_1 and B_2[10]. Wave B_1 increases with increasing concentration of chlorate, clearly indicating that the catalysis occurs at potentials of the B_1 wave. The peak potential (—0.32 V) is not affected by the chlorate concentration. From experiments which are not reported here in 0.1 m*M* molybdenum(VI) and 0.05 *M* sulfuric acid it appeared that the peak potential remains constant up to 0.05 *M* chlorate and then becomes slightly more negative.

It is of interest to note in Fig. 3 that the height of wave B_2 decreases from 2.1 μA in the absence of chlorate to 0.6 μA in 0.005 *M* chlorate solution. It becomes too small to be measured with any accuracy in 0.01 *M* chlorate.

Graphs of the effect of larger concentrations of chlorate in 1 and 0.05 *M* sulfuric acid and at different molybdenum(VI) concentrations are given in Fig. 4. Included in Fig. 4 (curve 4) is the effect of chlorate concentration on the first catalytic wave in 1 *M* sulfuric acid. In order to obtain well-defined first catalytic waves, both the sulfuric acid and sodium chlorate concentrations must be at least 0.2 *M*. Table VIII

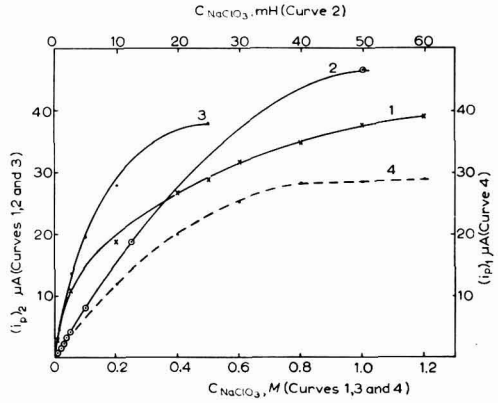

Fig. 4. Catalytic currents $(i_p)_2$ (curves (1), (2) and (3)) and $(i_p)_1$ (curve (4), dotted line) as a function of sodium chlorate concentration: (1) and (4), 0.1 m*M* Mo(VI), 1 *M* H_2SO_4; (2), 0.5 m*M* Mo(VI), 0.05 *M* H_2SO_4; (3), 0.1 m*M* Mo(VI), 0.05 *M* H_2SO_4.

TABLE VIII

EFFECT OF SODIUM CHLORATE CONCENTRATION ON THE CATALYTIC CURRENTS IN 1 *M* SULFURIC ACID IN THE PRESENCE OF 0.1 m*M* MOLYBDENUM(VI)

m = 1.60 mg/sec^{-1}, t = 4.60 sec, h = 86.8 cm

C_{NaClO_3} (*M*)	$(E_{1/2})_1$ (V)	First $(i_c)_1$ (μA)	$(i_c)_1/C_{ClO_3^-}$ (μA/*M*)	$-(E_{peak})_2$ (V)	$(i_p)_2$ (μA)	$(i_p)_2/C_{ClO_3^-}$ (μA/*M*)
0.2	+0.04	12.0	60	0.25	18.8	94
0.4	+0.02	20.1	50	0.25	26.8	67
0.5	+0.02	22.5	45	0.24	29.0	58
0.6	+0.02	25.7	43	0.25	31.7	53
0.8	+0.01	28.5	36	0.22	35.0	44
1.0	+0.02	28.7	29	0.27	37.7	38
1.2	+0.02	29.1	24	0.29	39.3	33

tabulates the results in 1 M sulfuric acid at chlorate concentrations higher than 0.2 M.

Effect of molybdenum(VI) concentration. The effect of molybdenum concentration has been studied at various acidities and sodium chlorate concentrations. Some of the results are presented in Figs. 5, 6, 7, and 8. It is of interest to note (Fig. 8) that in

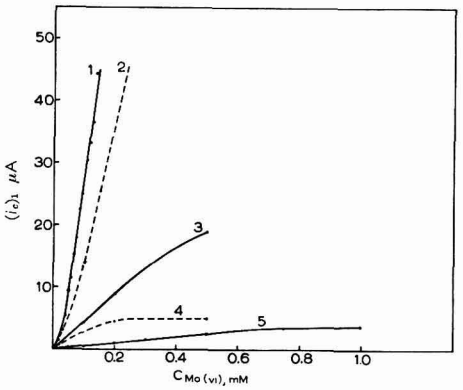

Fig. 5. $(i_c)_1$ as a function of molybdenum concentration. Drawn curves in 1 M, dotted curves in 0.05 M sulfuric acid. Curves (1) and (2), 0.5 M in sodium chlorate; curves (3) and (4), 0.05 M in sodium chlorate; curve (5), 0.005 M in sodium chlorate.

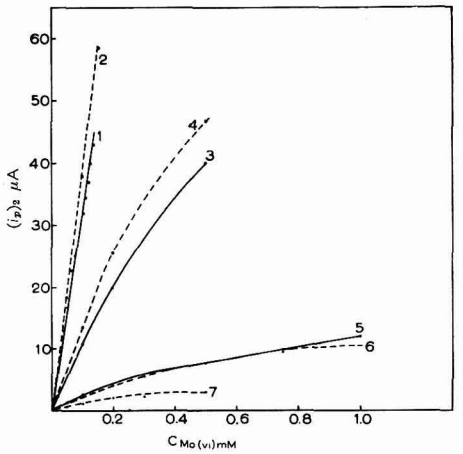

Fig. 6. $(i_p)_2$ as a function of molybdenum concentration. Drawn curves in 1 M, dotted curves in 0.05 M sulfuric acid. Curves (1) and (2), 0.5 M in sodium chlorate; curves (3) and (4), 0.05 M in sodium chlorate; curves (5) and (6), 0.005 M in sodium chlorate; curve (7), 0.002 M in sodium chlorate.

0.5 M sodium chlorate the second catalytic current is strictly proportional to molybdenum concentration at sulfuric acid concentrations between 0.05 and 1 M. From Fig. 7 it is seen that in 0.5 M chlorate the first catalytic current becomes proportional to molybdenum concentration when the latter becomes greater than about $4 \cdot 10^{-5}$ M

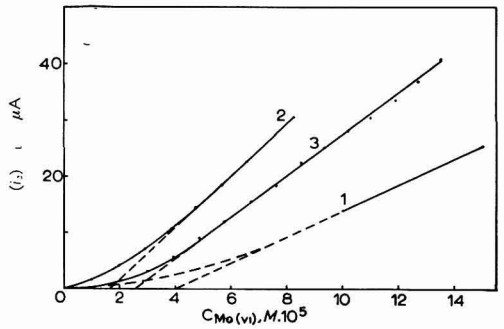

Fig. 7. $(i_c)_1$ as a function of molybdenum concentration in 0.5 M sodium chlorate at various acidities. Line (1), 0.05 M; line (2), 0.2 M; line (3), 1 M sulfuric acid.

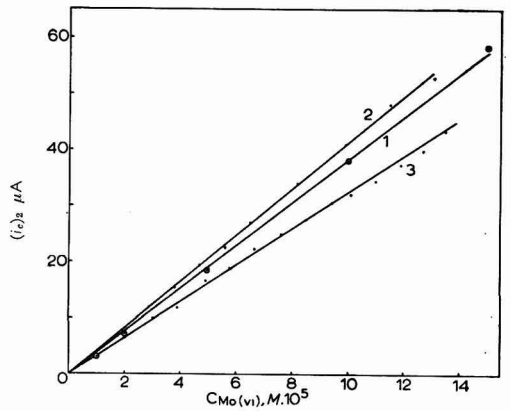

Fig. 8. $(i_c)_2$ as a function of molybdenum concentration in 0.5 M sodium chlorate at various acidities. Line (1), 0.05 M; line (2), 0.2 M; line (3), 1 M in sulfuric acid.

TABLE IX

CATALYTIC CURRENTS ($(i_p)_1$ AND $(i_p)_2$) AND POTENTIALS AS A FUNCTION OF MOLYBDENUM(VI) CONCENTRATION IN 0.2 M SULFURIC ACID AND 0.5 M SODIUM CHLORATE

$C_{Mo(VI)}$ ($M \cdot 10^5$)	*First peak*			*Second peak*			
	$-(E_{1/2})_1$ (V)	$(i_p)_1$ (μA)	$(i_p)_1/C_{Mo(VI)}$ (μA/mM)	$-(E_{1/2})_2$ (V)	$-E_{p2}$ (V)	$(i_p)_2$ (μA)	$(i_p)_2/C_{Mo(VI)}$ (μA/mM)
0.99	0.04	1.5	152	0.21	0.26	3.95	399
1.96	0.03	4.0	204	0.22	0.26	7.90	403
2.91	0.04	7.2	247	0.22	0.26	11.8	407
3.85	0.04	10.7	278	0.23	0.26	15.6	406
4.76	0.02	14.4	303	0.24	0.26	19.3	406
5.67	0.03	18.3	323	0.24	0.27	22.6	399
6.54	0.03	22.9	350	0.23	0.27	27.1	414
8.26	0.02	30.5	369	0.23	0.28	33.9	410
9.90	[a]				0.27	41.2	416
11.5	[a]				0.27	47.2	412
13.1	[a]				0.27	53.1	406
						Mean	404±5

[a] The two waves merge.

at sulfuric acid concentrations greater than 0.2 M, and greater than $7 \cdot 10^{-5}$ M in 0.05 M sulfuric acid. Because of the analytical significance of these results some detailed data in a medium 0.2 M in sulfuric acid and 0.5 M in chlorate are presented in Table IX.

Effect of height of mercury column (h_{Hg}). From data in Table X it appears that both peak currents in a solution of 0.05 mM molybdenum(VI) in 0.5 M sodium chlorate and 1 M sulfuric acid are practically independent of the height of mercury column and are therefore kinetic in nature.

TABLE X

EFFECT OF HEIGHT OF MERCURY (h_{Hg})

h_{Hg} (cm)	drop-time (sec)	$(i_p)_1$ (μA)	$(i_p)_2$ (μA)
61.0	6.70	8.7	17.2
73.4	5.66	9.0	17.2
88.4	4.60	9.0	17.1
105.8	4.06	9.0	17.1
123.4	2.88	8.7	16.6

Effect of phosphoric acid concentration. The effect of phosphoric acid concentration has been studied in a medium 0.05 mM in molybdenum(VI), 0.5 M in sodium chlorate and 1 M sulfuric acid. The results are listed in Table XI. While the half-peak and peak potentials are hardly affected by phosphoric acid, the peak heights become considerably reduced when the phosphoric acid concentration becomes greater than 0.1 M.

TABLE XI

EFFECT OF PHOSPHORIC ACID ON THE CATALYTIC CHLORATE WAVES
Solution 0.05 mM in Mo(VI), 0.5 M in sodium chlorate and 1 M in sulfuric acid

$C_{H_3PO_4}$ (M)	1st reduction			2nd reduction		
	$(E_{1/2})_1$ (V)	$-(E_p)_1$ (V)	$(i_c)_1$ (μA)	$-(E_{1/2})_2$ (V)	$-(E_p)_2$ (V)	$(i_p)_2$ (μA)
0	+0.04	0	9.7	0.15	0.21	17.9
0.01	+0.04	0.03	10.4	0.15	0.22	17.4
0.05	+0.05	0.01	11.6	0.15	0.22	16.9
0.1	+0.05	0.01	11.1	0.15	0.23	15.8
0.2	+0.06	0.01	8.1	0.14	0.22	13.7
0.3	+0.07	[a]	5.8	0.12	0.23	11.4
0.4	+0.07	[a]	4.1	0.11	0.24	9.7
0.5	+0.07	[a]	2.9	0.10	0.25	8.4

[a] Wave.

DISCUSSION

One of the most interesting results of this study is that chlorate in acid medium yields two catalytic reduction waves in the presence of molybdenum(VI) (Fig. 2), whereas perchlorate and nitrate yield only one (Fig. 1). The half-wave potential of the second catalytic chlorate wave occurs at a potential slightly less negative (0.08 V) than that

of wave B_1 (see ref. [10] and also Fig. 3) of molybdenum alone at the same acid concentration and 0.05 V less negative than the half-wave potentials of the nitrate and perchlorate waves. Evidently, the reduction of Mo(V) to Mo(III) catalyzes the polarographic reduction of chlorate, nitrate and perchlorate. No indication of formation of Mo(IV) was found in a polarographic study[10] of Mo(VI) at different concentrations of sulfuric acid and it is postulated that the Mo(III) formed at the surface of the electrode is the catalyst. HAIGHT[3,5,12] and HAIGHT AND SAGER[13] attribute the perchlorate reduction to catalysis by Mo(IV) and not by Mo(III), since they found that Mo(III) does not catalyze the reduction of perchlorate in the bulk of solution. However, it should be realized in the interpretation of all the molybdenum waves, including the catalytic currents, that polymerization equilibrium of the various valence forms of Mo(V) and Mo(III) (and Mo(IV)(?)) is not expected to be established on the surface of the growing drop of mercury and that reduction studies carried out in the bulk of a solution with equilibrated reduced molybdenum species may yield different rates and other characteristics than those observed at dropping mercury. In this connection it is of interest to note that the second chlorate wave yields a well-defined peak (see Fig. 2); at potentials more negative than $(E_{peak})_2$ the current drops. On the other hand, perchlorate and nitrate yield limiting catalytic currents which are constant over a range of potentials covering at least 0.2 V. The appearance of the peak on the second chlorate wave could be attributed to participation of Mo(IV) in the catalysis; at more negative potentials than $(E_{peak})_2$ Mo(III) formation is favored upon reduction of Mo(V). The constancy of the limiting catalytic current of perchlorate and nitrate with change of potential shows almost conclusively that the catalysis must be due to Mo(III).

In 0.05 M sulfuric acid and in the absence of anions whose reduction is catalyzed, the Mo(V) to Mo(III) wave is split into 2 waves, B_1 and B_2 (ref. [10], see also curve 1, Fig. 3), whereas in 1 M sulfuric acid only one wave B (B_1) is observed. At all acidities the half-wave potentials of the kinetic waves of perchlorate, nitrate and chlorate $(i_c)_2$ closely correspond to that of wave B_1, but the kinetic currents of these anions hardly change when the sulfuric acid concentration is varied from 0.05 to 1 M. In a previous paper it was shown (see Table II, ref.[10]) that at small molybdenum concentrations the half-wave potential of B_1 does not change with acid concentration, while that of B_2 (Fig. 1, ref.[10]) becomes less negative with increasing acid concentrations, so that in 0.25 M sulfuric acid the two waves overlap and only one B wave is observed. Thus, it is possible that the ratio of the reduced species of Mo(V) responsible for the appearance of waves B_1 and B_2 does not change with acid concentration, and that the species giving rise to wave B_1 is responsible for the catalytic waves at all acidities. An alternative is that the "species B_2" is not formed in the presence of 0.5 M nitrate, perchlorate or chlorate. A clear indication that this may be the case is obtained from Fig. 3, which gives polarograms of molybdenum in the presence of small concentrations of chlorate. In the absence of chlorate the height of B_2 was 2 μA, but in the presence of 0.005 M chlorate only 0.6 μA. It is not possible to determine with any accuracy the height of B_2 at higher chlorate concentrations. However, there is strong indication that wave B_2 disappears and the species responsible for it is not formed at higher chlorate concentrations. Similar experiments have been carried out in the presence of small concentrations of nitrate and of perchlorate. For the sake of brevity these are not reported in the experimental part. As an illustration, some data obtained with nitrate follow: medium, 0.05 M in sulfuric acid and 0.5 mM in Mo(VI); $B_2 = 2.0\ \mu$A;

in the presence of 0.005 M nitrate $B_2 \leqslant 1.3\ \mu A$; in the presence of 0.015 M nitrate $B_2 \leqslant 0.4\ \mu A$ (no exact measurement possible).

Both catalytic waves of chlorate have been found proportional to the square root of its concentration in a range between 0.1 and 1.2 M chlorate (see Table VIII). Applying the equation developed by DELAHAY AND STIEHL[14] it is possible to calculate from the polarographic data the rate constants of the catalyzed reductions of chlorate and nitrate:

$$i_c = 3/5\ (1.255 \cdot 10^6\ nm^{2/3}t^{2/3}\ D_{Mo(VI)}^{1/2}\ C_{Mo(VI)}\ C_{A^-}^{1/2} k^{1/2})$$

in which i_c ($(i_c)_2$ for chlorate) is the catalytic current in μA, n the number of electrons involved and taken equal to 2 (Mo(V) to Mo(III)), $D_{Mo(VI)}$ the polarographic diffusion coefficient of molybdenum(VI) in $cm^2\ sec^{-1}$ which was taken from a previous paper[10], and k the rate constant. $C_{Mo(VI)}$ and C_{A^-} are expressed in mole/l. From the data obtained in solutions 0.5 M in A^-, the following values for k in 1 and 0.05 M sulfuric acid, respectively, are calculated, and shown in Table XII.

TABLE XII

	$k_{ClO_3^-}$	$k_{NO_3^-}$ (in $l\ mole^{-1}\ sec^{-1}$)	$k_{ClO_4^-}$
in 1 M H_2SO_4	$1.3 \cdot 10^3$	$2.3 \cdot 10^2$	$3.0 \cdot 10^1$
in 0.05 M H_2SO_4	$1.5 \cdot 10^3$	$2.5 \cdot 10^2$	$3.4 \cdot 10^1$

In the calculation of the rate constant for perchlorate reduction, the simplified equation given above could not be used because of the low value of the product kC_{A^-}, which should be higher than 100 to allow the use of the approximate equation. The graphical method described by DELAHAY AND STIEHL[14] was therefore used, inserting our experimental values in the figure presented in their paper. Only the order of magnitude of $k_{ClO_4^-}$ is thus obtained; it is about 10 times smaller than that of nitrate and about 100 times smaller than that of chlorate.

LAITINEN AND ZIEGLER[15] reported a value of $1.63 \cdot 10^3\ sec^{-1}$ for kC_{A^-} in the catalytic polarographic reduction of perchlorate in the presence of tungsten (W(VI) to W(V)) in solutions being 12 M in perchloric acid and 0.04 M in hydrochloric acid.

The first catalytic wave of chlorate has a half-wave potential which corresponds exactly to that of the first molybdenum(VI) reduction wave[10]; thus it can be definitely concluded that the catalysis is due to Mo(V).

From the analytical viewpoint, the determination of the second catalytic current (peak current) of chlorate in the estimation of traces of molybdenum(VI) has the following advantages over the use of the nitrate or perchlorate catalytic waves:

(1) The (second) peak current of chlorate at various sulfuric acid concentrations is strictly proportional to Mo(VI) concentration, at least in a range between 0.5 and $15 \cdot 10^{-5}$ M (see Fig. 8). On the other hand, no such proportionality is found for the limiting catalytic nitrate and perchlorate waves (Table III) and a calibration curve must be constructed when use of these ions is made.

(2) At the same molybdenum, anion and acid concentration, the ratio of the catalytic currents is of the order of 1 (perchlorate) to 2.6 (nitrate) to 8 (chlorate). Thus the chlorate reduction current is the most sensitive to traces of molybdenum.

(3) Phosphoric acid suppresses the peak current of chlorate (Table XI) to a much smaller extent than that of nitrate (Table V).

A disadvantage in the use of the second peak current of chlorate is that the residual current at the peak potential is considerably greater than those at potentials of the limiting catalytic currents of nitrate or perchlorate. However, in 0.05 M sulfuric acid the residual current in 0.5 M chlorate is only 0.6 μA as compared to a peak current corrected for i_r of 4.2 — 0.6 = 3.6 μA for $1 \cdot 10^{-5}$ M molybdenum(VI).

The first peak current in the chlorate reduction varies more with sulfuric acid concentration than that of the second one (compare Figs. 7 and 8). In 0.05 M sulfuric acid, the first peak current is about one third of that in 0.2 M acid, and one half of that in 1 M sulfuric acid. At the same molybdenum concentration, the first and second peak currents (corrected for i_r in 0.2 M sulfuric acid) are of the same order of magnitude when the molybdenum concentration is equal to or greater than $4 \cdot 10^{-5}$ M. Since the residual current at the first peak potential is only 0.4 μA in 0.2 M sulfuric acid, the measurement of the first peak current would have analytical advantages over the measurement of the second one. This is true when the molybdenum concentration is equal to or greater than $4 \cdot 10^{-5}$ M, when $(i_{peak})_1$ becomes proportional to molybdenum concentration. However, at smaller concentrations the first peak current decreases less than in proportion to the decrease of molybdate concentration (see Fig. 7).

ACKNOWLEDGEMENT

Partial financial support of this work was received from the United States Air Force Office of Scientific Research of the Air Research and Development Command under Contract No. AF 49(638)519. Reproduction in whole or in part is permitted for any purpose of the United States Government.

SUMMARY

Molybdenum catalyzes the polarographic reduction of chlorate in acid medium, giving rise to two catalytic waves. The half-wave potential of the first one corresponds to that of the normal reduction wave of Mo(VI) to Mo(V), indicating that Mo(V) acts as the catalyst. The half-wave potential of the second catalytic wave corresponds to that of B_1 (see ref.[10]) in the normal reduction of Mo(VI) to Mo(III). The second catalytic wave is characterized by a peak, the peak current (corrected for i_r) being strictly proportional to the molybdenum concentration in the range between $1 \cdot 10^{-5}$ (or less) and $1.3 \cdot 10^{-4}$ M and about 2.6 times greater than the catalytic nitrate and 8 times greater than the catalytic perchlorate waves measured under similar conditions. The first catalytic current becomes proportional to molybdenum(VI) concentration when $C_{Mo(VI)}$ is greater than $4 \cdot 10^{-5}$ M. The characteristics of catalytic chlorate, nitrate and perchlorate waves have been determined and interpreted under various experimental conditions.

REFERENCES

1 W. OSTWALD, *Z. Physik. Chem. (Leipzig)*, 2 (1888) 127.
2 I. M. KOLTHOFF, *Z. Anal. Chem.*, 60 (1921) 348, 352.
3 G. P. HAIGHT, JR., *Anal. Chem.*, 25 (1953) 642.
4 R. HÖLTJE AND R. GEYER, *Z. Anorg. Allgem. Chem.*, 246 (1941) 258.
5 G. P. HAIGHT, JR., *Anal. Chem.*, 23 (1951) 1505.
6 G. B. JONES, *Anal. Chim. Acta*, 10 (1954) 584.

[7] S. I. SIMYAKOVA AND M. I. GLINKINA, *J. Anal. Chem. USSR*, 11 (1956) 581; (*C.A.*, 51 (1957) 7228).
[8] H. E. PALMER, U.S.A.E.C.-H.W.-66057 (1960); *Anal. Abstr.*, 8 (1960) 3252.
[9] M. G. JOHNSON AND R. J. ROBINSON, *Anal. Chem.*, 24 (1952) 366.
[10] I. M. KOLTHOFF AND I. HODARA, *J. Electroanal. Chem.*, 4 (1962) 369.
[11] D. M. BRASHER AND F. R. JONES, *Trans. Faraday Soc.*, 42 (1946) 775.
[12] G. P. HAIGHT, JR., *J. Am. Chem. Soc.*, 76 (1954) 4718.
[13] G. P. HAIGHT AND W. F. SAGER, *J. Am. Chem. Soc.*, 74 (1952) 6056.
[14] P. DELAHAY AND G. L. STIEHL, *J. Am. Chem. Soc.*, 74 (1952) 3500.
[15] H. A. LAITINEN AND W. A. ZIEGLER, *J. Am. Chem. Soc.*, 75 (1953) 3045.

TRIANGULAR WAVE CYCLIC VOLTAMMETRY. I

Z. GALUS, H. Y. LEE AND RALPH N. ADAMS

Department of Chemistry, University of Kansas, Lawrence, Kan. (U.S.A.)

(Received May 22nd, 1962)

The technique of cyclic voltammetry employs a repetitive, triangular (isosceles) voltage sweep and was apparently first practiced by SEVCIK[1]. An excellent series of papers by KEMULA and coworkers should be credited with reviving interest in the method and especially pointing the way to studies of electrode mechanisms[2-5]. The technique has been found to be particularly well suited to mechanism studies at solid electrodes. This communication is intended to show the scope and utility of the method, especially as applied to complex organic electro-oxidations at solid electrodes. A review of triangular wave methods employing oscillographic recording has been given by NÜRNBERG[6,7]. KAUFMAN, LOVELAND AND ELVING have recently described a triangular wave sweep generator and its application to oscillographic recording at mercury electrodes[8]. No further discussion of oscillographic recording or triangular wave methods applied to the dropping mercury electrode is given here.

In cyclic voltammetry (CV) the current (both cathodic and anodic segements) is followed during the complete excursions of the applied triangular voltage sweep. The sweep rates can be about the same as in ordinary (single sweep) peak voltammetry, *i.e.*, 0.2–3 V/min, but values up to 10 V/min are frequently of interest. Large amplitude signals of 1–3 V are used, depending upon the potential range of interest. The latter condition distinguishes CV from small amplitude triangular wave methods in which much higher frequencies are used. The data is best presented on an X–Y recorder (1 sec pen response) although conventional X–time or strip chart recording can be used. The latter operation requires folding the chart paper and retracing the composite curve.

Since cyclic polarograms are observed at quiet electrodes and the time interval between reverse sweeps is relatively short, products of say, a cathodic reduction, are available at and near the electrode surface for re-oxidation on the anodic going segment of the cycle. Ideally CV should employ strictly linear diffusion conditions. However, after several sweeps the concentration profiles near the electrode surface are rather involved and, especially with the complexities of organic electrode processes, little is gained by using such refinements as shielded electrodes. For instance, vertical wire electrodes with sweep rates of 2–3 V/min give quite satisfactory results. While specific instrumentation is described elsewhere[9], Fig. 1 shows a block diagram

of suitable apparatus for CV. This indicates an operational amplifier controlled potential polarograph, but CV can be carried out, of course, using only two electrodes. In this case the triangular wave generator is a low resistance slide-wire driven in a cyclic fashion and connected directly to two electrodes, as with the usual polarographic bridge circuit. However, with the ease of construction of controlled potential circuits it is difficult to recommend the continued use of two-electrode polarography.

Intuitively it is easy to see that a rapid charge transfer process (reversible system)

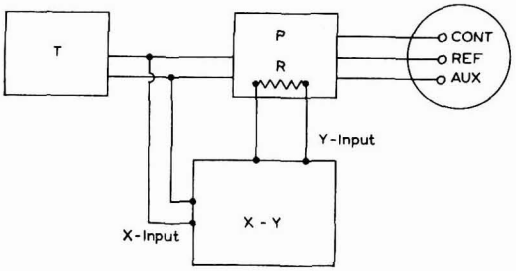

Fig. 1. Block diagram of equipment for cyclic voltammetry: T, slow sweep triangular wave generator (mechanical or electronic); P, operational amplifier type potentiostat; CONT, controlled electrode; AUX, auxiliary electrode; REF, reference electrode; X–Y, X–Y recorder, 1 sec pen responses; R, current measuring network in the potentiostat.

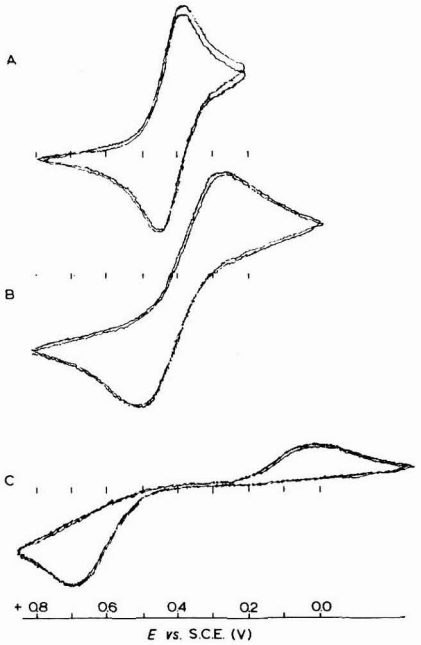

Fig. 2. Typical cyclic polarograms of the Fe(III)/Fe(II) system: A, 10^{-3} *M* Fe(III) in 1 *M* hydrochloric acid and 5 *M* calcium chloride background, scan rate 2 V/min, at carbon paste electrode; B, 10^{-3} *M* Fe(II) in 1 *M* sulfuric acid, scan rate 1 V/min, at platinum electrode; C, 10^{-3} *M* Fe(II) in 1 *M* sulfuric acid, scan rate 2 V/min, at carbon paste electrode. All currents on an arbitrary scale.

will show cyclic polarograms as in Fig. 2A, which represents several sweeps taken at a carbon paste electrode of a solution 10^{-3} *M* in Fe(III) and 1 *M* in hydrochloric acid and 5 *M* in calcium chloride. At this high chloride concentration the Fe(III)–Fe(II) system behaves almost reversibly at carbon paste with the scan rate of 2 V/min. Actually, for a truly reversible system, the anodic and cathodic peaks are not at exactly the same potential, but a separation is predicted (in V) as:

$$(E_{p(\text{anodic})} - E_{p(\text{cathodic})}) = \frac{0.058}{n} \qquad (1)$$

Equation (1) was given by MATSUDA AND AYABE[10] and is based on uniform concentrations of either *Ox* or *Red* prior to initiation of the potential sweep. Such conditions do not prevail, particularly at high sweep rates in CV, and eqn. (1) is not quite correct. However, it has been verified for cyclic sweep rates of *ca.* 2–3 V/min on several reversible systems[11].

A quasi-reversible system (nomenclature of MATSUDA AND AYABE[10]) shows a greater separation in E_p's than that of eqn. (1). The polarograms are more drawn out and the peaks more rounded. This behavior is seen in Fig. 2B which is of 10^{-3} *M* Fe(II) in 1 *M* sulfuric acid at a platinum electrode, using a sweep rate of 1 V/min in this case.

For a very slow charge transfer process, one sees the complete separation of anodic and cathodic processes as represented in Fig. 2C. This represents the same system as in Fig. 2B, but run on a carbon paste electrode where the reaction is markedly more irreversible. Obviously the artificial distinctions between reversible, quasi-, and irreversible reactions are only gradations of the charge transfer rate, but these terms are common and will undoubtedly remain in use. The examples above were used merely to illustrate the profound effect of both background electrolyte and electrode material on charge transfer rates as reflected in the CV.

Actually CV is not particularly well suited to the measurement of charge transfer rates. These parameters are better investigated with single sweep voltammetry following the treatment of MATSUDA AND AYABE, or by other techniques. Complications, such as follow-up chemical reactions after charge transfer, provide the area of greatest interest in CV. The method is ideally suited for investigating the *overall* processes, both chemical and electrochemical, which may occur in a complex organic electrode reaction. Coupled with single sweep methods for evaluating kinetic parameters, CV is a powerful tool for elucidating electrode mechanisms. The advantages are best illustrated by examples of some organic electrode processes carried out at solid electrodes.

A. OXIDATION OF N,N-DIMETHYLANILINE

A complex overall process which can be readily defined by CV is the anodic oxidation of N,N-dimethylaniline (DMA) at carbon paste or platinum electrodes. Figure 3 shows several cycles of a typical oxidation of DMA in pH 2–4 buffers. DMA is oxidized at *ca.* +0.6 V in this pH range and is represented by the large anodic wave in this potential region. Note first that there is no cathodic process corresponding to the oxidation at +0.6 V. This immediately marks the DMA oxidation as an overall irreversible process.

Often, one of the most significant features of a series of cyclic polarograms is a

marked difference between the first and all subsequent sweeps. In Fig. 3 it can be observed that no anodic processes occur on the *first sweep* until DMA itself is oxidized at 0.6 V. Note, however, on the first reverse (cathodic going) sweep, two

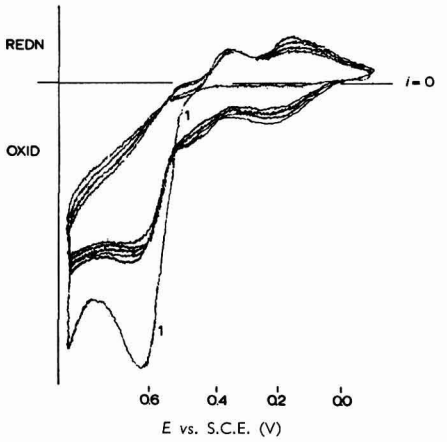

Fig. 3. Cyclic polarograms of dimethylaniline oxidation: 1, first anodic sweep.

reduction peaks occur with $E_{p/2}$ values of *ca.* +0.45 and 0.20 V. Now, on the second and subsequent anodic cycles two oxidation peaks develop at about the same potentials; *i.e.*, two almost reversible redox systems appear *after* the initial oxidation of DMA. By running cyclic polarograms of suspected products, these redox systems can then be identified. It is possible to establish without doubt that the redox system at +0.45 V is due to the reversible oxidation–reduction of N,N′-tetramethylbenzidine (TMB) and its corresponding diquinoid (TMBOx). TMB is formed in a follow up chemical reaction between the initial oxidation product of DMA (a dipositive ion intermediate resulting from the loss of 2 electrons) with a molecule of unoxidized DMA.

The system at +0.2 V is more difficult to identify in an absolute sense. Since the material was suspected of being a coupling product between TMBOx and excess DMA, TMBOx was prepared by chemical oxidation of TMB with lead peroxide and isolated as the perchlorate. A solution of this was made up in pH 4 buffer and divided into two parts. To one solution, DMA was added and after standing for about 1/2 h cyclic polarograms were run on both solutions. In the solution containing only TMBOx, the cyclic polarograms consisted of only the redox system at 0.45 V. In the solution which had been mixed with DMA, the additional peaks at 0.2 V were clearly evident. During the latter runs, the anodic sweep was not allowed to go beyond +0.5 V so that no DMA was electrochemically oxidized. Hence the 0.2 V redox system could only develop *via* TMBOx–DMA interaction. Further details on the mechanism of DMA oxidation have been given[12–14].

B. OXIDATION OF *p*-PHENYLENEDIAMINE IN STRONG ACID

The CV of *p*-phenylenediamine (PPD) in 1 *M* perchloric acid illustrates another

situation where the first anodic sweep is significantly different from all subsequent sweeps. This is seen in Fig. 4 where only a very small anodic peak at *ca.* 0.5 V (wave A) is obtained on the first sweep. This peak is greatly increased on the second sweep, showing that the reductant species which it represents is generated on a previous

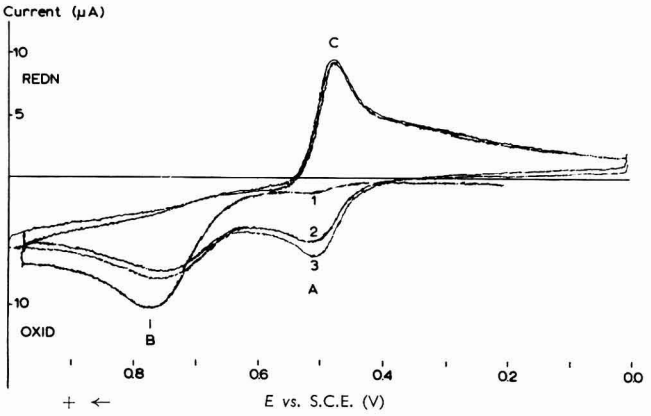

Fig. 4. Oxidation of *p*-phenylenediamine in 1 *M* perchloric acid: (1), first sweep, starting anodic; (2) and (3), second and third sweeps.

cathodic cycle. The fact that any wave A is obtained on the first sweep indicates this species can also arise to a small extent by homogeneous chemical reactions. While the complete interpretation of PPD oxidation is quite complex, the following general picture can be given: peak B represents the 2-electron oxidation of PPD to the corresponding diimine. (*In situ* electron paramagnetic resonance studies show no PPD cation radical from the 1-electron oxidation is present during oxidation in strong acid medium.) Since there is no corresponding reduction peak for the diimine, a rapid chemical transformation of diimine is suspected. This is born out by the fact that peak C (and its anodic counterpart A) are coincident with the CV of *p*-quinone imine and its reduced form, *p*-aminophenol. Thus *p*-phenylenediimine undergoes rapid hydrolysis of one imine group to give the quinone imine whose reduction is seen as peak C. The subsequent oxidation of *p*-aminophenol formed during C appears as the anodic peak A. The small current for peak A observed on the first sweep is due to a small amount of hydrolysis of PPD in the strong acid solution prior to electrolysis. A complication which is not apparent in Fig. 4 is that hydrolysis of both amino groups of the quinone imine leads to *p*-benzoquinone. Indeed, the hydrolysis rate of *p*-benzoquinone imine can be studied by CV and a full interpretation of these systems will be given soon[11].

SUMMARY

Cyclic voltammetry using moderately slow sweep rates, and hence pen and ink recording, is advantageous for examining the overall mechanisms of complex organic electrode processes. The method is particularly well suited to the study of organic oxidations at solid electrodes. When coupled with single sweep peak voltammetry for measuring charge transfer rates and other kinetic parameters, it can be a powerful tool for the study of organic electrode processes.

ACKNOWLEDGEMENTS

This work was supported by the Atomic Energy Commission through contract AT(11-1)-686 and the Air Force through Air Force Office of Scientific Research and this support is gratefully acknowledged.

REFERENCES

1 A SEVCIK, *Collection Czech. Chem. Commun.*, 13 (1948) 349.
2 W. KEMULA AND Z. KUBLIK, *Anal. Chim. Acta*, 18 (1958) 104.
3 W. KEMULA AND Z. KUBLIK, *Bull. Acad. Polon. Sci. Ser. Sci. Chim.*, 6 (1958) 653.
4 W. KEMULA, Z. GALUS AND Z. KUBLIK, *Bull. Acad. Polon. Sci. Ser. Sci. Chim.*, 7 (1959) 613, 723.
5 W KEMULA, Z. GRABOWSKI AND M. KALINOWSKI, *Naturwissenschaften*, 22 (1960) 514.
6 H. W. NÜRNBERG AND M. V. STACKELBERG, *J. Electronal. Chem.*, 2 (1961) 181.
7 H. W. NÜRNBERG, *Z. Anal. Chem.*, 186 (1962) 1.
8 D. C. KAUFMAN, J. W. LOVELAND AND P. J. ELVING, *J. Phys. Chem.*, 63 (1959) 217.
9 J. R. ALDEN, J. Q. CHAMBERS AND R. N. ADAMS, *J. Electronal. Chem.*, [2] 5 (1963).
10 H. MATSUDA AND Y. AYABE, *Z. Elektrochem.*, 59 (1955) 494.
11 H. Y. LEE AND R. N. ADAMS, unpublished data.
12 T. MIZOGUCHI AND R. N. ADAMS, *J. Am. Chem. Soc.*, 84 (1962) 2058.
13 Z. GALUS AND R. N. ADAMS, *ibid.*, 84 (1962) 2061.
14 Z. GALUS, R. M. WHITE, F. S. ROWLAND AND R. N. ADAMS, *ibid.*, 84 (1962) 2065.

ELECTROCHEMISTRY OF DISSOLVED GASES

III. OXIDATION OF HYDROGEN AT PLATINUM ELECTRODES

DONALD T. SAWYER AND EDDIE T. SEO

Department of Chemistry, University of California, Riverside, Calif. (U.S.A.)

(Received February 9th, 1962)

The electrochemical behavior of hydrogen has been extensively studied and was first discussed by HAMMETT in 1924[1]. This early investigation, concerned with the hydrogen indicator electrode, discussed the preparation of the metal surface to ensure reversible behavior. A later discussion of hydrogen and its electrolysis at platinum electrodes was presented by BUTLER AND ARMSTRONG in 1934[2] and also in 1947[3]. Recently FRANKLIN AND COOKE have suggested that molecular hydrogen is oxidized at the platinum electrode by three different processes (a bibliography of hydrogen dissolution reactions is included in this paper)[4]. Another recent study by SHIBATA suggests that a pre-cathodized electrode gives supersaturated hydrogen at the platinum surface which is seen when the electrode is subsequently anodized[5].

Because the previous work, in many respects, presents conflicting views and because there are a number of new techniques available for studying electrode mechanisms and kinetics, a further investigation of the behavior of hydrogen at platinum electrodes is desirable. The present discussion is concerned with the results of such an investigation and is directed toward elucidating how dissolved hydrogen gas is oxidized at platinum electrodes. This study is also concerned with the effect of solution conditions and preconditioning of the electrode surface. Much of the work follows the techniques used in an earlier study of dissolved oxygen[6].

EXPERIMENTAL

Equipment

Both the voltammetric and chronopotentiometric studies were carried out using a versatile electronic instrument which has been previously described by DEFORD[7]. This instrument is based on the use of Philbrick operational amplifiers and permits precise measurements of current and potential. The potentials were measured to an accuracy of $\pm$ 2 mV and the currents to an accuracy of $\pm$ 0.1%. The voltammetric measurements were made in a modified H-cell which prevented attack of the agar salt bridge by strongly alkaline solutions[8]. The cell for chronopotentiometric measurements was of conventional design and utilized a platinum foil working electrode and a platinum gauze auxiliary electrode. The working electrode potential was measured relative to a saturated calomel electrode in all cases. The electrode for chronopotentiometric measurements was prepared from reagent grade platinum foil, 1 cm^2 on each side, welded to 22 gauge platinum wire and sealed into soft glass in such a manner as

to incorporate the weld in the seal[9]. The electrodes for voltammetric studies were prepared from 18 and 22 gauge platinum wire sealed in soft glass to give a planar surface. Because platinum is subject to poisoning and oxide-film formation, frequent reconditioning of the platinum surface was necessary. This was best accomplished by dipping the platinum electrode into a solution of aqua regia. After this treatment, the electrodes were extensively rinsed and then pre-cathodized electrolytically to remove any platinum salts or freshly formed oxide film. After an electrode was pre-reduced it could be surfaced with platinum oxide by anodizing it in a sulfuric acid solution briefly. Such pre-oxidation was usually accomplished by applying 1½–3 V in a 1 *F* sulfuric acid solution. Pre-cathodization could either be accomplished just short of the evolution of hydrogen (which was normally desirable), or more severely, in which case hydrogen was evolved at the electrode surface. The latter treatment normally would cause a high degree of hydrogen adsorption.

Gold electrodes were prepared by sealing gold wire in a glass tube with deKotinsky cement. The boron carbide electrodes were prepared as described by MUELLER AND ADAMS[10]. The boron carbide was obtained from the Norton Company.

The pH of the solutions was measured using a Leeds and Northrup line operated pH meter, equipped with high-range glass electrodes. All measurements were made in a thermostated bath at 25.0 ± 0.1°.

Reagents

The supporting electrolyte and buffer solutions were prepared from reagent grade chemicals. The buffer solutions were from the Britton–Robinson series involving acetate, phosphate and borate with potassium sulfate added to maintain constant ionic strength. The hydrogen gas, purified grade, was obtained from the Liquid Carbonic Division of General Dynamics Corporation and was further purified by passing it over heated copper turnings at 475°.

RESULTS

The study of the oxidation of dissolved hydrogen has resulted in several general observations. First, hydrogen is not oxidized under any conditions at gold or boron carbide electrodes; the inability to oxidize hydrogen at gold electrodes has been observed previously[11]. In the case of platinum electrodes, anion adsorption tends to deactivate the electrode, which has been a problem in terms of finding effective buffers for the study of dissolved hydrogen. Phosphate ion, in part, shows some of this effect, but less so than other anions that are commonly encountered in buffer solutions. As has been observed by others[4,12], hydrogen gas reacts with platinum oxide in solution to form water and reduced platinum. This has been observed in a number of different ways and found to be a rather rapid reaction, particularly with a freshly oxidized platinum surface and under acidic conditions.

Voltammetry

A number of voltammetric studies have been made of dissolved hydrogen on a platinum surface. Figure 1 presents some experimental curves for 0.1 *F* potassium sulfate solutions. Curve A is for a platinum electrode, which has been allowed to stand for 1½ h in a solution saturated with hydrogen. The massive peak at 0.0 V undoubtedly is due to absorbed hydrogen, as discussed by FRANKLIN AND COOKE[4].

More recently, PRESBREY AND SCHULDINER have also substantiated the presence of absorbed hydrogen[13]. The two lesser peaks of Curve A at approximately −0.2 V result from adsorbed hydrogen on the surface[4]. If the scan of Curve A is stopped as

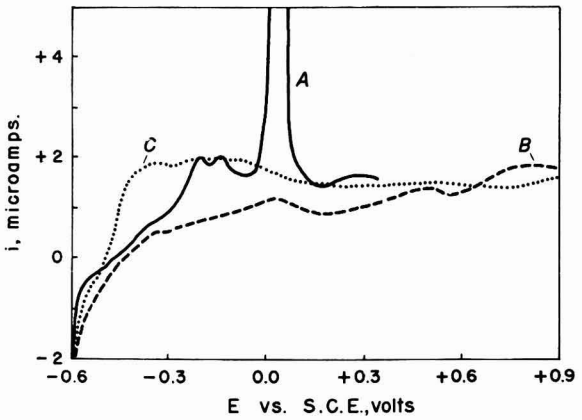

Fig. 1. Voltammetric oxidation of dissolved hydrogen in 0.1 *F* potassium sulfate. Curve A is for dissolved hydrogen at one atm; the electrode was aged for 1½ h in a hydrogen saturated solution. Curve B is a repeat of the scan represented by Curve A. Curve C is a repeat of the scan represented by Curve B.

indicated and a re-scan is initiated, Curve B results, with the two lesser peaks no longer present. The absorbed hydrogen of Curve A is again indicated, although to a much lesser extent, due to the slow rate of diffusion of hydrogen from the interior of the platinum surface, and its inability to reabsorb hydrogen in the short interval that has lapsed. This time the scan is carried out to 0.9 V and a peak for the production of a platinum oxide is shown. Now, if the scan is repeated, Curve C results with a rather reversible anodic wave for the oxidation of hydrogen. From the curves in Fig. 1 it

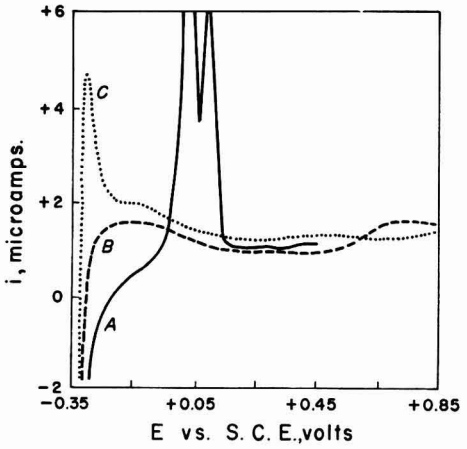

Fig. 2. Voltammetric oxidation of dissolved hydrogen in 0.1 *F* sulfuric acid. Curve A is for the oxidation of hydrogen at one atm pressure after the electrode was aged for 1 h in a hydrogen saturated solution. Curve B is a repeat of the scan represented by Curve A. Curve C is a repeat of the scan represented by Curve B.

would appear that the reversible oxidation of dissolved hydrogen requires an initial formation of platinum oxide.

By changing the supporting electrolyte to 0.1 F sulfuric acid, a series of anodic waves are observed for hydrogen under various conditions. Curve A in Fig. 2 represents a platinum electrode which has been aged for 1 h in a solution saturated with hydrogen. Again, a massive maxima due to absorbed hydrogen is observed at approximately 0.0 V; the double peak is not always observed and it may not be significant. A repeat of this sweep gives Curve B, which represents a much more reversible condition. Again a hump at approximately 0.6 V appears, due to the formation of a platinum oxide. After this sweep, a repeat scan gives Curve C with a much larger maxima, which is apparently due to adsorbed hydrogen on the surface. This wave is more reversible than the wave observed for Curve B and again emphasizes the importance of forming platinum oxide on the surface of the electrode.

Chronopotentiometry

In addition to the voltammetric studies, a series of chronopotentiometric oxidations of dissolved hydrogen have been carried out to demonstrate more fully the effect of

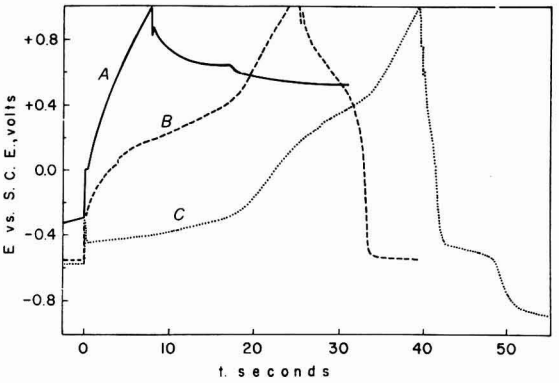

Fig. 3. Chronopotentiograms for dissolved hydrogen in 0.1 F potassium sulfate. Current is 300 μA. Curve A is for a solution saturated with nitrogen. The discontinuity at 9 sec represents the point where the current was stopped. Curve B is for an unconditioned platinum electrode in a solution saturated with one atm of hydrogen. Before the chronopotentiogram was started, the electrode was aged for 5 min in hydrogen. The current was stopped at approximately 28 sec. Curve C is a chronopotentiogram for a pre-oxidized platinum electrode in a solution saturated with hydrogen; at 40 sec the current was reversed.

electrode conditioning. Figure 3 shows the chronopotentiograms that result for a solution containing 0.1 F potassium sulfate. Curve A represents the scan for a solution containing only dissolved nitrogen; the discontinuity at approximately 9 sec indicates the point where the current is stopped. The remainder of the curve indicates that the potential of the working electrode is maintained at a high level, even after the current is stopped. Curve B is for an unconditioned platinum electrode which has been allowed to age for 5 min in a solution saturated with hydrogen. The curve indicates a large overpotential and an irreversible oxidation reaction. Again, the discontinuity in the curve at 25 sec shows where the current is turned off and also indicates the rather

rapid fashion with which the potential of the working electrode goes negative. The transition at approximately 0.6 V for the decay apparently represents the chemical reduction of platinum oxide by hydrogen. Curve C results from a pre-oxidized platinum electrode; under these conditions a much more reversible anodic scan is obtained, although the transition time is approximately the same for Curves B and C. On Curve C a second transition appears to occur at approximately 0.3 V. This potential is in the region where platinum might be expected to be oxidized to platinum oxide, although the length of time far exceeds that which is observed for solely oxidizing the platinum surface (Curve A). In this particular scan, the discontinuity at approximately 38 sec represents a reversed scan, in which the transition between 40 and 50 sec is due to the hydrogen ions resulting from the oxidation reaction. The amount of platinum oxide reduced is almost insignificant, although it is barely perceptible in the vicinity of 41 sec.

An additional series of chronopotentiometric studies has been carried out in 1 *F* sodium hydroxide. The results of these are shown in Fig. 4, where Curve A represents

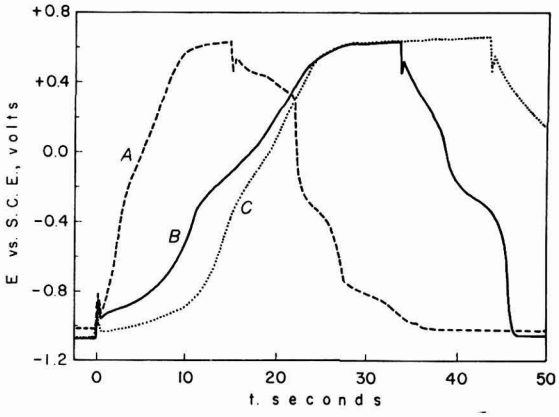

Fig. 4. Chronopotentiograms for dissolved hydrogen at a platinum electrode in 1 *F* sodium hydroxide. Current is 300 μA. Curve A is for a solution which has been degassed with nitrogen; the current was discontinued at 12 sec, and at 20 sec hydrogen was introduced into the solution. Curve B is for a solution saturated with one atm of hydrogen and is for an unconditioned platinum electrode. The current was stopped at approximately 35 sec. Curve C is for a hydrogen saturated solution using a pre-oxidized platinum electrode.

the anodic scan for a solution saturated with nitrogen gas. The slight transition at 0.0 V is probably due to the formation of platinum oxide. The discontinuity at 12 sec represents the point where the current is turned off; again the potential remains positive until almost 20 sec. At that point, hydrogen gas is introduced into the cell and a rapid negative shift in the working electrode potential is observed. A transition occurs at about −0.3 V which appears to be due to the reduction of platinum oxide by the dissolved hydrogen. Curve B represents the anodic scan which results with an unconditioned platinum electrode in the presence of one atmosphere of dissolved hydrogen. A large overpotential is observed, together with a rather irreversible chronopotentiogram. There appears to be a second transition in the vicinity of the potential where platinum oxide is formed. The discontinuity at 33 sec represents the point where the current is turned off. Again, the reduction of the platinum oxide by

the dissolved hydrogen is apparent. Curve C of this figure represents a pre-oxidized platinum electrode used for the oxidation of dissolved hydrogen. A much more reversible wave is observed with a two-step oxidation. The first one undoubtedly represents an almost reversible oxidation of dissolved hydrogen, while the second step in the vicinity of the potential for the oxidation of platinum probably is due to an alternative mechanism. The high degree of activation that results from pre-oxidizing the platinum electrode is demonstrated by the differences between Curves B and C in this figure, as well as in Fig. 3.

To demonstrate further the effect of electrode pre-conditioning a series of chronopotentiometric studies has also been carried out in the presence of 1 *F* sulfuric acid (Fig. 5). Curve A again represents an anodic scan for a solution saturated with nitrogen. At approximately 0.5 V a slight inflection is noted, which probably represents formation of platinum oxide; the current is discontinued at 9 sec. The potential

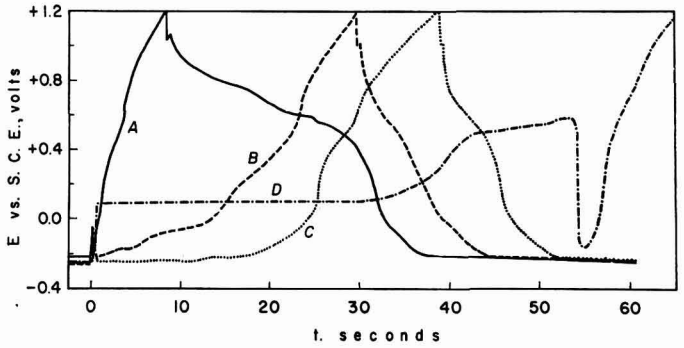

Fig. 5. Chronopotentiograms for dissolved hydrogen in 1 *F* sulfuric acid. The current was 300 μA. Curve A is for a solution saturated with nitrogen. The current was discontinued at 9 sec and hydrogen was introduced at 24 sec. Curve B is for a hydrogen-saturated solution at an unconditioned platinum electrode. The current was discontinued at 30 sec. Curve C is for a pre-oxidized platinum electrode and a hydrogen-saturated solution. The current was discontinued at approximately 40 sec. Curve D is for a platinum electrode which has been aged for $6\frac{1}{2}$ h in a hydrogen-saturated solution.

remains quite positive until hydrogen is introduced at approximately 24 sec, after which the potential goes negative rather rapidly. There is a brief period during which the potential remains high before it becomes negative, and probably is due to the reduction of platinum oxide by the hydrogen. Curve B is the anodic scan for an unconditioned platinum electrode in the presence of dissolved hydrogen. The wave is quite irreversible, with several ill-defined transitions. The first probably is due to the direct oxidation of hydrogen gas, while the others appear to occur in the vicinity of the potential where platinum is oxidized to platinum oxide. The discontinuity at 30 sec is brought about by stopping the current; a transition for the decay is noted in the vicinity of the potential for platinum oxide reduction. Curve C of Fig. 5 results when a pre-oxidized platinum electrode is used for the oxidation of hydrogen. The oxidation is essentially reversible, with a second small inflection in the vicinity of the platinum oxide oxidation potential. When the current is discontinued at approximately 40 sec, an inflection is observed at a potential roughly analogous to where platinum oxide is reduced. Again, the importance of pre-oxidizing the platinum electrode for reversible

oxidation of hydrogen is emphasized. This factor is observed for neutral and basic solutions as well as for the acidic solution represented by Fig. 5. If a platinum electrode is allowed to stand in a hydrogen-saturated sulfuric acid solution for $6\frac{1}{2}$ h, an anodic scan gives Curve D (Fig. 5). The overpotential has increased by almost 0.3 V as a result of aging the electrode in hydrogen. Also, the transition time has increased by almost a factor of two over Curve C, which represented a reversible oxidation of dissolved hydrogen. After 40 sec the potential of the electrode rises to approximately the potential where platinum oxide is formed, where it remains until approximately 54 sec. Then the potential rapidly drops almost to the reversible potential, before it finally rises to the oxidation potential of the solvent.

In an effort to understand the oscillatory behavior of an electrode aged in hydrogen better, a series of additional studies using lower current densities has been undertaken. Curve A of Fig. 6 represents a platinum electrode which has been aged for 3 h in a

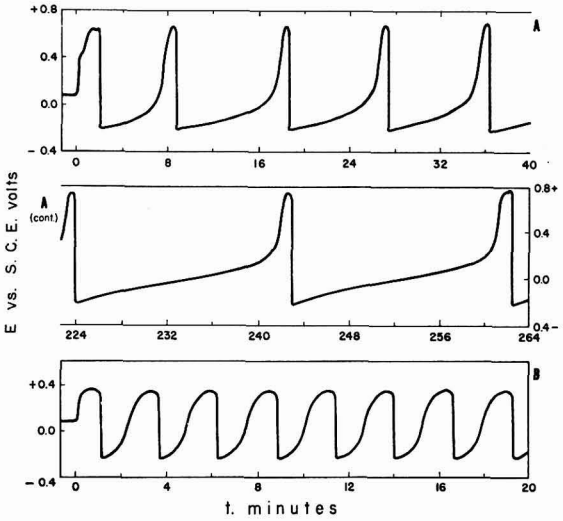

Fig. 6. The oscillographic behavior of a platinum electrode under constant current conditions. Curve A is for the oxidation of dissolved hydrogen in 1 F sulfuric acid. The electrode was aged for 3 h in a hydrogen-saturated solution. Current density was 50 μA. Curve B is for the oxidation of dissolved hydrogen in 1 F hydrochloric acid. Current density was 20 μA.

hydrogen-saturated solution of 1 F sulfuric acid. The curve shows an initial transition to a potential approximating to the oxidation potential for platinum to platinum oxide and then sweeps down to a potential of approximately -0.2 V, which is essentially the potential for a reversible hydrogen electrode. The potential remains at this level for a short period of time before it again rises to that for the oxidation of the platinum electrode. This behavior repeats itself, as indicated by many cycles, although the length of each cycle increases with time. Also, the potential of the high portion of these oscillations becomes more positive as the length of the study increases. This phenomenon, which has been observed a number of times, has also been reported by ARMSTRONG AND BUTLER[3]. Curve B of Fig. 6 represents a similar set of oscillations for a supporting electrolyte composed of 1 F hydrochloric acid. The positive side of these oscillations occurs at a less positive potential than in the case of sulfuric acid.

This potential is essentially that which is observed for the oxidation of platinum metal in hydrochloric acid, and probably represents the point where platinum chloride is formed[14]. Again the potential falls to a point approximately equal to the reversible potential of a hydrogen electrode. For these conditions the period of the oscillations does not increase in time and the oscillations continue indefinitely. Furthermore, stirring of the solution has no effect on the oscillations shown by Curve A or Curve B of Fig. 6.

Figure 7 summarizes the potentiometric data for the oxidation of hydrogen as a function of the pH for the supporting electrolyte solution. The potentials for the solid

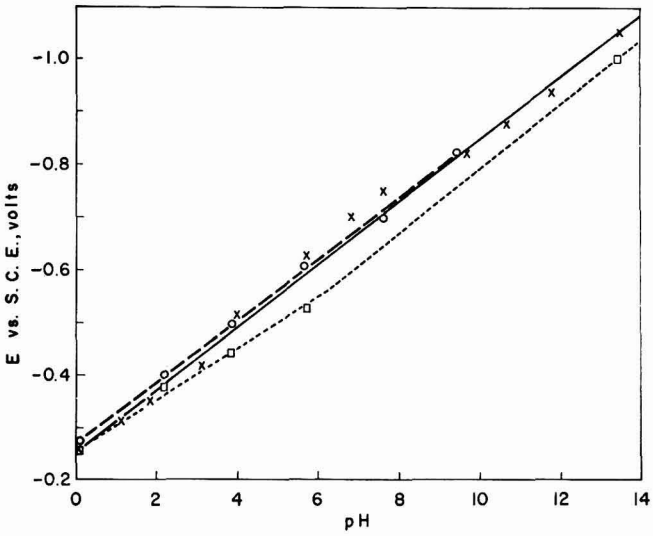

Fig. 7. The effect of pH upon the oxidation potential for dissolved hydrogen. ×, potential at zero current for voltammetric scans using a pre-oxidized electrode. O, rest potential for a pre-oxidized platinum electrode in a chronopotentiometric scan. □, quarter wave-potential for a pre-oxidized platinum electrode used in the oxidation of dissolved hydrogen chronopotentiometrically. All solutions were buffered and a current of 300 μA was used for the chronopotentiometric data.

curve have been measured at the point where the current is zero for the current voltage scan, using a pre-oxidized electrode. As is seen in Figs. 1 and 2, pre-oxidized electrodes are essentially reversible and go through zero current in the vicinity of the middle of the total wave. The slope for this curve is −0.060 V per pH unit. The long dashed line is for the rest potential for a pre-oxidized electrode, and is obtained from the chronopotentiometric studies. This again should coincide with the reversible potential for the hydrogen electrode; this curve also has a slope of −0.060 V per pH unit. The short dashed line represents the quarter-wave potential for the chronopotentiograms as a function of pH using a pre-oxidized platinum electrode. The slope for this curve is −0.043 V per pH unit, and indicates that the system is less reversible than is observed for the zero current curves. Thus, the system is not totally reversible. The deviation of the points from the other curves is greater in the vicinity of pH 7 than at more acidic or basic pH's, and emphasizes the effect of pH upon the reversibility. The system

appears to be most reversible in acidic solutions, then next most reversible in basic solutions, and least reversible in neutral solutions. This can be seen from Figs. 3, 4, and 5 which represent neutral, basic, and acidic solutions, respectively.

For those studies of the oxidation of hydrogen where the electrode has been pre-oxidized, $i\tau^{\frac{1}{2}}$ is independent of i. This behavior indicates that adsorption of hydrogen is not a kinetically limiting factor in the electrochemical oxidation of this gas. The data also clearly indicate that pre-oxidation of the platinum electrode activates it for the subsequent oxidation of dissolved hydrogen. If this activation is destroyed by continued exposure of the electrode to dissolved hydrogen, deactivation manifests itself by a much higher overpotential and an entirely different electrochemical reaction. The importance of the pre-oxidation of the platinum surface is also emphasized by the fact that neither gold nor boron carbide gives oxidation waves for dissolved hydrogen. In other words, platinum (and possibly other platinum metals) appears to be somewhat unique in its behavior for the oxidation of hydrogen.

DISCUSSION AND CONCLUSIONS

The preceding results indicate that the oxidation of hydrogen can occur by several routes. The two small maxima shown by Curve A in Fig. 1 are evidence for adsorbed hydrogen on the platinum electrode surface; FRANKLIN AND COOKE have given additional evidence for adsorbed hydrogen at platinized platinum[4]. The adsorbed hydrogen apparently is formed by pre-cathodizing of the electrode to the point of evolution of hydrogen. There is no evidence for adsorbed hydrogen in the chronopotentiometric studies. Thus it can be concluded that the oxidation of hydrogen by an adsorption process is of minor importance in terms of the total quantity of hydrogen that is normally oxidized under electrolytic conditions.

A second mechanism for the oxidation of dissolved hydrogen, and one of considerably more importance, involves the absorption of hydrogen by platinum. This occurs when platinum is exposed for a considerable period of time to dissolved hydrogen in solution and is best represented by Curve A of Fig. 1 and Curve A of Fig. 2. In both cases, a large quantity of hydrogen has been absorbed by the platinum surface. The potential of this particular electrode oxidation is independent of pH. Another clear example of this type of behavior is shown on the chronopotentiogram represented by Curve D of Fig. 5. In this particular figure an exceedingly long transition time relative to normal hydrogen oxidation is observed. This apparently is due to the rather extensive quantity of hydrogen absorbed by the platinum surface which diffuses outward to the surface, to be oxidized under electrolytic conditions.

The third and most important mechanism for the oxidation of dissolved hydrogen involves the pre-oxidation of the platinum electrode. This pre-oxidation apparently forms platinum oxide, which is subsequently reduced by the dissolved hydrogen in the solution. This reduction produces an activated surface which in all probability is platinized platinum. This particular platinized surface is of limited life; continued exposure to dissolved hydrogen apparently destroys the activated surface by recrystallization or poisoning. With a pre-oxidized electrode an almost reversible oxidation reaction for hydrogen occurs. In the voltammetric studies this is seen as Curve C in Figs. 1 and 2; these two systems indicate an essentially reversible reaction with the current going through zero from an anodic to a cathodic reaction. The chronopotentiometric studies also indicate an almost reversible reaction when the electrode

has been pre-oxidized. This is seen by Curve C in Figs. 3, 4, and 5. In all of these systems, the pre-oxidized platinum electrode gives a much more reversible reaction with a much lower overpotential than under other types of pre-conditioning. The quite negative potential for the oxidation reaction of hydrogen under these conditions, however, precludes the existence of any platinum oxide. A somewhat similar activated surface can be obtained by plating the electrode briefly at low current density in a chloroplatinate solution; this surface also is of limited life.

A fourth and important mechanism for the oxidation of hydrogen occurs at a more positive potential than the reversible reaction. The potential for this particular reaction occurs in all cases in the vicinity of the potential for the oxidation of the platinum surface. As seen in Fig. 3, the amount of current that is necessary to pre-oxidize the surface is represented by Curve A and is indeed negligible, relatively speaking. At the 30-sec point on Curve C in Fig. 3, however, there is a rather long step in the vicinity of this potential. To a lesser extent this is also seen in Curve C of Figs. 4 and 5. This phenomenon is somewhat analogous to the mechanism proposed for the reduction of dissolved oxygen, where platinum oxide plays an active role in the electrode reaction[6].

These four mechanisms are represented more clearly by the following equations

$$H_2 \xrightarrow{Pt} 2\,H\,(Pt) \longrightarrow 2\,H^+ + 2\,e^- \tag{1}$$

$$H_2 + Pt \longrightarrow Pt(H_2) \longrightarrow Pt + 2\,H^+ + 2\,e^- \tag{2}$$

$$Pt + H_2O \longrightarrow PtO + 2\,H^+ + 2\,e^- \tag{3a}$$

$$PtO + H_2 \longrightarrow Pt^* + H_2O \tag{3b}$$

$$H_2 \xrightarrow{Pt^*} 2\,H^+ + 2\,e^- \tag{3c}$$

$$Pt + n\,H_2O \longrightarrow PtO_n + 2n\,H^+ + 2n\,e^- \tag{4a}$$

$$PtO_n + H_2 \longrightarrow PtO_{n-1} + H_2O \tag{4b}$$

Equations (1) and (2) represent the oxidation of adsorbed hydrogen on the platinum surface and the oxidation of absorbed hydrogen, respectively. The reversible oxidation at an activated platinum surface, Pt*, of molecular hydrogen to hydrogen ion is represented by equations (3a), (3b), and (3c), where equation (3c) is the actual reversible step. A cyclic mechanism is indicated by equations (4a) and (4b), involving the formation of platinum oxide and its subsequent reduction by dissolved hydrogen to a lower oxidation state, or to the metal itself. This mechanism cyclicly repeats itself, and is observed on the chronopotentiograms in the vicinity of the potential for platinum oxide formation.

The oscillations shown in Fig. 6 appear to be a combination of the proposed mechanisms. Apparently the electrode attains a potential where the reactions represented by equations (4a) and (4b) occur. As platinum oxide is built up on the electrode surface and is subsequently reduced by the dissolved hydrogen, an activated platinized surface is produced. When this occurs, the potential becomes much more negative for the oxidation reaction and the reversible process represented by equation (3c)

occurs. As continued exposure to hydrogen takes place, the electrode becomes deactivated by recrystallization or some other phenomenon, and the potential again becomes positive, where equations (4a) and (4b) again represent the controlling process. This phenomenom repeats itself again and again*.

The conclusions reached here are in general conformity with much of the work of other workers[1-4]. However, an overall consideration of the multitude of mechanisms that occur at the electrode when hydrogen is oxidized has not been made previously. Similarly, the oscillations shown in Fig. 6 have also been observed and discussed by BUTLER AND ARMSTRONG[3]. In their discussion they note that the platinum surface was activated, but do not indicate a mechanism for the activation. A number of workers have also indicated that adsorbed hydrogen plays a role in the oxidation of hydrogen[1,4]. However, our work indicates that this particular mode of oxidation is of minor importance and only occurs to an observable extent when the electrode is pre-cathodized to the point of production of hydrogen.

Absorbed hydrogen, also noted by FRANKLIN AND COOKE[4], appears to occur only when the electrode is exposed, for a relatively long period of time, to dissolved hydrogen. This is a phenomenon which is not observed if the electrode is pre-oxidized, for two reasons. First, the hydrogen that is at the surface is oxidized at the same time that the electrode is; and second, the production of platinum oxide ensures that any additional absorbed hydrogen will be oxidized chemically when it reaches the surface rather than electrolytically.

Although BUTLER AND ARMSTRONG[2] indicated that a more reversible reaction is obtained by activating the electrode, the conclusion as to how this might take place was left unanswered. We believe that our data support the general conclusion that a platinized surface is formed best by pre-oxidizing the electrode and then having it re-reduced by the dissolved hydrogen itself. This has, of course, been a common practice by organic chemists who want an active catalytic surface of platinum. By adding Adams catalyst, PtO_2, to the solution and then introducing hydrogen, a finely divided, highly activated platinum surface is obtained. Apparently, this also is an effective means of activating the platinum electrode for hydrogen oxidation. Such platinized surfaces are easily poisoned (even by dissolved hydrogen) and must be used shortly after formation.

Additional studies are currently in progress to determine the kinetic parameters for the several proposed mechanisms for the oxidation of hydrogen at platinum surfaces.

SUMMARY

Voltammetric and chronopotentiomatic studies have been made to determine the effect of supporting electrolyte, pH, and electrode pre-conditioning upon the oxidation of dissolved hydrogen at platinum electrodes. The results of these investigations lead to the conclusion that hydrogen can be electrolytically oxidized by four different mechanisms; (a) atomic hydrogen adsorbed on the platinum surface (observed with pre-cathodized electrodes), (b) absorbed hydrogen in the platinum electrode (observed after the electrode is exposed for long periods of time to dissolved hydrogen), (c)

* While this paper was in press the research of A. J. KOLK, JR. came to our attention. His masters' thesis "Periodic Phenomena at Platinum Electrodes", was presented at the Case Institute of Technology in 1953. The observations and mechanisms proposed here for the oscillations are in general agreement with those in KOLK's thesis.

molecular hydrogen at an activated platinum electrode (accomplished by first forming platinum oxide electrolytically, which subsequently is reduced by hydrogen to give the activated surface), and (d) cyclic reaction of molecular hydrogen with platinum oxide and the electrolytic re-formation of the platinum oxide (observed with unconditioned electrodes). The third mechanism is the most important, as well as the most reversible, reaction. Only the second mechanism is independent of pH. In acidic solutions a platinum electrode, which has been aged in dissolved hydrogen, exhibits an oscillating potential for the electrolytic oxidation of hydrogen. This behavior appears to be due to a combination of mechanisms (c) and (d). Hydrogen is not oxidized under similar conditions at gold or boron carbide electrodes, which supports the conclusion that platinum is a somewhat unique electrode for the electrolytic oxidation of hydrogen.

ACKNOWLEDGEMENT

This work was supported by the United States Air Force, Geophysics Research Directorate, Air Force Cambridge Research Laboratories, under contract No. AF 19(604)-8347.

REFERENCES

1 L. P. HAMMETT, *J. Am. Chem. Soc.*, 46 (1924) 7;
H. T. BEANS AND L. P. HAMMETT, *ibid.*, 47 (1925) 1215;
L. P. HAMMETT AND A. E. LORCH, *ibid.*, 55 (1933) 70;
L. P. HAMMETT, *Trans. Faraday Soc.*, 29 (1933) 770.
2 J. A. V. BUTLER AND G. ARMSTRONG, *J. Chem. Soc.*, (1934) 734.
3 G. ARMSTRONG AND J. A. V. BUTLER, *Discussions Faraday Soc.*, 1 (1947) 122.
4 T. C. FRANKLIN AND S. L. COOKE, JR., *J. Electrochem. Soc.*, 107 (1960) 556.
5 S. SHIBATA, *Bull. Chem. Soc. Japan*, 33 (1960) 1635.
6 D. T. SAWYER AND L. V. INTERRANTE, *J. Electroanal. Chem.*, 2 (1961) 310.
7 D. D. DEFORD, Private Communication, presented at the *133rd American Chemical Society Meeting, San Francisco, Calif., April, 1958.*
8 R. L. PECSOK AND R. S. JUVET, JR., *Anal. Chem.*, 27 (1955) 165.
9 R. G. BATES, *Electrometric pH Determinations*, John Wiley and Sons, Inc., New York, N.Y., 1954, p. 166.
10 T. R. MUELLER AND R. N. ADAMS, *Anal. Chim. Acta.*, 23 (1960) 467.
11 K. I. ROSENTAL AND V. I. VESELOVSKII, *Zh. Fiz. Khim.*, 31 (1957) 1555; *C.A.*, 52 (1958) 6060.
12 M. J. N. POURBAIX, J. VAN MUYLDER AND N. DE ZOUBOV, *Platinum Metals Rev.*, 3 (1959) 47.
13 C. H. PRESBREY, JR. AND S. SCHULDINER, *J. Electrochem. Soc.*, 108 (1961) 986.
14 J. LLOPIS AND A. SANCHEZ, *ibid.*, 720.

DETERMINATION OF SILVER IONS IN SOLUTION WITH A GLASS ELECTRODE*

ALLAN L. BUDD

Beckman Instruments, Inc., Fullerton, Calif. (U.S.A.)

(Received April 26th, 1962)

INTRODUCTION

Since the discovery of the hydrogen ion function at glass membranes by CREMER[1], HABER AND KLEMENSIEWICZ[2] and BORELIUS[3], the glass electrode has been a subject of curiosity. Its application in the measurement of pH is well known. One of the problems encountered with the glass electrode in pH measurements is the sodium error. HOROWITZ[4] and SCHILLER[5] studied the response of glass electrodes to other ions, such as sodium and potassium. LENGYEL AND BLUM[6] studied the relationship between composition of the glass and response and concluded that the oxides of aluminum and boron enhance the sodium function of glass electrodes.

EISENMAN, RUDIN AND CASBY[7] extended the work of LENGYEL AND BLUM and produced sodium aluminum silicate glasses with high alumina content and very satisfactory sodium function. Their 18 *M* per-cent alumina glass was about 250 times more sensitive to sodium than potassium.

LEONARD[8] reported on two glass electrodes; one a sodium aluminum silicate and the other a lithium aluminum silicate. The former was found to be equally responsive to sodium and potassium, while the latter showed a 1000 to 1 selectivity for sodium over potassium.

None of the above workers was able to find a glass which was specific for any metal ion over hydrogen. As a result, it was found necessary to raise the pH of a solution if the cation function of the glass electrode was to be observed.

EXPERIMENTAL

Electrodes used in this study were commercially available glass electrodes (Beckman Electrode No. 39278 of lithium aluminum silicate composition and No. 39137 of sodium aluminum silicate composition).

A pH meter with a full scale sensitivity of 1400, 700, 200, or 100 mV (Beckman No. 76000) was used for all cation measurements. All pH measurements were made with a type E-2 glass electrode to minimize cation error.

Analytical reagent grade chemicals were used in all cases.

RESULTS

The electrodes were tested for their response to a large number of cations and the

* A Paper Presented at the 13th Pittsburgh Conference on Analytical Chemistry and Applied Spectroscopy, March, 1962.

results are given in Table I. In all cases where response was observed, it was approximately 55 mV per decade change in concentration. No response was observed for multivalent ions.

TABLE I

RESPONSE OF THE TWO GLASS ELECTRODES TO VARIOUS IONS

Ion	*No. 39137*	*No. 39278*
H^+	+	+
Na^+	+	+
K^+	+	−
Li^+	+	−
Ca^{2+}	−	−
Mg^{2+}	−	−
Ba^{2+}	−	−
Cu^+	−	−
Tl^+	−	−
Ag^+	+	+
NH_4^+	+	−

+ Responds
− Does not respond

The new and interesting observation is the response to silver ions and further experiments were performed to determine how sensitive these electrodes are for silver.

Electrode No. 39137 showed no great selectivity for any of the ions except hydrogen. The silver ion was favored over other monovalent metal cations. The electrode was about 1000 times more sensitive to hydrogen ion and 25 times more sensitive to silver than to other ions. The order of sensitivity for various ions was $H^+ \gg Ag^+ > K^+, NH_4^+ > Na^+ > Li^+$.

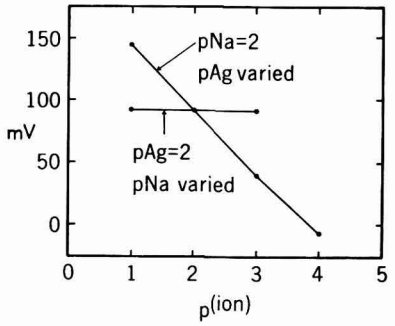

Fig. 1. Response of electrode 39278 to (Ag^+) relative to (Na^+).

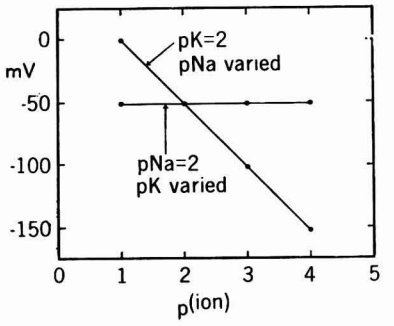

Fig. 2. Response of electrode 39278 to (Na^+) relative to (K^+).

Electrode No. 39278 had some very interesting selectivity properties. In Fig. 1, potentials are given for mixtures of silver and sodium ions as one is varied relative to the other. It can be seen that even a 1000-fold excess of sodium over silver has very little effect on the response of the electrode to silver. Similar data for mixtures of sodium and potassium ions are given in Fig. 2 and reveal that potassium has no measur-

able effect on the sodium measurement. Likewise, potassium has no effect on the silver measurement (Fig. 3).

Apparently, the lithium aluminum silicate electrode is more sensitive to silver ions than to hydrogen ions. It can be seen in Fig. 4 that the hydrogen ion seems to have much less effect on the silver response than silver has on the hydrogen response. The indicated change in response, for a given silver concentration with changing pH, is shown in Fig. 5. When the pH is one unit below pAg there is apparently no hydrogen ion error.

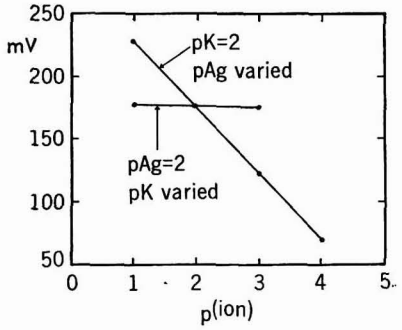

Fig. 3. Response of electrode 39278 to (Ag^+) relative to (K^+).

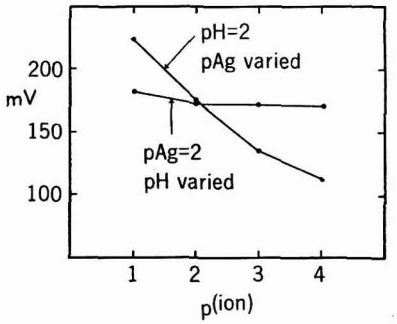

Fig. 4. Response of electrode 39278 to (Ag^+) relative to (H^+).

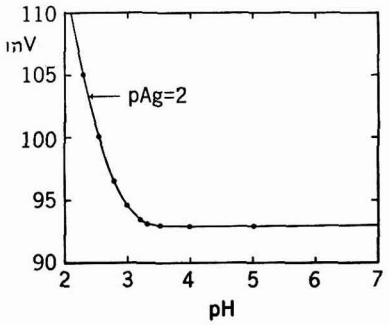

Fig. 5. Response of electrode 39278 to (Ag^+) with changing pH.

DISCUSSION

The mechanism of the glass electrode process is complex and, as yet, not fully understood. It may be assumed that the following factors influence the response for a given ion:

(1) the size of the ion relative to the size of the "electron rich holes" in the glass membrane.

(2) Lewis acidity of the ion.

(3) polarizability of the ion.

(4) energy of electron transfer (proportional to the E_0 of the ion–metal equilibrium).

(5) relative population of the ions, *i.e.* concentration.

The degree to which the electrode responds to one ion in the presence of another is probably based upon ability of the ion to compete for the active sites on the electrode surface.

In the case of pH glass electrodes, the size of the "holes" in the glass membrane is such that only hydrogen ions can fit. As a result, these electrodes respond to other ions only at high pH values. This response for sodium, often called sodium error, is then due primarily to sodium ions occupying active sites. A 10^8–10^{10}-fold excess of sodium ions is required, however, to compete with the hydrogen ion.

If the active sites, or the "holes", are made larger, then other ions can more easily occupy the sites. This appears to be the case with electrodes with increased cation functions.

If the above considerations are true, it is logical that an electrode which responds to sodium and/or potassium should also respond to silver and, in fact, probably be more responsive to silver than the other two. Conductance data[9] show that the size of the silver ion is in the same range as sodium and potassium. The available sites for covalent bonding make silver a better Lewis acid than sodium or potassium; silver is more polarizable than either sodium or potassium and has an E_0 of -0.7991 *vs.*N.H.E., whereas sodium and potassium are high on the positive side[10]. All these factors tend to favor silver over sodium and potassium. The most important factor is the nature of the glass surface. Ionic properties such as size, Lewis acidity, and polarizability, will have greater or lesser effect, depending on the nature of the glass. The data presented here certainly support the theoretical inference that silver ion will be favored over sodium and potassium.

CONCLUSIONS

The most important fact to arise out of this study is the observation that a glass electrode can respond in a Nernstian manner to changes in silver concentration in the presence of all other ions. Such an electrode has many practical analytical applications in the area of argentometric determinations. The glass electrode is not poisoned by cyanide, sulfide or any other substance except fluoride and concentrated alkali. Figure 6 is a typical titration curve using the 39278 lithium aluminum silicate glass electrode as the sensor.

More work must be done before the mechanism of the response of the glass electrode can be fully explained. The present work suggests that an adsorption and electron transfer type of equilibrium controls the electrode response.

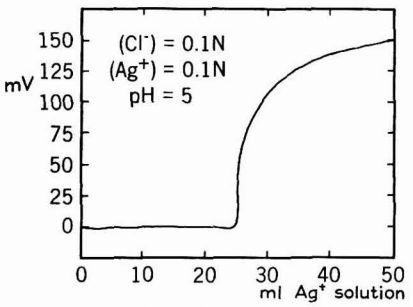

Fig. 6. Typical titration curve.

SUMMARY

Two glass electrodes were found to respond to changes in silver ion concentration. One of the electrodes is somewhat more sensitive to silver than to hydrogen ions, and is highly selective for the silver ion over other cations. A response of 55 mV per decade is observed at 25°. Theoretical implications and applications are discussed.

REFERENCES

1 M. CREMER, *Z. Biol.*, 47 (1906) 562.
2 F. HABER AND Z. KLEMENSIEWICZ, *Z. Physik. Chem.*, 67 (1909) 385.
3 G. BORELIUS, *Ann. Physik.*, 45 [4] (1914) 929.
4 K. HOROWITZ, *Z. Physik.*, 15 (1923) 389.
5 H. SCHILLER, *Ann. Physik.*, 74 [4] (1924) 105.
6 B. LENGYEL AND E. BLUM, *Trans. Faraday Soc.*, 30 (1934) 461.
7 G. EISENMAN, D. O. RUDIN AND J. U. CASBY, *Science*, 126 (1957) 831.
8 J. E. LEONARD, Paper presented at the *Instrument Society of America, 5th Instrumental Methods of Analysis Symposium, May 1959, Houston, Texas*, Beckman Reprint R-6148.
9 H. HARNED AND B. B. OWEN, *Physical Chemistry of Electrolytic Solutions*, 2nd ed., Reinhold, New York, N.Y., 1950, p. 538.
10 W. LATIMER, *The Oxidation States of the Elements and their Potentials in Aqueous Solutions*, 2nd ed., Prentice-Hall, Englewood Cliffs, N.J., 1952, pp. 340–343.

POLAROGRAPHIC AND SPECTROPHOTOMETRIC BEHAVIOUR OF RHODIUM IN PYRIDINE AND γ-PICOLINE SOLUTIONS

FRANCESCO PANTANI

Institute of Analytical Chemistry, University of Florence (Italy)

(Received February 12th, 1962)

INTRODUCTION

Rhodium solutions in the presence of pyridine were investigated polarographically by WILLIS[1]. This author found a step at —0.414 V in 1 *M* pyridine + KCl or KBr, which could indicate the reduction of a Rh^{3+}–hexapyridine complex to Rh^{2+}, because of the similarity of the diffusion coefficient with that of analogous Co^{3+} complexes.

Some data on this argument were also obtained by REPIN[2]. In $\sim$ 3 *M* pyridine + $\sim$ 2 *M* HCl, Rh^{3+} yields a polarographic step, which, however, is well developed only up to 0.4 m*M* Rh^{3+}. In REPIN's opinion, the electrode process could be a reduction from $[Rh(pyrid)_4Cl_2]^+$ to $[Rh(pyrid)_4Cl_2]^\circ$.

No further information on the behaviour of such solutions is found in the available literature. Moreover, the above mentioned 1-electron reductions should involve the formation of the +2 oxidation state, which has, hitherto, hardly been investigated.

Further data are reported here on rhodium–pyridine solutions, in order to clarify the mechanism of the electrode process. The behaviour of the solutions in the presence of γ-picoline was also investigated for analytical applications in a wider range of rhodium concentrations than those considered by REPIN.

APPARATUS AND REAGENTS

A Sargent Model XV recording polarograph and a Beckman DU spectrophotometer were used. Standard 0.02 *M* Rh^{3+} solutions were made from $Na_3RhCl_6.2H_2O$. Polarographic measurements were generally carried out at 25°, against a saturated calomel electrode.

RESULTS AND DISCUSSION

Preliminary work was carried out in order to confirm REPIN's data[2]: in a supporting electrolyte similar to that used by this author, a cathodic step can be found in the range of —0.4 V *vs.* S.C.E. With a rhodium concentration higher than 0.4 m*M*, however, the step is poorly developed and shows a sharp maximum. The position of the wave along the axis of the applied electric tension depends on the amount of Rh^{3+} present in solution, according to the experimental points shown in Fig. 1.

By using α-picoline instead of pyridine, only very poorly developed steps can be observed. With β-picoline, sufficiently well-defined steps can be obtained, but maxima

are present mainly for high Rh^{3+} concentrations. The best results were obtained in the presence of γ-picoline; for this reason, in the present paper, the data obtained using either pyridine or γ-picoline are reported at the same time.

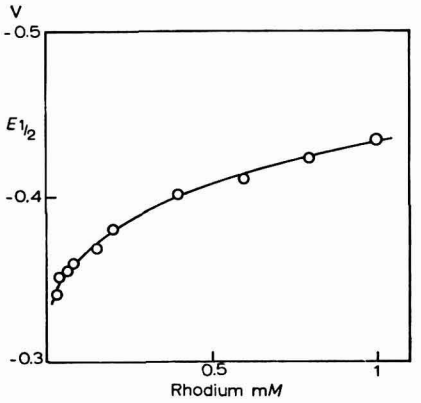

Fig. 1. Variation of $E_{\frac{1}{2}}$ with rhodium concentration in REPIN's supporting electrolyte.

The pink Rh^{3+} chloride solutions, on heating several minutes at 100° in the presence of γ-picoline, turn pale yellow and show a polarographic step in the range —0.4 to —0.5 V *vs.* S.C.E., which is well defined for any rhodium concentration up to 4 m*M*. The limiting current being proportional to the C_{Rh}, a polarographic determination of this element can be performed under better conditions than those used by REPIN. Among the platinum metals, iridium does not yield observable reduction in this medium; therefore, rhodium can also be determined in the presence of iridium, as is shown by the data in Table I. Acidic solutions, however, cannot be used since chloro-complexes are not destroyed by pyridine or γ-picoline in acid media.

TABLE I

POLAROGRAPHIC DETERMINATION OF RHODIUM IN THE PRESENCE OF IRIDIUM, IN 25 ml OF 1 *M* γ-PICOLINE SOLUTIONS

Taken (mg)			*Found (mg)*
Rh^{3+}	Ir^{3+}	Ir^{4+}	*Rh*
2.06	3.86	—	2.11
2.06	7.72	—	1.92
2.06	11.58	—	2.08
4.12	3.86	—	4.12
4.12	7.72	—	4.03
4.12	15.44	—	4.06
6.18	5.79	—	6.31
6.18	9.65	—	6.15
6.18	17.37	—	6.04
2.06	—	5.05	2.04
2.06	—	12.6	2.08
2.06	—	22.6	2.12

The limiting current appears to be proportional to the square root of the mercury column height, (see Table II), in the presence of either pyridine or γ-picoline, showing it to be diffusion-controlled. Identical results are also obtained using solutions pre-

TABLE II

VARIATION OF POLAROGRAPHIC CHARACTERISTICS WITH MERCURY COLUMN HEIGHT, IN SOLUTIONS OF 2 mM Rh^{3+} IN THE PRESENCE OF PYRIDINE (OR γ-PICOLINE) AND KCl

h_{Hg} (mm)	$\sqrt{h_{Hg}}$	Drop time (sec)	Pyridine			γ-Picoline		
			$E_{1/2}$ (V vs. S.C.E.)	i_d (μA)	$i_d/\sqrt{h_{Hg}}$	$E_{1/2}$ (V vs. S.C.E.)	i_d (μA)	$i_d/\sqrt{h_{Hg}}$
71.0	8.43	2.4	—0.420	12.7	1.51	—0.465	11.0	1.31
54.5	7.38	3.0	—0.425	11.3	1.53	—0.475	9.8	1.33
40.5	6.37	4.0	—0.415	10.0	1.56	—0.470	8.4	1.32
31.5	5.61	5.2	—0.435	8.8	1.56	—0.465	7.4	1.32

pared at room temperature, in which no stabilized pyridine or γ-picoline complexes are present; unstabilized solutions will be taken into account later in this paper. The data obtained at increasing temperatures with stabilized solutions are reported in Table III, and show a shift of $E_{\frac{1}{2}}$ to less negative values.

TABLE III

VARIATION OF POLAROGRAPHIC CHARACTERISTICS WITH TEMPERATURE

$t°$	0.4 mM Rh^{3+} in Repin's supporting electrolyte		1 mM Rh^{3+} in 0.1 M KCl + 0.1 M HCl + 0.2 M γ-picoline	
	$E_{1/2}$ (V vs. S.C.E.)	i_d (μA)	$E_{1/2}$ (V vs. S.C.E.)	i_d (μA)
25	—0.402	2.17	—0.470	4.45
35	—0.394	2.72	—0.454	4.98
45	—0.385	3.27	—0.440	5.70
55	—0.378	3.96	—0.427	6.30
average variation per degree	+0.8 mV	2.2%	+1.4 mV	1.2%

In 1 mM Rh^{3+} solutions, in the presence of 0.1, 0.2, 1, and 2 M γ-picoline, the following values of $E_{\frac{1}{2}}$ were found; —0.464, —0.470, —0.500, and —0.522 V. Corresponding i_d values were; 4.55, 4.45, 4.15, and 3.90 μA. Similar variations can also be observed in pyridine solutions.

In order to acquire some information on the electrode process, the polarographic curves and absorption spectra obtained from the same solutions were investigated. Polarograms of Rh^{3+} in the presence of pyridine or γ-picoline are respectively reported in Figs. 2 and 3*, the analogous effect of these two ligands being shown by the

* In the presence of KBr, K_2SO_4 or KNO_3 instead of KCl identical results were obtained.

similar shape of the curves. The usual waves of chloro-complexes are observed in (A), which are similar to those obtained in previous work at this Institute[3]. Very different curves are recorded when a small amount of the ligand is added, (B). The original reduction step is transformed into a peak, which, however, is not eliminated by a

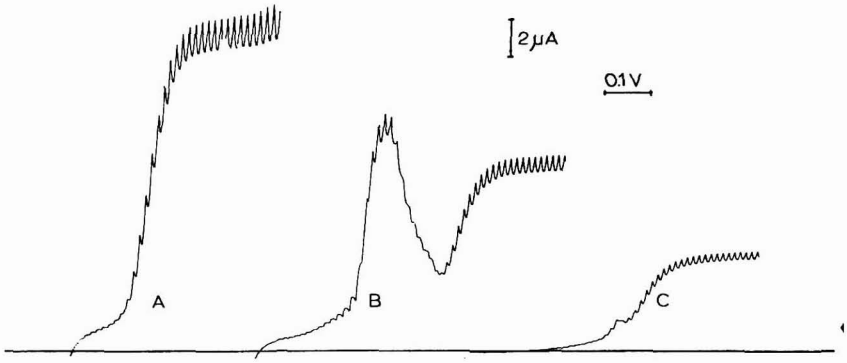

Fig. 2. (A), Polarograms of 2 m*M* Rh^{3+} in 3 *M* KCl + 0.1 *M* HCl; (B), after addition of 0.2 *M* pyridine at room temperature; (C), the same, after heating 10 minutes at 100°.

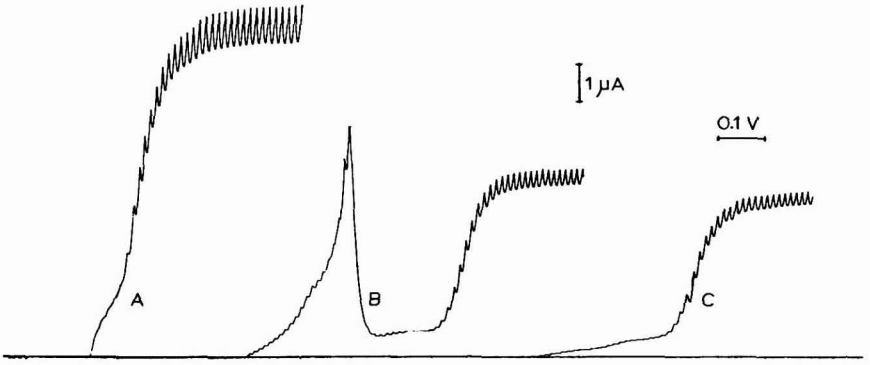

Fig. 3. (A), Polarograms of 1 m*M* Rh^{3+} in 0.1 *M* HCl + 0.1 *M* KCl; (B), after addition of 0.2 *M* γ-picoline at room temperature; (C), the same, after heating 10 minutes at 100°.

maximum suppressor. The current then decreases almost to zero and, finally, a true step appears with a diffusion plateau much lower than that of the starting solution. Despite such different shapes in the polarographic curves, the reducible form in the solution has remained unchanged: this is evident from the absorption spectra in Figs. 4 and 5 (in the presence of pyridine and γ-picoline, respectively); on addition of the ligand to the pink solutions of chloro-complexes at room temperature, practically n change is observed within the few minutes necessary to record a polarogram. A sensible variation becomes evident only after some hours when using γ-picoline, and after a much longer time when using pyridine. Such a difference may be ascribed to the more basic properties of γ-picoline. On the other hand, quite different spectra are

observed on heating the same solutions for some minutes at 100°: the new absorption maximum of the yellow solutions can be ascribed to the presence of Rh–pyridine or Rh–γ-picoline complexes. The polarograms formed under such conditions are reported

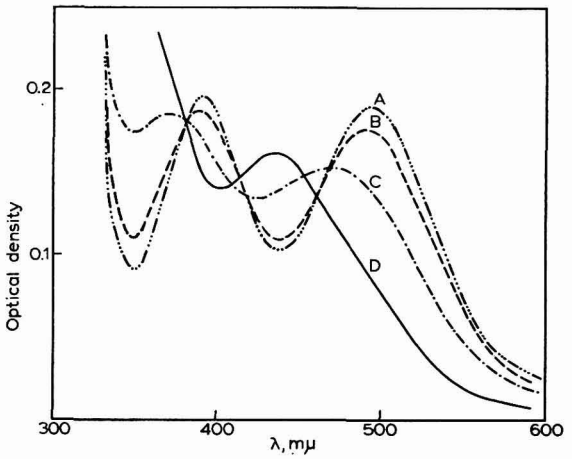

Fig. 4. Spectra of 2 mM Rh^{3+} in 1 M KCl after addition of 0.02 M pyridine at room temperature: (A), after 30 minutes (the same as chloro-complexes); (B), after 5 days; (C), after 3 weeks; (D), after heating 10 minutes at 100°.

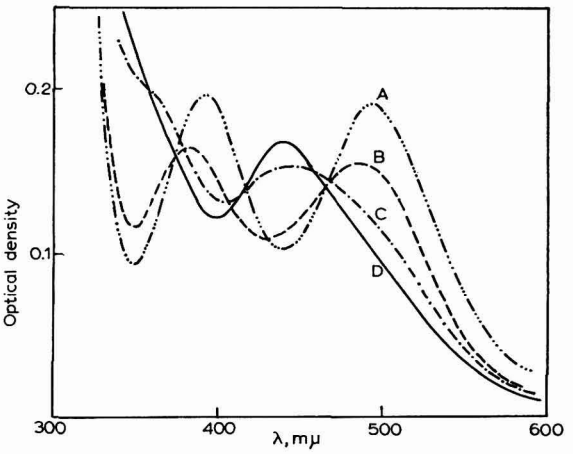

Fig. 5. Spectra of 2 mM Rh^{3+} in 1 M KCl (A), after addition of 0.02 M γ-picoline at room temperature: (B), after 30 minutes; (C), after 1 day; (D), after 5 days (the same as after heating 10 minutes at 100°).

in Figs. 2(C) and 3(C). Besides the absence of the peak, the steps appear to be at the same applied electric tension and have an identical slope, 58–60 mV per logarithmic unit of $i/(i_d - i)$, as the curves (B).

Such unusual behaviour can be explained by taking into account a paper by HEYROVSKÝ and coworkers[4], who observed an absorption film on the dropping electrode in the presence of pyridine, which can hinder some reduction processes. Actually, measurements of electro-capillary curves in the present work (some examples are given in Fig. 6) show the considerable modification of the drop time in

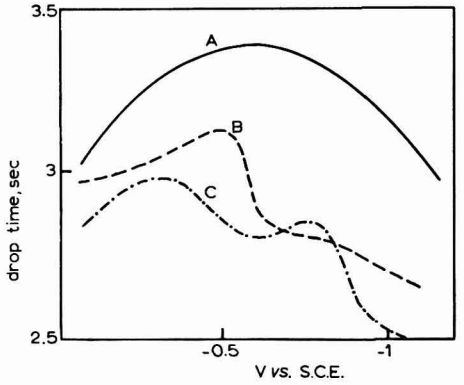

Fig. 6. Electrocapillary curves: (A), 2 mM Rh^{3+} in 0.4 M KCl; (B), the same + 0.1 M pyridine; (C), the same + 0.5 M γ-picoline.

the presence of both pyridine and γ-picoline. Hence, the absorbed film can be assumed to mask the true reduction step of chloro-complexes, which is transformed into a peak: the reduction may take place only at a more negative applied electric tension. The reduction of the complexes with pyridine or γ-picoline is hindered in a similar way: such reduction, however, should take place at a little more negative electric tension than that of chloro-complexes, since not even a peak, indicating the beginning of a reduction, is observed with stabilized solutions. In any case, when pyridine or γ-picoline is present, and the solution contains either chloro-complexes or other reducible forms, the polarographic step does not represent the true reduction at that electric tension; on the contrary, the true reduction, which should take place at a more positive electric tension, is hindered by the absorption of the ligand on the electrode,

TABLE IV

CHARACTERISTICS OF THE ABSORPTION SPECTRA OF 2 mM Rh^{3+} STABILIZED IN THE PRESENCE OF PYRIDINE OR γ-PICOLINE AT DIFFERENT KCl CONCENTRATIONS

KCl (molarity)	*0.15 M pyridine*		*0.15 M γ-picoline*	
	λ_{max} *(mμ)*	ε_{max}	λ_{max} *(mμ)*	ε_{max}
0	414	76	406	98
0.2	424	82	411	91
0.5	428	84	416	88
1	431	86	426	83
2	436	88	—*	—
3	441	88	—	—

* A precipitate is obtained in the presence of γ-picoline at KCl concentrations greater than 1 M.

and may be observed only when such absorption shows a relatively small influence. The considerable modification of the electrode surface is tested also by the difference in the diffusion current of the polarograms (A) and (B); the further decrease in the polarograms (C) can be ascribed (at least partially) to the lower mobility of the pyridine- and γ-picoline-complexes, with respect to the chloro-complexes.

The optical density at the maximum of the absorption spectrum is proportional to the rhodium concentration. In addition, the wavelength and the molar extinction coefficient depend on the salt concentration in the solution, according to the data in Table IV.

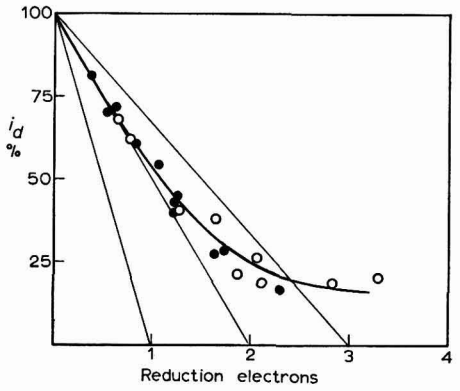

Fig. 7. Coulometric measurements on Rh^{3+}, stabilized in the presence of pyridine (○) or γ-picoline (●).

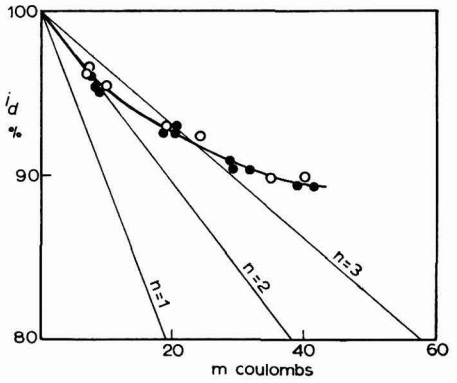

Fig. 8. Current measurements on 1 ml 1 mM Rh^{3+}, stabilized in the presence of pyridine (○) or γ-picoline (●).

Further experimental work was directed towards ascertaining the number of electrons involved in the electrochemical process. When using unstabilized solutions, no useful results were obtained, as could be expected. On the other hand, the data from coulometric measurements with a mercury pool cathode on stabilized solutions are reported in Fig. 7. The decrease of i_d is at first in agreement with a two-electron

process; near the end of the reduction the current efficiency appears to be lower and the curve deviates from the theoretical slope. The same phenomenon is better observed during current measurements (Fig. 8), when using a dropping mercury capillary as the cathode in the electrolysis. On the basis of these data, a two-electron reduction can be assumed to occur, from which the formation of monovalent rhodium could be presumed; such a species, however, appears to be highly unstable and the products of its conversion (which is likely to be by re-oxidation) lead to a higher consumption of

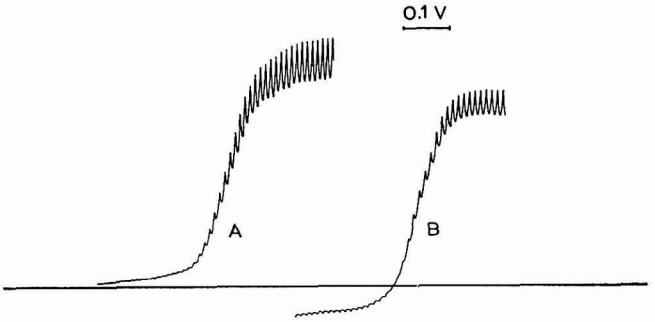

Fig. 9. Polarograms of 1 mM Rh^{3+}, stabilized in the presence of 0.2 M pyridine, (A), at the beginning, and (B), at $\sim 2/3$ reduction, with sensitivities, respectively of 0.15 and 0.06 μA/mm.

current in the electrolysis. The hypothesis of the formation of Rh^+ can be supported, in addition to these coulometric data, by the absence of a metal precipitate during the electrolysis (contrary to halide complexes); moreover, on reduced solutions a cathodic–anodic step can be recorded (Fig. 9), whose anodic current rapidly disappears on ageing. Finally, it must be remembered that many more data are found in the literature on Rh(I) than on Rh(II)[5].

SUMMARY

Well-shaped polarographic steps are obtained with Rh^{3+} in pyridine or γ-picoline solutions, suitable for a quantitative determination of Rh in the presence of Ir. Maxima in the absorption spectrum are found in the range 400–440 mμ, depending on the composition of the solutions. The effect of pyridine and γ-picoline as masking agents for the true polarographic step of Rh is studied. The electrode process appears to be, in both cases, a 2-electron reduction.

REFERENCES

1 J. Willis, *J. Am. Chem. Soc.*, 66 (1944) 1067.
2 S. A. Repin, *J. Appl. Chem. USSR*, 20 (1947) 46, 55.
3 D. Cozzi and F. Pantani, *J. Inorg. Nucl. Chem.*, 8 (1958) 385.
4 J. Heyrovský, F. Sorm and J. Forejt, *Collection Czech. Chem. Commun.*, 12 (1947) 11.
5 L. Malatesta and L. Vallarino, *J. Chem. Soc.*, (1956) 1867; L. Vallarino, *J. Chem. Soc.*, (1957) 2287, 2473.

POLAROGRAPHIE À ONDES CARRÉES

G. GEERINCK*, H. HILDERSON, C. VAN HULLE ET F. VERBEEK

Laboratoire de Chimie Analytique, Université de Gand (Belgique)

(Reçu le 7 avril, 1962)

INTRODUCTION

Le facteur limitant dans l'application de la polarographie conventionelle ou la polarographie alternative à tension sinusoidale superposée pour la détermination de faibles concentrations ($\leq 10^{-5}\ M$) est le courant capacitif associé à la double couche de la goutte de mercure. BARKER ET JENKINS[1] ont montré que l'on pouvait éliminer ce courant capacitif gênant en superposant à la tension continue E, appliquée entre les deux électrodes d'une cellule polarographique classique, une tension carrée de quelques mV d'amplitude. Le courant alternatif résultant est composé d'un courant capacitif et d'un courant d'électrolyse correspondant à la réduction d'un ion. Si la constante de temps de la cellule polarographique est suffisamment faible, le courant capacitif tombe très rapidement à zero, tandis que le courant d'électrolyse varie beaucoup plus lentement. Ce dernier est déterminé séparément en mesurant immédiatement avant la variation de la tension. Il en résulte une plus grande sensibilité qu'en polarographie classique.

La polarographie alternative a d'autre part l'avantage de donner des courbes dérivées. Ainsi la séparation de vagues voisines est plus distincte c. à d. la sélectivité est plus grande. L'estimation d'une petite vague suivant une grande se fait également plus aisément.

A cause de ces avantages la polarographie à ondes carrées a déjà trouvé de nombreuses applications en chimie analytique[2–6].

Cette recherche a pour but la construction d'un polarographe à ondes carrées suivant le principe décrit par HAMM[7]. Quelques modifications introduites et les résultats obtenus sont également décrits. Ce polarographe est moins sensible que celui de BARKER, mais le circuit électronique est par contre plus simple.

INSTRUMENTATION

Le polarographe à ondes carrées dont le montage électrique simplifié est représenté dans la Fig. 1, comprend les parties suivantes: source de tension continue, moteur synchrone et potentiomètre, cellule et enregistreur automatique comme dans la polarographie classique, ainsi qu'un générateur à ondes carrées, un générateur de signaux de porte, un amplificateur, un circuit à porte, un détecteur et un filtre pour l'amortissement des oscillations dues au grossissement périodique des gouttes.

* Membre de l'Institut Interuniversitaire des Sciences Nucléaires.

HAMM[7] adapta le circuit à tension alternative à un polarographe Sargent, Modèle XXI. Dans cette recherche ce dernier est remplacé par un potentiomètre helipot à dix tours (100 Ω), entrainé par un moteur synchrone Sapmi Modèle 700 avec une vitesse d'un demi tour/min dans les deux sens de marche. A l'aide d'un réducteur, la vitesse de polarisation est réglable à 0.2, 0.1, 0.05 ou 0.025 V par minute. Le millivolt mètre enregistreur est un Speedomax G de Leeds et Northrup à sensibilité réglable de 2.5, 5 ou 10 mV fond d'échelle (25 cm).

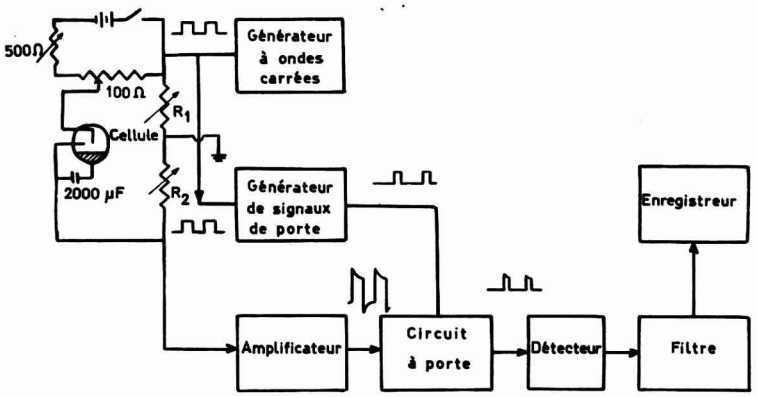

Fig. 1. Montage électrique simplifié du polarographe à ondes carrées.

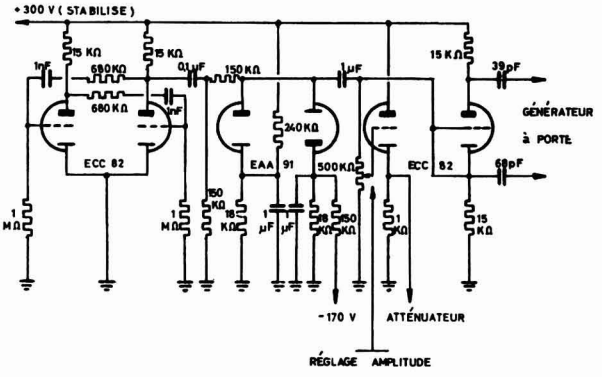

Fig. 2. Générateur à ondes carrées (f = 250 Hz).

Le générateur à ondes carrées est un appareil de General Radio, Unit KS Oscillator, type 1210 B, à fréquence réglable. Après l'étude de l'influence de la fréquence, ce générateur à été remplacé par un appareil plus simple d'une fréquence fixe de 250 Hz et à amplitude réglable de 5, 10, 25 ou 50 mV crête à crête (Fig. 2).

L'amplificateur est un Radiometer, Type 33 aj. Le générateur de signaux de porte est identique à celui décrit par HAMM. Le circuit à porte, le détecteur et le circuit de sortie sont cependant considérablement modifiés (Fig. 3). Le bistable de délai et le générateur de signaux de porte ne sont pas reproduits dans cette figure (cfr. HAMM).

Le quadruple filtre T de KELLEY ET FISHER[8] fut employé dans les premiers essais pour amortir les oscillations du courant. Cependant dans les expériences ici décrites ce filtre est remplacé par un condensateur de 32 μF (Fig. 3).

La cellule polarographique avec une capacité de 40 ml est constituée d'une électrode au calomel saturée (E.C.S.) à faible résistance et un tube capillaire ordinaire Tinsley comme électrode à gouttes de mercure (Fig. 4).

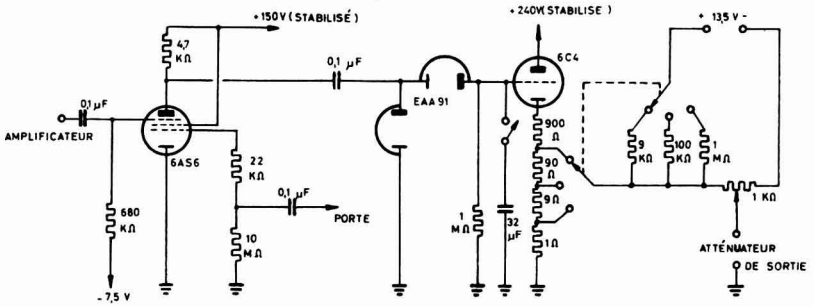

Fig. 3. Circuit à porte, détecteur et circuit de sortie.

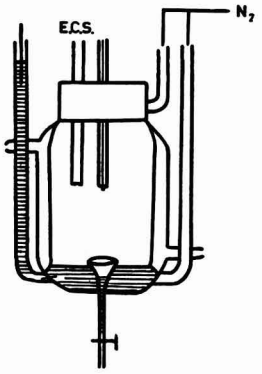

Fig. 4. Cellule polarographique.

L'électrode au calomel est reliée à une couche de mercure sur le fond de la cellule par un condensateur de 2.000 μF. Les gouttes de mercure contaminées sont éliminées par un entonnoir. La résistance de cette cellule n'atteint pas 200 Ω.

Dans la construction de ce polarographe, un soin spécial doit être pris du blindage afin d'éviter des troubles dans les mesures. A cause de cela le moteur synchrone du potentiomètre et les batteries ont été séparées de la partie électronique.

CARACTÉRISTIQUES DU POLAROGRAPHE

Les produits et réactifs, surtout l'électrolyte indifférent (principalement KCl, 1 *M*), doivent être très purs, et l'eau bidistillée. L'oxygène dissous gène beaucoup moins que dans la polarographie classique à cause de sa réduction irréversible. La désoxy-

génation se fait en barbotant de l'azote dans la solution pendant dix minutes. Le temps de goutte (3 sec hors du circuit) ainsi que la distance entre la goutte et la couche de mercure reste constante pendant les différentes mesures. La température est constante, 25° ± 0.1°.

Examen des facteurs variables

Les facteurs variables sont d'abord examinés afin d'établir les conditions optima de travail:

1), l'amplitude de la tension carrée, 5, 10, 25 ou 50 mV;
2), la largeur de porte, réglable entre 0–40% du cycle complet de la tension carrée;
3), la fréquence de la tension carrée, examinée entre 150–300 Hz;
4), la résistance R_2 montée en série avec la cellule, 10, 25, 50, 100 ou 200 Ω;
5), l'amplification avec position 10 (facteur de l'amplification × 3.2), 20 (× 10), 30 (× 32), 40 (× 100), 50 (× 320), 60 (× 1,000), 70 (× 3,200), 80 (× 10,000), 90 (× 32,000), 100 (× 100,000);
6), l'atténuation à la sortie du détecteur avec 4 positions (× 1, × 10, × 100, × 1000);
7), la vitesse de polarisation réglable à 0.025, 0.050, 0.100 ou 0.200 V/min.

En contrôlant ces facteurs les autres variables sont tenues constantes:

1), l'amplitude, 25 mV;
2), la largeur de porte, 1/4 de cycle ou 25%;
3), la fréquence, 250 Hz;
4), la résistance R_2, 100 Ω;
5), l'amplification, 320 fois;
6), l'atténuation, position 2;
7), la vitesse de polarisation, 0.1 V/min;
8), l'enregistreur, 2.5 mV;
9), la solution: $CdCl_2$ $5 \cdot 10^{-5}$ *M* en KCl 1 *M*.

De ces essais on peut déduire:

1), dans les conditions d'enregistrement citées ci-dessus, l'électrolyte indifférent KCl 1 *M* donne un polarogramme stable et reproductible. La stabilité ainsi que la précision de la mesure diminuent progressivement en augmentant la sensibilité;
2), il existe un rapport linéaire entre les hauteurs des pics et la résistance R_2, l'amplification et l'atténuation à la sortie du détecteur;
3), la hauteur du pic augmente légèrement suivant que la vitesse de polarisation diminue. Cette augmentation est due à la distorsion causée par le filtre pour l'amortissement des oscillations dues au grossissement périodique des gouttes;
4), pour de faibles amplitudes (5–25 mV) il existe un rapport linéaire entre la hauteur du pic et l'amplitude, ceci en accord avec la théorie[9–11]. Pour des valeurs plus élevées la hauteur du pic augmente moins vite;
5), en théorie il existe un rapport linéaire entre la hauteur du pic et la racine carrée de la fréquence ($\omega^{1/2}$). Cette linéarité est vérifiée entre 175–260 Hz. Par conséquent les essais suivants sont exécutés à une fréquence fixe de 250 Hz;
6), la hauteur du pic augmente en fonction de la largeur de porte. Puisque par contre le courant capacitif ne peut plus être éliminé complètement pour de très grandes largeurs de porte, une largeur de 25% ou 1/4 de cycle paraît optima.

Sélectivité de la méthode

La séparation de pics voisins est étudiée à l'aide d'une solution de Cd^{2+} + In^{3+} en milieu KCl 1 *M* + HCl 0.1 *M* comme électolyte indifférent. Le milieu acide prévient l'hydrolyse de In^{3+}. Un polarogramme classique donne dans ces conditions une différence de 45 mV entre les potentiels de demi-vague: —0.602 V pour In^{3+} et —0.647 V pour Cd^{2+}. La Fig. 5 montre qu'en ces conditions l'on n'obtient pas de séparation pour un mélange de Cd^{2+} et In^{3+} dans un rapport 1/1 (concentration de chaque ion: $5 \cdot 10^{-5}$ *M*).

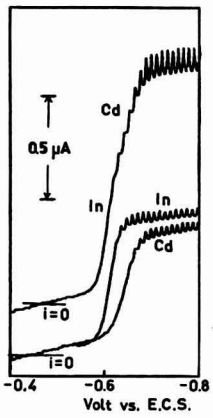

Fig. 5. Polarogrammes classiques de In^{3+} et Cd^{2+}, séparément et en mélange; concentration de chaque ion est $5.0 \cdot 10^{-5}$ *M* en KCl 1 *M*, HCl 0.1 *M*.

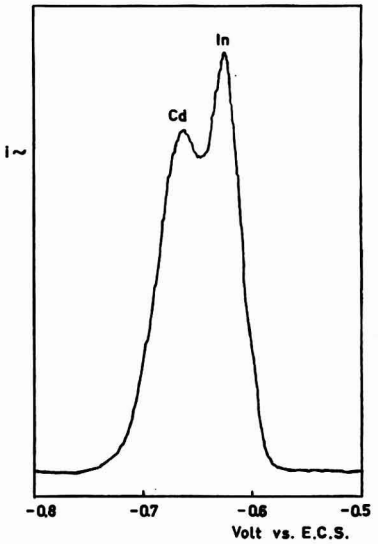

Fig. 6. Polarogramme à ondes carrées d'un mélange de In^{3+} + Cd^{2+}; concentration de chaque ion est $5.0 \cdot 10^{-5}$ *M* en KCl 1 *M*, HCl 0.1 *M*.

La polarographie à ondes carrées donne par contre une séparation bien nette pour un rapport de 1/1. Figure 6 donne un polarogramme à ondes carrées enregistré à une vitesse de polarisation de 0.025 V min^{-1} et à une amplitude de 10 mV. Pour des amplitudes de 50–10 mV la sélectivité augmente à mesure que l'amplitude diminue; il n'y a pas de séparation pour une amplitude de 50 mV. A cause de la distorsion dans l'enregistrement produite par le système d'amortissement la sélectivité augmente apparemment pour des petites vitesses de polarisation.

La sélectivité de ce polarographe est du même ordre de grandeur que celui de BARKER, le "Mervyn-Harwell square wave polarograph"[12].

Estimation d'une petite vague après une grande

Dans la polarographie classique la détermination d'une petite vague (ion *B*) suivant une grande (ion *A*) n'est possible que si le rapport *A*/*B* ne dépasse pas 50/1. Pour des rapports plus élevés, il est difficile de compenser le courant provenant de la première vague. En polarographie dérivée et surtout en polarographie à ondes carrées, ce rapport peut être beaucoup plus élevé[12].

Le polarographe ici décrit permet, sans perte de précision la détermination de traces de Cd^{2+} (10^{-5}–10^{-6} M) en présence de grandes quantités de cuivre ou d'autres ions précédents. La concentration de l'ion A ne peut cependant pas dépasser 10^{-2} M, sinon des troubles se produisent. Tout ceci est comparable aux résultats obtenus avec le polarographe de BARKER[13].

Sensibilité

La plus faible concentration des ions réduits réversiblement comme le Cd^{2+} qui peut être déterminée par ce polarographe est de $5 \cdot 10^{-7}$ M. Ceci est environ 12 fois moins qu'avec le polarographe de BARKER dont la sensibilité limite atteint $4 \cdot 10^{-8}$ M pour des ions réversibles.

MÉTHODES DE DOSAGE

Trois méthodes ont été étudiées et comparées afin de déterminer la précision de ce polarographe à ondes carrées surtout pour de faibles concentrations: courbe d'étalonnage, méthode par addition[14] et méthode de l'étalon interne[15].

Courbe d'étalonnage

Les hauteurs des pics ont été mesurées pour des concentrations de 10^{-3}–10^{-6} M de Cd^{2+} en KCl 1 M. Il y a un rapport linéaire entre la hauteur du pic et la concentration au-dessous de 10^{-4} M. A des concentrations entre 10^{-3}–10^{-4} M, la hauteur du pic est plus basse que prévue. Ces résultats sont en rapport avec ceux obtenus par HAMM[7].

TABLEAU I

DOSAGE DE CADMIUM EN KCl, 1 M

Concentration (M)	R_2 (Ω)	*Courbe d'étalonnage*		*Méthode par addition*
		Hauteur de pic H_1 *(mm)*	k	*Concentration trouvée (x) (M)*
$1.0 \cdot 10^{-3}$	10	245	24.5	—
$5.0 \cdot 10^{-4}$		160	32.0	—
$2.5 \cdot 10^{-4}$		99.5	39.8	—
$1.0 \cdot 10^{-4}$	50	202.5	40.5	—
$9.0 \cdot 10^{-5}$		181.5	40.3	—
$8.0 \cdot 10^{-5}$		162.0	40.5	—
$7.0 \cdot 10^{-5}$		144.5	41.3	—
$6.0 \cdot 10^{-5}$		121.5	40.5	—
$5.0 \cdot 10^{-5}$		100	40.0	—
$4.0 \cdot 10^{-5}$		84	42.0	—
$3.0 \cdot 10^{-5}$		59.5	39.7	—
$2.0 \cdot 10^{-5}$		38.5	38.5	—
$1.0 \cdot 10^{-5}$	200	85	42.5	$1.02 \cdot 10^{-5}$
$9.0 \cdot 10^{-6}$		77.5	43.1	$9.09 \cdot 10^{-6}$
$8.0 \cdot 10^{-6}$		67.5	42.2	$8.32 \cdot 10^{-6}$
$7.0 \cdot 10^{-6}$		57.5	41.1	$7.07 \cdot 10^{-6}$
$6.0 \cdot 10^{-6}$		47.5	39.6	$6.24 \cdot 10^{-6}$
$5.0 \cdot 10^{-6}$		40	40.0	$5.15 \cdot 10^{-6}$
$4.0 \cdot 10^{-6}$		32.5	40.6	$4.12 \cdot 10^{-6}$
$3.0 \cdot 10^{-6}$		25	41.7	$3.02 \cdot 10^{-6}$
$2.0 \cdot 10^{-6}$		15	37.5	$2.08 \cdot 10^{-6}$
$1.0 \cdot 10^{-6}$		7.5	37.5	$0.99 \cdot 10^{-6}$

Quelques résultats sont résumés dans le Tableau I. Les hauteurs des pics dans la colonne 3 sont la moyenne de trois mesures consécutives de la même solution. La constante k (colonne 4) est obtenue en divisant la hauteur du pic en mm (H_1) par la résistance R_2 montée en série avec la cellule et la concentration en mmol ($k = H_1/R_2C_{\text{mmol}}$).

L'erreur moyenne sur k (40.5 entre 10^{-4} en 10^{-6} M) est:

$$\frac{\Sigma \Delta k}{n} = 1.5\% \text{ (entre } 10^{-4}\text{–}10^{-5}\ M;\ 11.2\text{–}1.12\ \mu\text{g/ml)}$$

$$= 3.8\% \text{ (entre } 10^{-5}\text{–}10^{-6}\ M;\ 1.12\text{–}0.112\ \mu\text{g/ml)}$$

et l'erreur quadratique: $\sqrt{\frac{\Sigma \Delta k^2}{n-1}} = 2.5\%$ (10^{-4}–10^{-5} M).

$= 4.8\%$ (10^{-5}–10^{-6} M).

Méthode par addition

Un polarogramme d'une solution inconnue est d'abord enregistré (vol V_1, hauteur de pic H_1). Un volume exact (V_2) d'une solution de concentration connue (a mol) est ensuite ajouté à cette solution et un second polarogramme est enregistré (hauteur de pic H_2). La concentration de la solution inconnue (x mol) est calculée comme suit:

$$x = \frac{aV_2H_1}{H_2(V_1 + V_2) - V_1H_1}$$

La précision de la méthode est maxima pour $H_2 \simeq 1.5\ H_1$. Les résultats pour des concentrations entre 10^{-5}–10^{-6} M sont donnés dans le Tableau I (colonne 5).

L'erreur moyenne: $\frac{\Sigma \Delta k}{n} = 2.4\%$

et l'erreur quadratique: $\sqrt{\frac{\Sigma \Delta k^2}{n-1}} = 2.9\%$.

Méthode de l'étalon interne

A une solution de concentration inconnue (x mol) est ajouté un élément de référence de concentration connue (a mol) comme étalon interne, et le polarogramme est enregistré. Les hauteurs respectives des pics sont H_1 et H_2 pour l'inconnue et l'élément de référence. Un polarogramme est ensuite enregistré d'une solution de deux ions de concentrations connues d'où suit le rapport K pour le couple des éléments considérés.

La concentration inconnue est donnée par:

$$x = \frac{H_1}{H_2} \cdot \frac{a}{K}$$

Avec le Cu^{2+} comme étalon interne le Cd^{2+} peut être déterminé avec une précision encore légèrement meilleure que dans la méthode par addition. La précision est la meilleure pour $H_1 \simeq H_2$.

La précision de ces trois méthodes étudiées est satisfaisante. La méthode par

addition et surtout la méthode de l'étalon interne donnent les meilleurs résultats pour des concentrations de 10^{-5}–10^{-6} M. En employant une courbe d'étalonnage de légères fluctuations peuvent se produire dues à l'amplification en fonction du temps, ce qui diminue la précision.

DOSAGE DE CUIVRE EN ALLIAGES D'ALUMINIUM

Ce polarographe à ondes carrées a été essayé pour le dosage de cuivre dans une série d'alliages d'aluminium de Johnson et Matthey, selon la méthode de l'étalon interne. A côté de l'aluminium comme élément de base, il y a en outre du manganèse, du fer, du silicium, du cuivre et du zinc.

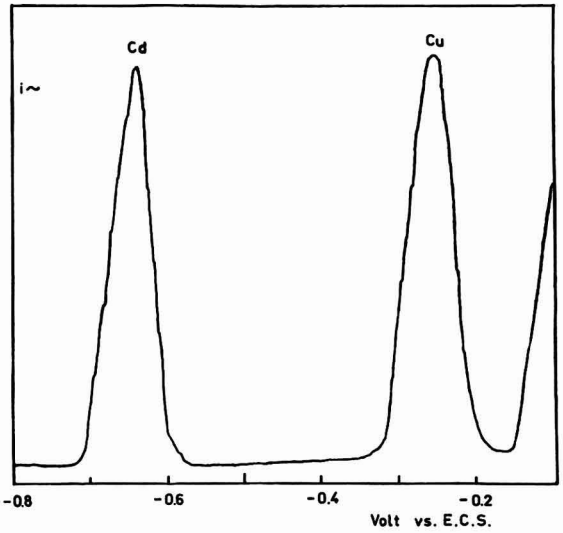

Fig. 7. Dosage de cuivre en alliages d'aluminium suivant la méthode de l'étalon interne (Cadmium); concentration de Cu^{2+} et Cd^{2+} est $5.0 \cdot 10^{-5}$ M en HCl 1 M.

TABLEAU II

DOSAGE DU CUIVRE EN ALLIAGES D'ALUMINIUM

Méthode	AB_1 (%)	AB_2 (%)	AB_3 (%)	AB_4 (%)
chimique	0.02	0.05	0.11	0.20
spectrographie	0.024	0.046	0.11	0.20
polarographie à ondes carrées	0.0198	0.0476	0.105	0.191

Une quantité adéquate d'alliage est d'abord dissoute en acide chlorhydrique et puis diluée jusqu'à 50 ml, contenant à côté de $\pm$ $5 \cdot 10^{-5}$ M Cu en HCl 1 N, également $5 \cdot 10^{-5}$ M Cd^{2+} comme étalon interne.

Les résultats sont représentés dans le Tableau II. Les valeurs trouvées sont en accord avec les certificats d'analyse qui donnent les résultats obtenus par analyse chimique et spectrographique.

CONCLUSION

En ce qui concerne la sélectivité et la détermination d'ions en faibles concentrations en présence de larges excès ($\leq 10^{-2}$ M) d'ions réductibles à des potentiels plus positifs, ce polarographe à ondes carrées est comparable à celui de BARKER. Il est toutefois 12 fois moins sensible: la sensibilité limite est de $5 \cdot 10^{-7}$ M pour des ions réduits réversiblement par rapport à $4 \cdot 10^{-8}$ M[12]. Le circuit électronique est par contre plus simple et l'appareil peut être construit à un prix relativement modéré.

Pour le moment des essais sont fait avec un polarographe à ondes carrées entièrement transistorisé. Cet appareil a l'avantage d'avoir une plus grande stabilité et sécurité que l'appareil décrit.

RÉSUMÉ

Un polarographe à ondes carrées a été construit selon le principe de HAMM. Quelques modifications et aussi les caractéristiques de l'appareil sont décrites. La sélectivité et d'autres facteurs sauf la sensibilité sont comparables au polarographe à ondes carrées de BARKER. Le circuit électronique est toutefois plus simple. Trois méthodes de dosage sont comparées: courbe d'étalonnage, méthode par addition et méthode d'étalon interne. Cette dernière méthode est employée pour la détermination de cuivre en alliages d'aluminium.

SUMMARY

A square-wave polarograph was constructed according to the principle of HAMM. Some modifications were introduced and its characteristics were determined. The apparatus is 12 times less sensitive than the BARKER square-wave polarograph, but its electronic circuits are simpler. Other important properties, such as resolution and the possibility of determining small quantities of more difficultly reducible substances in the presence of large quantities ($\leq 10^{-2}$ M) of more easily reducible substances, are approximately the same.

Three methods of standardization were studied and compared: by a calibration curve, by the method of standard additions and the internal standard method. The reliability and accuracy of the polarograph were tested, for the determination of copper in aluminum alloys, using the internal standard method.

BIBLIOGRAPHIE

1 G. C. BARKER ET I. L. JENKINS, *Analyst*, 77 (1952) 685.
2 D. J. FERRETT, G. W. C. MILNER ET A. A. SMALES, *ibid.*, 79 (1954) 731.
3 D. J. FERRETT ET G. W. C. MILNER, *ibid.*, 80 (1955) 132; 81 (1956) 193.
4 D. J. FERRETT ET G. W. C. MILNER, *J. Chem. Soc.*, (1956) 1186.
5 G. W. C. MILNER ET L. J. SLEE, *Industrial Chemist*, 33 (1957) 494.
6 G. W. C. MILNER ET L. J. SLEE, *Analyst*, 82 (1957) 139.
7 R. E. HAMM, *Anal. Chem.*, 30 (1958) 350.
8 M. T. KELLEY ET D. J. FISHER, *ibid.*, 28 (1956) 1130.
9 T. KAMBARA, *Bull. Chem. Soc. Japan*, 27 (1954) 523, 527, 529.
10 G. C. BARKER, R. L. FAIRCLOTH ET A. W. GARDNER, *A.E.R.E. Report*, A.E.R.E.-C/R (1958) 1786.
11 G. C. BARKER, *Anal. Chim. Acta*, 18 (1958) 119.
12 D. J. FERRETT, G. W. C. MILNER, H. I. SHALGOSKY ET L. J. SLEE, *Analyst*, 81 (1956) 506.
13 R. L. FAIRCLOTH, *Talanta*, 2 (1959) 135.
14 H. HOHN, *Chemische Analysen mit dem Polarographen*, Berlin, 1937, p. 51-52.
15 E. FORCHE, *Mikrochemie*, 25 (1938) 217.

TITRATION OF SULPHYDRYL SUBSTANCES BY LEAD TETRAACETATE

LUDMILA SUCHOMELOVÁ AND JAROSLAV ZÝKA

Department of Analytical Chemistry, Charles University, Prague (Czechoslovakia)

(Received April 2nd, 1962)

Standard lead tetraacetate solutions have proved their importance in the last few years as a stable and effective oxidizing agent, suitable for titrating and investigating the oxidation process in a number of inorganic and organic systems[1-7].

As part of a project on the study of further applications of this reagent to the determination of organic compounds, we have investigated the reactions of lead tetraacetate with organic substances containing the -SH group; TOMÍČEK AND VALCHA[8] have already referred to this reaction, without, however, giving any details.

In our experiments we have observed that, in a medium of glacial acetic acid, lead tetraacetate may be used for potentiometric, as well as visual, titration of mercaptans, and that this method is suitable for the needs of industrial process analysis. In addition, by using other sulphur-containing compounds (thioglycollic acid, cysteine, thiourea and thiosemicarbazide) we have demonstrated how aqueous or non-aqueous media, or the presence of mineral acids, can influence the manner and degree of oxidation of these substances by lead tetraacetate solutions.

EXPERIMENTS AND RESULTS

Reagents and apparatus

An approximately 0.05 *M* lead tetraacetate solution was prepared by reacting Pb_3O_4 with glacial acetic acid[5]. Its strength was determined by titration against a standard hydrazine sulphate solution[1]. A 0.05 *M* hydroquinone solution was prepared from the pure substance, and its strength determined by bichromate titration[13]. Thioglycollic acid solutions were estimated by iodate titration[9], and thiourea solutions by Chloramine T[10]. The strength of the thiosemicarbazide solutions was determined by nitrite[11] and mercaptan solutions (*n*-butylmercaptan, *sec*-butylmercaptan and benzylmercaptan) were determined by iodometric titrations[12]. Potentiometric titrations were carried out with the electronic potentiometer Multoscop III, using a platinum indicating electrode and a saturated calomel reference electrode. For visual indication a 0.2% solution of quinalizarin in glacial acetic acid was used.

Titrations in glacial acetic acid media

Glacial acetic acid is a very good solvent for mercaptans, which can then be oxidised by lead tetraacetate to the appropriate disulphides according to the reaction:

$$2\ RSH + Pb(CH_3COO)_4 \rightarrow RSSR + Pb(CH_3COO)_2 + 2\ CH_3COOH$$

The reaction is immediate and its end-point may be indicated potentiometrically, the point of equivalence being shown by a large potential change (250 mV for 0.05 ml of a 0.05 *M* $Pb(CH_3COO)_4$ solution); the potential at the inflexion is in the region of 400 mV *vs.* S.C.E. Titrations were carried out in a volume of 30 ml, using samples of about 20 mg. Results given in Table I show that the method is sufficiently accurate,

TABLE I

TITRATION OF -SH SUBSTANCES IN GLACIAL ACETIC ACID MEDIUM (1 ml 0.05 *M* LEAD TETRAACETATE SOLUTION CORRESPONDS TO 9.211 mg $C_2H_4O_2S$, 9.018 mg $C_4H_{10}S$ AND 12.419 mg C_7H_8S)

	Taken (mg)	*Found (mg)*	*Deviation (%)*
Thioglycollic acid	5.768	5.878	+ 1.90
	5.768	5.800	+ 0.60
	11.536	11.765	+ 2.00
	11.536	11.652	+ 0.90
	28.840	28.669	− 0.49
	28.840	28.669	− 0.49
	28.840	28.898	+ 0.20
	46.145	46.460	+ 0.70
	57.681	57.110	− 0.98
n-butylmercaptan	11.30	11.40	+ 0.90
	15.80	16.05	+ 1.60
	21.90	21.68	− 0.80
	23.70	24.43	+ 3.00
	26.95	27.97	+ 3.70
sec-butylmercaptan	18.76	18.70	− 0.32
	19.50	19.44	− 0.30
	19.60	19.59	− 0.07
	20.32	20.30	− 0.09
	21.60	21.52	− 0.39
	22.60	22.52	− 0.39
benzylmercaptan	20.80	20.74	− 0.30
	21.80	21.68	− 0.55
	22.27	22.20	− 0.32
	28.16	28.04	− 0.41
	32.16	32.10	− 0.18
	34.65	34.49	− 0.46

and as simple as methods used up to now for the titration of -SH substances. It even improves upon these by allowing the use of quinalizarin as a visual indicator. (5–10 drops of the quinalizarin solution are added, and the end-point is indicated by a colour change from red to blue). The method is suitable for routine analysis of mercaptans; using potentiometric indication, it is suitable also for micro-determinations.

Titrations in aqueous media

We have already remarked in previous papers on the fact that lead tetraacetate may be used as a volumetric agent for oxidative reactions not only in glacial acetic acid media, but also in aqueous or mineral acid solutions[5,7]. In the oxidation of organic compounds, various oxidation products are formed, depending on the medium employ-

ed. The rate of reaction is also largely influenced by the medium; we have observed this mainly in the case of α-hydroxy acids[2,3].

For the present work we have chosen as examples some sulphur-containing compounds, and have investigated whether a similar influence due to the medium also exists in these cases. Since in some cases the reaction was too slow and could not be used for a direct titration, we have added an excess of lead tetraacetate volumetric solution to the substance investigated, and after a certain period of time have titrated the excess potentiometrically using standard hydroquinone solution.

Oxidations in 80–30% acetic acid media (in more dilute solutions the tetraacetate salt hydrolyses) were investigated by adding various amounts of hydrochloric, sulphuric or perchloric acid. The influence of the length of time for which excess tetraacetate salt was present was also examined. Only those results are mentioned, which have led to positive conclusions; these conclusions varied for each compound.

Thioglycollic acid. Whereas thioglycollic acid is oxidised rapidly and by a definite route in glacial acetic acid to the corresponding disulphide, application of lower acetic acid concentrations (from 80–30%) leads to oxidation to higher valency states; even though the rate of reaction increases, an excess of the reagent must be used and back titrated with standard hydroquinone solution. In 60% solutions of acetic acid a defined oxidation state is reached after 60 min, and the rate of oxidation increases with decreasing acetic acid concentration. Therefore, in 30% acetic acid, oxidation is complete after 15 min. One mole of thioglycollic acid reacts with 2 moles of lead tetraacetate, showing that thioglycollic acid is oxidised to sulphinic acid in this reaction.

For the oxidation of thioglycollic acid by lead tetraacetate in 30–60% acetic acid media and in the presence of hydrochloric acid, this latter acid must not be present in concentrations higher than 2%, to prevent liberation of elementary chlorine which is formed as a result of oxidation of the HCl by the tetraacetate salt. In solutions of

TABLE II

DETERMINATION OF THIOSEMICARBAZIDE USING LEAD TETRAACETATE

(1 ml 0.05 *M* $Pb(CH_3COO)_4$ corresponds to 0.911 mg CH_5N_3S)

Thiosemicarbazide taken (mg)	*Time of reaction with $Pb(CH_3COO)_4$, (h)*	*Thiosemicarbazide found (mg)*	*Deviation (%)*
2.359	2	2.362	+ 0.10
2.359	2	2.358	0.00
2.359	2	2.362	+ 0.10
3.774	1	3.695	− 2.10
3.774	1.5	3.722	− 1.40
3.774	2	3.770	− 0.12
4.718	2	4.692	− 0.50
		4.673	− 0.94
		4.719	0.00
		4.700	− 0.37
		4.755	+ 0.80
		4.737	+ 0.40
7.077	2.5	7.060	− 0.23
9.436	2	9.001	− 4.63
	2.5	9.217	− 2.32
	3	9.279	− 1.67
	3.5	9.474	+ 0.40
	3.5	9.492	+ 0.60

50% acetic acid and 0.3% hydrochloric acid, a defined oxidation state is reached after 15 min, which corresponds to a reaction of 1 mole of thioglycollic acid with 3 moles of tetraacetate salt, the appropriate sulphochloride probably being formed.

Cysteine and thiourea. In the case of cysteine and thiourea, satisfactory results have been obtained only in the direct titration of 30–80% acetic acid solutions (for cysteine) and of 50% acetic acid solutions (in the presence of 1–5 *N* H_2SO_4 or 0.1 *N* HCl) at room or elevated temperature (60°), for thiourea. Cysteine reacts in the ratio of 1 mole: 2 moles tetraacetate salt, forming the appropriate sulphinic acid. Thiourea reacts with the tetraacetate salt in the molar ratio of 1 : 1. For both acids, however, the reaction is very slow, and is not well suited to the needs of volumetric analysis.

Thiosemicarbazide. Analytically favourable results have been obtained by oxidation with excess reagent in perchloric acid medium, followed by back titration with hydroquinone. The reaction is suitable for determinations on the microscale. The favourable course of the reaction may be explained by the fact that sulphate is formed in the oxidation, 1 mole thiosemicarbazide reacting with 5 moles of the reagent:

$$\begin{matrix} \diagup\!\!\diagup NH \\ C—SH \\ \diagdown NHNH_2 \end{matrix} + 5\ Pb(CH_3COO)_4 + 4\ H_2O \rightarrow PbSO_4 + HCN + N_2 + 4\ Pb(CH_3COO)_2 + 12\ CH_3COOH$$

The sulphate formed reacts with Pb^{2+} ions orginating in reduction of the reagent to form lead sulphate, thus shifting the direction of the oxidation process favourably and speeding up the reaction. Best results were obtained in the determination of 2–10 mg thiosemicarbazide, to which 30 ml 30% $HClO_4$ and 15–30 ml 0.05 *N* $Pb(CH_3COO)_4$ were added. After a suitable period of time, the mixture was titrated by hydroquinone, using potentiometric indication of the end-point (see Table 2).

ACKNOWLEDGEMENT

The authors wish to thank Doz. Dr. V. HORÁK of the Department of Organic Chemistry, Charles University, for preparing the mercaptan samples used in these studies, as well as for valuable discussions in the course of the work described.

SUMMARY

Mercaptans may be titrated by standard lead tetraacetate solutions in glacial acetic acid media, using potentiometric or visual control with quinalizarin as indicator, the appropriate disulphide being formed. The method is well suited for routine analysis. Using thiglycollic acid, cysteine, thiourea and thiosemicarbazide as model substances, it has been found that -SH substances can be oxidised to various oxidation states according to the medium employed (*e.g.* dilute acetic acid, possibly containing mineral acids). These reactions were investigated using an excess of the reagent. The excess was determined by back titration with standard hydroquinone solution.

REFERENCES

1 A. BERKA AND J. ZÝKA, *Collection Czech. Chem. Commun.*, 24 (1959) 105.
2 A. BERKA AND J. ZÝKA, *ibid.*, 23 (1958) 2005.
3 A. BERKA AND J. ZÝKA, *Cesk. Farm.*, 7 (1958) 141.
4 A. BERKA, *ibid.*, 8 (1959) 561.
5 A. BERKA, V. DVOŘÁK, I. NĚMEC AND J. ZÝKA, *Anal. Chim. Acta*, 23 (1960) 380.
6 A. BERKA, *ibid.*, 24 (1961) 171.

[7] A. BERKA, J. DOLEŽAL, I. NĚMEC AND J. ZÝKA, *ibid.*, 25 (1961) 533.
[8] O. TOMÍČEK AND J. VALCHA, *Chem. Listy*, 44 (1950) 283.
[9] K. J. STEEL, *J. Pharm. Pharmacol.*, 10 (1958) 574; *C.A.*, 53 (1959) 1634c.
[10] J. ČÍHALÍK AND J. RŮŽIČKA, *Chem. Listy*, 49 (1955) 1731.
[11] J. VULTERIN AND J. ZÝKA, *Chem. Listy*, 50 (1956) 364.
[12] J. W. KIMBALL, R. L. KRAMER AND E. E. REID, *J. Chem. Soc.*, 43 (1921) 1199.
[13] V. SIMON AND J. ZÝKA, *Chem. Listy*, 49 (1955) 1646.

OSZILLOGRAPHISCHE BESTIMMUNG VON BISMUTH UND CHLORIDIONEN

DALIBOR WEISS

Institut für Erzforschung, Prag (Tschechoslowakei)

(Eingegangen am 26. Februar, 1962)

Mit der oszillographischen Bestimmung des Bismuths beschäftigte sich eine Reihe von Autoren. Es waren vor allem die japanischen Forscher ITSUKI UND NAGAO[1], die das oszillographische Verhalten von Bismuth im Chloridmedium studierten. Sie fanden, dass sich zur oszillographischen Bestimmung dieses Elements am besten eine Elektrolytenlösung von 1 *M* Chlorwasserstoffsäure eignet. Ihre Erfahrungen benutzten sie zur quantitativen Bestimmung von Bismuth in metallischem Silber.

Die Depolarisation dreiwertiger Bismuthionen in anderen Elektrolyten, z.B. in Schwefelsäure, Salpetersäure, Perchlorsäure und Essigsäure verfolgten GLADYŠEV UND KOZLOVSKIJ[2]. Gleichfalls HEYROVSKÝ UND FOREJT[3] erwähnen die irreversibele Depolarisation von Bismuth in Sulfat- und Nitratlösungen mit der Bemerkung, dass sich diese Depolarisation durch Zusatz von konzentrierten Chloriden in eine reversibele verwandelt. In Zusammenhang mit dem gesagten, erwähnen die letztgenannten Autoren auch den selbständigen Depolarisationseffekt der Chloridionen in saueren Sulfatlösungen. Später nützten KALVODA UND GLADYŠEV[4] diesen Effekt zur quantitativen Chloridbestimmung in Mineralwasser.

In der vorliegenden Arbeit beschäftigten wir uns mit dem beschriebenen Depolarisationseffekt des Bismuths. Wir verfolgten den Einfluss wachsender Chloridkonzentration auf die Depolarisation des Bismuths in perchlorsaurem Medium. Die gewonnenen Erfahrungen wendeten wir zur quantitativen Bismuthbestimmung und indirekten Chloridbestimmung an.

EXPERIMENTELLES UND ERGEBNISSE

Reagentien und Apparatur

Die Standardlösung wurde durch Lösen 1 g metallischen Bismuths in 100 ml heissem Perchlorsäure–Salpetersäuregemisch (3 : 2) hergestellt. Diese Lösung wurde bis zum Entweichen dichter weisser Perchlorsäuredämpfe erhitzt und nach Kühlung mit Wasser auf 1 l aufgefüllt.

Alle verwendeten Reagentien waren höchsterreichbarer Reinheit. Die Salpetersäure sowie Perchlorsäure enthielten keine Chloride.

Die oszillographischen Messungen wurden mit dem Polaroskop Křižík P 576 durchgeführt. Die Quecksilbertropfelektrode war aus einer abgebogenen Kapillare hergestellt. Die konstante Tropfdauer (3 sec) war durch einen mechanischen Tropfenabreisser gewährleistet. Die Elektrode wurde mit Wechselstrom 0.1–0.3 μA, 50 Hz

polarisiert. Als Vergleichselektrode verwendeten wir den Quecksilberboden oder eine spektralreine Graphitelektrode. Zur Bestimmung der Ausscheidungspotentiale verwendeten wir eine gesättigte Kalomelelektrode, die mittels einer Brücke, aus gesättigter Natriumperchlorat oder Ammoniumsulfatlösung bestehend, mit der untersuchten Lösung verbunden war. Die Tiefe der Einschnitte auf der oszillographischen Kurve $dE/dt = f(E)_5$ wurde mittels des kalibrierten Lichtschiebers nach KALVODAS gemessen. Die Potentialwerte der Einschnitte wurden mittels der ebenfalls von KALVODA[6] beschriebenen Methode gemessen. Die oszillographischen Kurven wurden aus 20 cm Entfernung mit einem Pentaconapparat unter Verwendung eines Objektivzwischenringes fotografiert. Als Negativmaterial benutzten wir den Agfa-Röntgen fluorapid 25 DIN Film, Exposition 1/20 sec.

Auf der oszillographischen Kurve $dE/dt = f(E)$ bildet Bismuth einen kaum sichtbaren kathodischen Einschnitt und einen irreversibelen, deutlicheren anodischen Einschnitt. Chloride in einer Konzentration von $2 \cdot 10^{-4}$ M bewirken, dass sich der kathodische Einschnitt verdeutlicht und gleichzeitig zeigt sich der kathodische Depolarisationseinschnitt der Chloridionen, dessen Potential bei 0.25 V, gegen G.K.E. gemessen, liegt. Durch steigende Chloridkonzentration vertiefen sich die Bismutheinschnitte, sie werden reversibeler und gleichzeitig zeigt sich der anodische Depolarisationseinschnitt des Chlorids. Der kathodische Einschnitt vergrössert sich und sein Potential verschiebt sich zu negativeren Werten. Bei einer $1.0 \cdot 10^{-3}$ M Chloridkonzentration hat der kathodische Chlorideinschnitt ein Potential von 0.22 V. Gleichzeitig entwickelt sich dicht neben ihm ein nadelförmiger Kapazitätseinschnitt. Dasselbe ist am anodischen Teil der Kurve zu beobachten.

Wird die Chloridkonzentration auf den Wert $3 \cdot 10^{-3}$ M gesteigert, wird der kathodische Chloridioneneinschnitt kleiner, sein Potential liegt bei 0.19 V und die Kapazitätseinschnitte berühren sich. Durch weitere Erhöhung der Chloridkonzentration auf $6 \cdot 10^{-3}$ M beginnt die Kurve, die schon sehr positiven Potentialen entspricht, zu sinken und an den Chlorideinschnitten wird sie abgeschnitten. Bei noch höherer

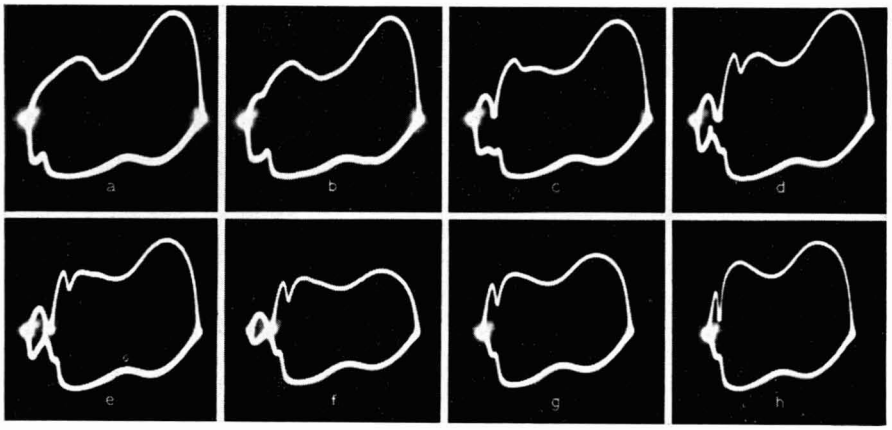

Abb. 1. Depolarisation des Chlorids und Einfluss der steigenden Chloridkonzentration auf die Bismutheinschnitte in 1 M $HClO_4$. Konzentration des Bi^{3+} $1.0 \cdot 10^{-4}$ M. Konzentration des NH_4Cl: a), 0 M; b), $1.0 \cdot 10^{-4}$ M; c), $5.0 \cdot 10^{-4}$ M; d), $1.0 \cdot 10^{-3}$ M; e), $2.0 \cdot 10^{-3}$ M; f), $3.0 \cdot 10^{-3}$ M; g), $5.0 \cdot 10^{-3}$ M; h), $1.0 \cdot 10^{-2}$ M. Quecksilbertropfelektrode, Polaroskop.

Chloridkonzentration, $1.0 \cdot 10^{-2}$ *M*, schwindet die Kurve vollkommen. Es bleibt nur die den negativen Potentialen entsprechende Kurve, die Bismutheinschnitte verwandeln sich in vollkommen reversibele und der linke Grenzpunkt der Kurve, deren Potential in diesen Stadium bei 0.05 V liegt, wandert langsam zu den negativen Potentialen. Steigt die Chloridkonzentration auf den Wert $1.0 \cdot 10^{-1}$ *M*, begrenzt sich der kathodische Bismutheinschnitt und sein Potential liegt dann bei −0.07 V. Durch weitere Erhöhung der Chloridkonzentration nimmt die oszillographische Kurve die Form, die der Form des Chloridmediums entspricht, an und die Bismutheinschnitte verringern sich. Die beschriebenen Veränderungen der oszillographischen Kurve zeigt die Abbildung (Abb. 1).

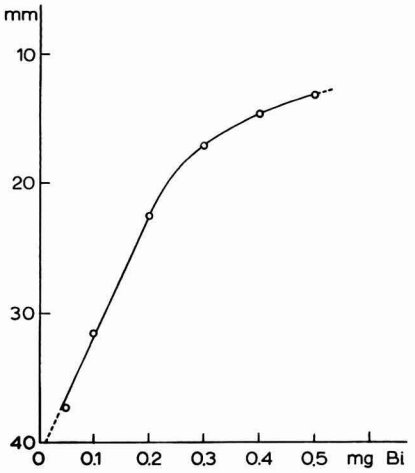

Abb. 2. Kalibrationskurve zur Bismuthbestimmung in 1 *M* $HClO_4$ und 0.2 *M* NH_4Cl.

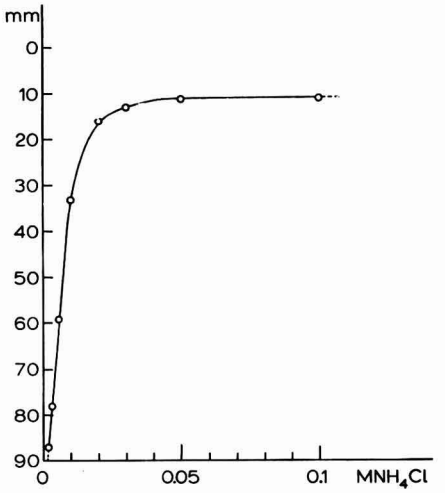

Abb. 3. Einfluss der steigenden Chloridkonzentration auf die Grösse des kathodischen Bismutheinschnittes in 1 *M* $HClO_4$. Gleichzeitig Kalibrationskurve zur Chloridbestimmung. Konzentration des Bi^{3+} $1.0 \cdot 10^{-4}$ *M*.

In 1 *M* Perchlorsäure ist demnach bei konstanter Bismuthkonzentration die Grösse der Bismutheinschnitte der Chloridkonzentration proportional, und umgekehrt. In einer Lösung von 1 *M* Perchlorsäure und 0.2 *M* Chlorid ist die Einschnittgrösse der Bismuthkonzentration proportional. Die Verhältnisse sind am besten an der Kalibrationskurve ersichtlich (Abb. 2 und 3).

DISKUSSION

Der Depolarisationseffekt des Bismuths in 1 *M* Perchlorsäure und 0.2 *M* Chloridlösung ist mehr ausgeprägt als in dem beschriebenen 1 *M* Chlorwasserstoffsäuremedium. Bei einer Konzentration von $9.0 \cdot 10^{-6}$ *M* Bi in 1 *M* Perchlorsäure und 0.2 *M* Ammonium- oder Natriumchlorid zeigt sich auf der oszillographischen Kurve ein gut messbarer Einschnitt. In 1 *M* Chlorwasserstoffsäure ist dagegen der Einschnitt erst bei der Konzentration $2.5 \cdot 10^{-5}$ messbar. Ein Nachteil der Bestimmung ist der störende Einfluss einiger Elemente, deren Abscheidungspotential in der Nähe des

Bismuths liegt, oder die mit Chloridionen in Perchlorsäure ähnliche Effekte bieten. Hauptsächlich wird die Bismuthbestimmung durch Kupfer gestört. Dasselbe gilt von der beschriebenen indirekten Chloridbestimmung.

Auf den Depolarisationseffekt von Chloriden, Bromiden, Jodiden und einiger weiteren Anionen, die mit Quecksilberionen schwer lösliche Verbindungen bilden, wiesen schon HAUL UND SCHOLZ[7]. Da die Depolarisation der Chloride, die mit der Kalomeladsorption auf der Quecksilberelektrodenoberfläche verbunden ist, bei sehr positiven Potentialen verläuft, ist sie für analytische Zwecke nur in einem verhältnismässig engen Konzentrationsbereich von $2.5 \cdot 10^{-4}$ *M* bis $1.0 \cdot 10^{-3}$ *M* Cl^- anwendbar. Dagegen ist die beschriebene indirekte Chloridbestimmung mittels Bismuthionen nur für höhere Konzentrationen in einem Bereich von $1.0 \cdot 10^{-3}$–$1.0 \cdot 10^{-1}$ *M* Cl^- anwendbar.

Im Vergleich zur direkten ist die indirekte Chlorbestimmung selektiver, da nur Chloridionen den erwähnten Depolarisationseffekt mit Bismuthionen bieten. Bromide und Jodide äussern sich nicht in der beschriebenen Weise, sie stören aber die Bestimmung von Bismuth bzw. der Chloride, weil sich in ihrer Anwesenheit der Bismutheinschnitt überhaupt nicht bildet.

ANALYTISCHE ANWENDUNG

Die Bestimmung von Bismuth in 1 *M* Perchlorsäure und 0.2 *M* Ammoniumchlorid (Natriumchlorid) oder die Bestimmung von Chloriden in 1 *M* Perchlorsäure und $1.0 \cdot 10^{-4}$ *M* Bi^{3+} wird durch Kupfer und Arsen gestört. Weitere Elemente, wie Zn^{2+}, Sb^{3+}, Sn^{4+}, Cd^{2+}, Fe^{3+} und Pb^{2+} stören nur dann, wenn ihre Konzentration die des Bismuths übersteigt. Der störende Einfluss dieser Elemente liegt darin, dass sie durch ihre Reduktion die ganze oszillographische Kurve deformieren. In Anwesenheit der erwähnten Elemente, soweit ihre Konzentration nicht extrem hoch ist, ist die Bismuth-, resp. Chloridbestimmung nur mittels einer vergleichenden Titrierung mit zwei synchronisierten Elektroden nach KALVODA[8] oder mit einer Elektrode nach JEZDÍNSKÝ[9] durchführbar.

Von den Anionen wirken auf die Bismuth- und Chloridbestimmung Bromide, Jodide, Sulfide und Sulfite störend. Von oberflächenaktiven Stoffen vermindert Gelatine die Bismutheinschnitte. Die Bestimmung von Bismuth und Chloriden ist also nur bei einigen Materialen, bei denen der störende Einfluss der erwähnten Elemente nicht in Frage kommt, anwendbar. So z.B., ist es möglich Bi^{3+} und Cl^- in Mineralwasser, Nitraten, Sulfaten, Chloraten, Perchloraten und manchen biologischen Materialen zu bestimmen. Der Analysenfehler liegt in einem Bereich von 6–7% rel.

Bei Anwendung der Methode zur Bismuthbestimmung in mineralischen Rohstoffen war es in einigen Fällen möglich, eine vergleichende Titrierung anzuwenden. In anderen Fällen, z.B. in Kupfer-, Eisen- und Zinn-Bleierzen musste Bismuth erst abgeschieden werden. Dazu eignete sich am bestem eine schnelle, von ŠEDIVEC UND VAŠÁK[10] vorgeschlagene Extraktionsmethode. Bismuth wird als Diethyldithiocarbamat (weiter DDTC) aus alkalischem Tartrat- und Cyanidmedium mit Chloroform extrahiert. Bei hohem Eisen- oder Bleigehalt ist aber die Extraktion des Bismuths nicht quantitativ. Blei wird zusammen mit Bismuth extrahiert, das dreiwertige Eisen bildet mit dem anwesenden Cyanid, Ferricyanid, und dieses oxydiert das DDTC. Aus diesem Grunde wählten wir zur Extraktion des Bi-DDTC ein

aus alkalischem Tartrat, EDTA, Triethanolamin und Cyanid bestehendes Medium. Bi-DDTC wurde mittels Kohlenstofftetrachlorid extrahiert. In diesem Medium blieb das Blei, sowie das dreiwertige Eisen gebunden. Kleine Bleimengen, die in den Extrakt übergingen, konnten die Bismuthbestimmung nicht mehr gefährden. Als Beispiel der Anwendung führen wir eine Bismuthbestimmung in Eisenerz an.

ARBEITSVORGANG

3–5 g der Probe werden in einem Becherglas mit 30 ml Königswasser zersetzt und zur Trockene verdampft. Der Rückstand wird mit 10 ml konz. Chlorwasserstoffsäure zersetzt und kurze Zeit digeriert, und danach mit 30 ml siedendem Wasser extrahiert. Die Lösung wird aufgekocht und durch einen Papierfilter in einem Scheidetrichter, in dem sich 80 ml gesättigte EDTA-Lösung befindet, filtriert. Der Filter wird in mit Chlorwasserstoffsäure angesäuertem heissen Wasser gewaschen. Die Lösung im Scheidetrichter wird mit konzentriertem Ammoniak zur ersten Rotfärbung neutralisiert und 25 ml Triethanolamin, 1 : 1 mit Wasser verdünnt, zugefügt. Weiter werden 10 ml 20% Natrium–Kaliumtartratlösung, 20 ml 10% Cyankalium zugegeben und die Lösung abgekühlt. Nach Zusatz von 0.25 g DDTC und 15 ml Kohlenstofftetrachlorid wird 1 min extrahiert. Die Extraktion wird noch zweimal wiederholt. Die gesammelten, mit Wasser gewaschenen Extrakte werden in einem Becherglas zur Trockene abgedampft. Zum Abdampfrückstand werden 5 ml eines Gemisches von Perchlorsäure und Salpetersäure (3 : 2) zugefügt und ebenfalls zur Trockne verdampft. Der Rückstand wird mit 2 ml Perchlorsäure befeuchtet, mit 5 ml heissem Wasser verdünnt und in einen 25-ml Messkolben überführt. Danach wird 1 ml 5 *M* Ammoniumchlorid zugegeben, temperiert und bis zur Marke gefüllt. Nach Mischung wird ein Teil der Lösung in ein polarographisches Gefäss abgegossen und oszillographiert. Die Tiefe des kathodischen Einschnitts wird mittels des verstellbaren Lichtschiebers gemessen und die gefundenen Werte mit der Kalibrationskurve, die durch Messung einer Reihe Standardlösungen konstruiert wurde, verglichen.

ZUSAMMENFASSUNG

Die irreversibele Depolarisation dreiwertiger Bismuthionen in 1 *M* $HClO_4$ wurde oszillographisch verfolgt. Die steigende Konzentration von Chloridionen in der Lösung beeinflusst den Vorgang in der Weise, dass sich die irreversibele Depolarisation allmählich in eine reversibele verwandelt. Bei konstanter Konzentration der Bismuthionen ist die Grösse des kathodischen Bismutheinschnittes in 1 *M* $HClO_4$ der Chloridionenkonzentration proportional. Umgekehrt ist bei konstanter Chloridkonzentration in gleicher Elektrolytlösung die Grösse des Bismutheinschnittes der Konzentration des Bismuths proportional. Da der beschriebene Depolarisationseffekt des Bismuths in 1 *M* $HClO_4$ nur in Anwesenheit von Chloridionen verläuft, war es möglich, denselben zur direkten quantitativen Bismuthbestimmung und zur indirekten Chloridbestimmung in einigen mineralischen und biologischen Materialen auszunützen.

SUMMARY

The irreversible depolarisation of Bi(III) in 1 *M* $HClO_4$ was followed oscillographically. Increasing concentration of chloride ions in the solution influences the reaction,

and the irreversible depolarisation gradually becomes reversible. At constant Bi(III) concentration in 1 *M* $HClO_4$, the magnitude of the cathodic bismuth indentation is proportional to the concentration of chloride ions. At constant chloride concentration, in a solution containing the same electrolyte, the magnitude of the bismuth indentation is proportional to the bismuth concentration. Because this depolarisation effect occurs only in the presence of chloride ions, it was possible to use this method for the direct quantitative determination of bismuth, and also for the indirect determination of chloride in some mineral and biological materials.

LITERATUR

1 K. ITSUKI UND M. NAGAO, *Japan Analyst*, 8 (1959) 800.
2 V. P. GLADYŠEV UND M. T. KOZLOVSKIJ, *Izv. Akad. Nauk Kaz. SSR*, [2] 16 (1959) 61.
3 J. HEYROVSKÝ UND J. FOREJT, *Oscilografická polarografie*, S.N.T.L., Prag, 1953.
4 V. P. GLADYŠEV UND R. KALVODA, *Zavodsk. Lab.*, [12] 27 (1961) 1450.
5 R. KALVODA, *Chem. Listy*, 49 (1955) 759.
6 R. KALVODA, *Chem. Listy*, 49 (1955) 1631.
7 R. HAUL UND E. SCHOLZ, *Z. Elektrochem.*, 52 (1948) 226.
8 R. KALVODA UND J. MACKŮ, *Collection Czech. Chem. Commun.*, 20 (1955) 257.
9 R. JEZDÍNSKÝ, *Chem. Zvesti*, Im Druck.
10 V. ŠEDIVEC UND V. VAŠÁK, *Chem. Listy*, 46 (1952) 607.

HYDROGEN ION EQUILIBRIA OF TRANSFUSION GELATIN

WAHID U. MALIK AND SALAHUDDIN

Chemical Laboratories, Aligarh Muslim University, Aligarh (India)

(Received February 24th, 1962)

The problem of hydrogen ion equilibria of proteins has been investigated extensively by a number of eminent workers, notably CANNAN[1], STEINHARDT[2] and TANFORD[3,5,6]. The latter author, assuming the protein molecule to be a sphere with the net charge spread over its surface, derived the equation[3]

$$\mathrm{pH} - \log \frac{r_i}{n_i - r_i} = (\mathrm{p}K_{\mathrm{int}})_i - 0.868\, ZW \qquad (1)$$

where

$$W = \frac{Ne^2}{2\,DRT}\left(\frac{1}{b} - \frac{k}{k_a}\right)$$

n_i is the number of ionisable groups with intrinsic association constant $(\mathrm{p}K_{\mathrm{int}})_i$, r_i is the number of groups ionised, Z is the mean charge on the protein sphere of radius b, a is the radius of exclusion and N, e, D, R and k have the usual significance as in the Debye–Huckel theory.

The equation was criticized by HILL[4], who had discussed the whole problem from the view point of discrete charge distribution on the protein molecule, but TANFORD[5] still maintains that any deviation from his original approach might lead to serious errors in the evaluation of W. The problem of abnormal binding of protons by a protein molecule in the acid range has also been considered by TANFORD[6] who thinks that the penetration of the solvent and small ions into the swollen spherical protein molecule might be the probable cause of such an abnormality, while BEYCHOK AND STEINHARDT[7] are of the opinion that the increase in proton binding is due to the unmasking of the binding sites as a result of acid denaturation.

Potentiometric methods are mainly employed to study the H^+ ion equilibria in proteins (more recently WISHNIA, WEBER AND WARNER[8] have also employed electrophoretic methods in studying conalbumin) and most of the work deals with the interpretation of titration curves. But very little appears to have been done in applying the results of proton binding to specific proteins.

Among the collagen type of proteins, some work has been done by COMBET[9] on the acid–base behaviour of gelatin by electrometric titration methods. He not only successfully employed the theory of dissociation of a polyelectrolyte of spherical molecular symmetry in explaining the results, but also calculated the values of different acid and basic groups (carboxyl, imadazole and amino) per 10^5 g of the gelatin.

The present communication deals with our studies on hydrogen ion equilibria of transfusion gelatin[10]. This particular protein, which has found use as a plasma expander (intravenous injection) has been selected for these investigations in view of

the simpler configuration of the degraded product and the certainty of its molecular weight.

The work also includes spectro-photometric studies on the tyrosine content, besides the usual potentiometric titration method employed for determining quantitatively the ionisable groups present in the gelatin.

EXPERIMENTAL

Reagents and solutions

Transfusion gelatin[10] (conc. 6%) supplied by the Director, National Chemical Laboratories, Poona (India), was used throughout these investigations.

Solutions of hydrochloric acid, caustic potash and potassium chloride (all A.R.) were prepared with water doubly distilled in all-glass apparatus. Carbonate free potassium hydroxide was prepared and its concentration determined.

Apparatus and technique

E.m.f. measurements were carried out with a Pye Precision Vernier Potentiometer (Cat. No. 7568). The titration cell consisted of a hydrogen electrode (Clark type) and a saturated calomel electrode. The reversibility of the hydrogen electrode was checked by measuring the e.m.f. of 0.05 *M* potassium hydrogen phthalate for the acid range and that of 0.05 *M* sodium borate for the alkaline range. Pure hydrogen was passed slowly for about 15 min to attain equilibrium.

Optical density measurements were carried out using a Beckman Spectrophotometer Model DU, using a hydrogen lamp (light path 1 mm) and a 1 cm corex cell.

Procedure

Varying amounts of hydrochloric acid (26.04, 17.95, 13.06 $\cdot 10^{-3}$ moles/l etc.) and caustic potash (2.314, 4.629, 6.943 $\cdot 10^{-3}$ moles/l etc.), were taken in 50 cm^3 conical flasks and 2 cm^3 of the transfusion gelatin was added to each of them. The total volume was made up to 10 cm^3 by adding water and 1 *M* KCl, to make the total ionic strength

TABLE I

TEMPERATURE 20°, IONIC STRENGTH 0.15, CONCENTRATION OF TRANSFUSION GELATIN = 6.66 g/l

H^+ added (moles/l $\cdot 10^3$)	pH	Free H^+ (moles/l $\cdot 10^3$)	Bound H^+ (moles/mole protein)	Moles of H^+ dissociated per mole protein
26.04	1.868	15.38	120	—
17.095	1.985	11.75	69.8	0.2
13.06	2.224	6.77	70	0
8.34	2.724	2.103	70	0
6.49	3.336	0.46	68	2
3.72	4.238	0.058	41	29
1.82	4.791	0.016	20	50
0.00	5.500	0.00	00	70
OH^- added (moles/l $\cdot 10^3$)	pH	Free OH^- (moles/l $\cdot 10^3$)	Bound OH^- (moles/mole protein)	Moles of H^+ dissociated per mole protein
2.314	8.468	0.002	26	96
4.629	9.394	0.016	52	122
6.943	10.456	0.194	76	146
13.887	11.951	6.720	80.7	150.7
23.145	12.270	12.67	118	188

TABLE II

TEMPERATURE 30°, IONIC STRENGTH 0.15, CONCENTRATION OF PROTEIN = 6.66 g/l

H^+ added (moles/l·10³)	pH	Free H^+ (moles/l·10³)	Bound H^+ (moles/mole protein)	Moles of H^+ dissociated per mole protein
26.04	1.862	15.59	117.6	—
17.95	1.984	11.76	69.7	0.3
13.06	2.223	6.802	70	0
8.34	2.714	2.155	69	1
6.49	3.362	0.435	68	2
3.72	4.162	0.069	41	29
1.82	4.572	0.026	20	50
oo	5.4	oo	oo	70
OH^- added (moles/l·10³)	pH	Free OH^- (moles/l·10³)	Bound OH^- (moles/mole protein)	Moles of H^+ dissociated per mole protein
2.314	8.210	0.002	26	96
4.629	9.0120	0.015	52	122
6.943	10.132	0.199	76	146
9.258	11.190	4.00	56	129
13.887	11.454	6.697	81	151
23.145	11.744	13.06	113	183

TABLE III

TEMPERATURE 40°, IONIC STRENGTH 0.15, CONCENTRATION OF PROTEIN = 6.66 g/l

H^+ added (moles/l·10³)	pH	Free H^+ (moles/l·10³)	Bound H^+ (moles/mole protein)	Moles of H^+ dissociated per mole protein
26.04	1.863	15.55	118	—
17.95	1.982	11.83	69	1
13.06	2.220	6.849	70	0
8.34	2.734	2.050	70	0
6.49	3.312	0.487	67	3
3.72	4.104	0.078	41	29
1.82	4.504	0.034	20	50
oo	5.3	oo	0	70
OH^- added (moles/l·10³)	pH	Free OH^- (moles/l·10³)	Bound OH^- (moles/mole protein)	Moles of H^+ dissociated per mole protein
2.314	7.970	0.002	26	96
4.629	8.553	0.010	52	122
6.943	9.835	0.200	76	146
9.258	10.943	4.480	54	124
13.887	11.178	7.032	77	147
23.145	11.453	13.24	111	181

of the solution 0.15. The pH measurements were carried out at three different temperatures, *viz.* 20°, 30° and 40° by keeping the cell in a water thermostat. Typical results are tabulated in Tables I to III, and are graphically represented in Fig. 1.

Experiments were also performed to show the reversible nature of hydrogen ion equilibria in the acidic and basic ranges, as suggested by TANFORD[3]. Reversibility was found to exist except in the extreme acid and basic ranges.

Calculation

Assuming that the activity of hydrogen ions (a_{H^+}) in solutions containing protein depends only upon the non-protein constituents of the system at moderate protein

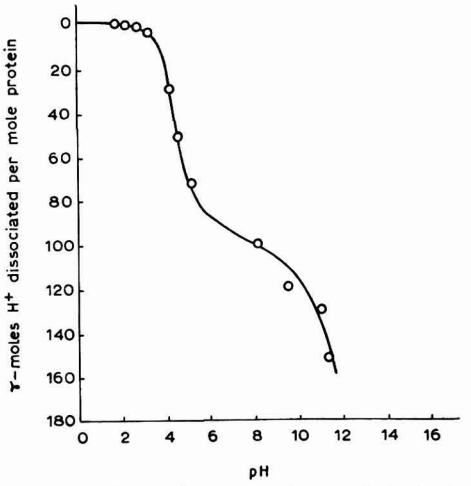

Fig. 1. Titration curve of transfusion gelatin at 30°; ionic strength = 0.15.

concentration, pH is given as:

$$\text{pH} = -\log a_{H^+} = \log m_{H^+} f_{H^+} = (E-E'_0)\ 2.303\ RT/nF$$

also, $\text{pH} = \log (m_{OH^-} f_{OH^-})/KW$.

The values of K_W were taken from those obtained by HARNED and co-workers[11], and those of activity coefficients (in extreme acid and basic regions) from those given by TANFORD[3]. The values of E (in V) at different temperatures were found by using the equation:

$$E = 0.242 - 7.6 \cdot 10^{-4}\ (t-25) \qquad (2)$$

Tyrosine content of the protein (in g mole per mole protein) was determined by the equation[12]:

$$M_{tyros} = (0.99\ E_{305} - 0.32\ E_{280}) \cdot 10^{-3}$$

where E_{305} and E_{280} represent molar extinction coefficients at wave lengths 305 mμ and 280 mμ respectively.

The apparent heat of ionization (ΔH_{ion}) was determined according to WYMAN'S[13] method, using the equation:

$$\Delta H_{ion} = -2.303\ RT^2 \frac{(\text{dpH})}{\text{d}T}$$

The apparent heat of ionization ΔH_{ion} was plotted against r, the number of protons

dissociated per protein molecule (Fig. 2). The values for different dissociable groups are given in Table IV.

The molecular weight of transfusion gelatin was taken to be 75,000.

TABLE IV

APPARENT HEAT OF IONIZATION OF IONISABLE GROUPS IN TRANSFUSION GELATIN

Groups	*Expected*[13] *range for ΔH ion (in Kcal per mole)*	*Observed average value for ΔH ion (in Kcal per mole)*
carboxyl	±1.5–3	2.6
imidazole	6.9–7.5	7.1
amino	10–12	11.2
guanidinium	12–13	12.4

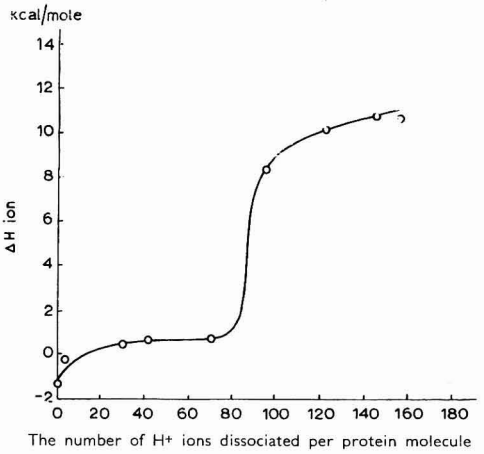

Fig. 2. The relation between the apparent heat of ionization and the number of protons dissociated per protein molecule.

DISCUSSION

The results of the hydrogen ion equilibria of transfusion gelatin provide useful information regarding the different ionisable groups in its solution, at different hydrogen ion concentrations. The whole titration curve of the protein consists mainly of three regions: (1), the first is due to carboxyl groups (α-carboxyl at the end of the peptide chain and β-carboxyl groups derived from aspartyl and glutamyl residues); (2), the second region is a very small one due to imidazole groups; and (3), the third is due to α-amino and ε-amino groups from lysine residues, phenoxyl groups from tyrosine and guanidinium groups from arginine protein residues.

The carboxyl region

The upper portion of the titration curve (Fig. 1) provides enough information re-

garding the number of carboxyl groups in the protein under investigation. Thus it may be seen that a sharp break exists at about pH 5.5, corresponding to $r = 84$, for the carboxyl groups. Moreover, the value of r in the vicinity of pH 3.2 becomes unity, showing that out of 84 carboxyl groups, only one is present in the α-form. Experimental results on the apparent heat of ionisation, shown in Fig. 2, also lend support to the above conclusions, since an inflexion occurs at $r = 84$, corresponding to $\Delta H_{ion} = 3.0$ — a value which is well below that of 4.0 Kcal, the maximum apparent heat of ionisation for carboxyl groups in protein. Further confirmation is forthcoming on the basis of EASTOE's[14] results on amino-acid analysis of bone gelatin. On inserting the value for aspartic and glutamic acid residues (37.8 and 59.0) and that for the amide groups (14.0) for 75,000 g protein ash (transfusion gelatin extracted from animal bone[10]), the value for carboxyl group is shown to be 83.8 ($37.8 + 59 + 1 - 14 = 83.8$ *vide* Table V), which is nearly the same as the value obtained by the two methods employed.

TABLE V

IONIZABLE GROUPS IN TRANSFUSION GELATIN

Groups	*Reasonable analytical value*[14]	*Observed*
α-carboxyl	—	(1)
β-carboxyl	83	83
imidazole	3.4	3.8
α-amino	—	(1)
ε-amino	22	22
phenolic	1	1.1
guanidinium	39	43
Total cationic	65	70

The non-carboxyl region

At the pH of maximum acid binding, all the basic nitrogen groups (imidazole, amino and guanidinium) bear a positive charge due to protonation. Hence, the number of such cationic groups may be obtained from the average value of the maximum number of protons bound, which is 70 (Tables I–III) — a number which differs only by 5 from the value which may be expected on the basis of amino acid analysis (Table V).

Since the expected range for the ionisation of imidazole groups is between pH 6–8, the value of r in this range will give the number of imidazole groups. This value comes to 3.8 (Fig. 1) which is nearly the same as the analytical value of 3.4 (Table V). However, the number of imidazole groups found from the results on ΔH_{ion} is slightly lower, *viz.* 2.0 (the average value of r in the range ΔH_{ion} 6.9–7.5 Kcal/mole, Fig. 2). Such behaviour is not unlikely in view of the low histidine content of gelatin.

In the higher pH range (beyond pH 8) no inflexion in the titration curves is observed. However, by considering the number of hydrogen ions dissociated in the pH range 9.2–11, the average value of r for the amino groups can be found. Its value is 23, including one for the α-amino group (corresponding to one α-carboxyl group). Results obtained from the apparent heat of ionisation also give the same value, since the value of r is approximately 23 for ΔH_{ion} values between 10–12 Kcal/mole (Fig. 2), which is the expected range for the ionisation of amino groups. Further confirmation is again

forthcoming from the amino acid analysis, where 22 amino groups corresponding to 22 lysine residues of gelatin are found. The average value of ΔH_{ion} calculated for imidazole groups is 7.1 Kcal/mole (Table IV).

No specific information could be obtained about the number of guanidinium groups from the titration curves. The splitting of the peptide linkage and denaturation of the base at a higher pH range might be probable explanations for such behaviour. However, the results from the apparent heat of ionisation can be used advantageously for this purpose. From Fig. 2 it is evident that the value of r for ΔH_{ion} values between 12–13 Kcal/mole, the range of ionisation for this group, is 43 — a value not very far from the analytical value of 39 per 75,000 dry protein ash.

As the method using pH determination could not be employed as such to find the number of phenolic groups derived from the tyrosine content of the gelatin, a spectrophotometric method was employed and was found to be quite successful. From the

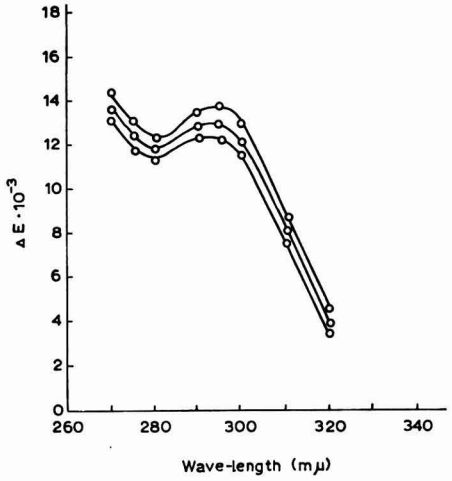

Fig. 3. Molar extinction coefficient as a function of wave length. Upper curve, pH 12; centre curve, pH 10; lower curve, pH 9.

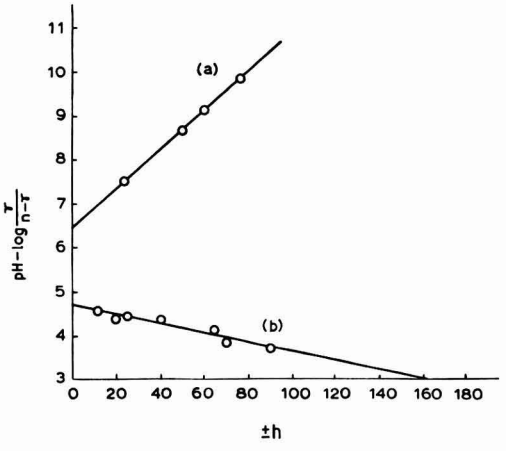

Fig. 4.

curve (Fig. 3) the tyrosine content of the gelatin was calculated using the Holliday equation and was found to be 1.1, and hence the number of phenoxyl groups will also be 1.1, which agrees fairly well with the analytical data.

The electrostatic interaction factor W

Applying Tanford's equation, a plot of $pH/\log(r/n-r)$ against h gives a straight line (Z replaced by h, the number of protons bound per protein molecule, Fig. 4). The value of W, the electrostatic interaction factor evaluated from the slope of the straight line (curve (b), Fig. 4) is 0.0279, which is usual in proteins. The value for the intrinsic association constant, $(pK_{int})_0$ for carboxyl groups determined from the intercept of the straight line on the ordinate is 4.7. For imidazole groups the value of $(pK_{int})_0$ is 6.5 (curve (a), Fig. 4). The values conform with results obtained by other workers[3,8].

Limitations of the method employed

Attention may be drawn to certain anomalies encountered during the study of hydrogen ion equilibria of transfusion gelatin.

(i) At very low pH values, the number of protons bound is quite high *i.e.* 120 (Table I), while the value of W calculated for an extreme acid range using eqn. (1) (values for pK_{int}, r, n and pH observed were substituted in the equation) is considerably lower (0.011). The deviation may be due to the increase in the radius, b, of the protein molecule, accompanied by penetration of protons and solvent molecules into the protein sphere, thus altering the molecular size[6].

(ii) In a basic range, the value for W is considerably higher *viz.* 0.111 (curve (a), Fig. 4). Such behaviour may be assumed to be due to unbalanced spacing of the ionisable groups in the protein structure and, hence, to non-applicability of the Tanford equation at higher pH values.

ACKNOWLEDGEMENTS

Thanks are due to Dr. A. R. KIDWAI for providing facilities, and to the C.S.I.R., Government of India, for the award of a fellowship to one of us (S). We also wish to express our thanks to Dr. JAGGANATHAN, Assistant Director, Biochemistry Division, N.C.L., Poona (India), for the supply of two bottles of transfusion gelatin.

SUMMARY

Hydrogen ion equilibria studies of transfusion gelatin carried out at different temperatures revealed the presence of 84 carboxyl, 23 amino, 3.8 imidazole and 43 guanidinium groups per $75 \cdot 10^3$ g of the protein. The results confirmed the values of amino acid analysis and also those obtained from observations of apparent heats of ionsation. TANFORD'S equation was found in this case to be applicable only in the carboxyl region, ($W = 0.027$).

Further work regarding the interaction of cations, other than hydrogen ions, with transfusion gelatin is in progress.

REFERENCES

1 R. K. CANNAN, A. C. KIBRICK AND A. H. PALMER, *Ann. N.Y. Acad. Sci.*, 41 (1941) 243.
2 J. STEINHARDT AND E. M. ZAISER, *Advances in Protein Chem.*, 10 (1955) 151.
3 C. TANFORD, *J. Am. Chem. Soc.*, 72 (1950) 441.

[4] T. L. HILL, *J. Am. Chem. Soc.*, 78 (1956) 5527.
[5] C. TANFORD, *J. Am. Chem. Soc.*, 79 (1957) 5340.
[6] C. TANFORD, *J. Phys. Chem.*, 59 (1955) 788.
[7] S. BEYCHOK AND J. STEINHARDT, *J. Am. Chem. Soc.*, 81 (1959) 5679.
[8] A. WISHNIA, I. WEBER AND R. C. WARNER, *J. Am. Chem. Soc.*, 83 (1961) 2071.
[9] SERGE COMBET, *J. Chim. Phys.*, 53 (1956) 422.
[10] S. L. KALRA, G. SINGH AND M. RAM, *Indian J. Med. Research*, 46 (1958) 171.
[11] H. S. HARNED AND B. B. OWNE, *The Physical Chemistry of Electrolytic Solutions*, Reinhold Publishing Corp., N.Y., 1950, p. 485.
[12] E. R. HOLLIDAY AND A. G. OGSTON, *Biochem. J.*, 32 (1938) 1166.
[13] J. WYMAN, *J. Biol. Chem.*, 127 (1939) 1.
[14] J. E. EASTOE, *Biochem. J.*, 61 (1955) 589.

Short Communication

An aid to the interpretation of data in chronopotentiometry with cylindrical electrodes

PETERS AND LINGANE[1] have derived an equation for the transition time in chronopotentiometry with cylindrical electrodes and have presented experimental data[1,2,3] supporting the validity of their equation. Because of the complexity of this equation, the interpretation of experimental data can be tedious. On the other hand, wire electrodes offer several experimental advantages, among which is their ease of fabrication. The following discussion analyzes the Peters and Lingane equation and provides a method for its rapid application.

The Peters and Lingane equation for symmetrical, cylindrical diffusion is the analog of the familiar Sand equation for linear diffusion. The Sand equation predicts that, under conditions of *linear* diffusion, the quantity $i\tau^{1/2}/AC^\circ$ is constant at all transition times. For *linear* diffusion, the area from which material can diffuse is independent of the thickness of the diffusion layer. For *cylindrical* diffusion, however, the area from which material can diffuse constantly increases as the electrolysis proceeds and the diffusion layer extends further into the solution. Thus more material is able to reach the electrode surface and the time required for the surface concentration to be reduced to zero, the transition time, is relatively longer than for linear diffusion at the same current density.

The Peters and Lingane equation differs from the Sand equation in that it contains an infinite series which accounts for the enhancement of $i\tau^{1/2}/AC^\circ$ due to the cylindricity of the diffusion field. Each term in the series must be derived separately. Using the method of these authors, we have extended this series by one more term. The final equation is:

$$\frac{i\tau^{1/2}}{AC^\circ} = \left[\frac{\pi^{1/2}nFD^{1/2}}{2}\right] \left[\frac{1}{1 - \frac{\pi^{1/2}}{4}\left(\frac{D^{1/2}\tau^{1/2}}{r_0}\right) + \frac{1}{4}\left(\frac{D^{1/2}\tau^{1/2}}{r_0}\right)^2 - \frac{3\pi^{1/2}}{32}\left(\frac{D^{1/2}\tau^{1/2}}{r_0}\right)^3 + \frac{21}{160}\left(\frac{D^{1/2}\tau^{1/2}}{r_0}\right)^4 - \frac{9\pi^{1/2}}{128}\left(\frac{D^{1/2}\tau^{1/2}}{r_0}\right)^5 + \ldots}\right] \quad (1)$$

where i is the current (in A), τ is the transition time (sec), A is the electrode area (cm^2), C° is the concentration of the electroactive substance (moles/cm^3), n is the number of Faradays of electricity per mole of reaction, F is the Faraday (96,493 coulombs), D is the diffusion coefficient of the substance (cm^2/sec), and r_0 is the radius of the electrode (cm).

The left hand side of eqn. (1) and the first factor of the right hand side constitute the Sand equation. The second factor, henceforth called R, introduces the effect of cylindricity.

We have investigated the properties of the function R in order: (1) to see within what limits of τ, D and r_0 eqn. (1) is valid, and (2) to provide a rapid and accurate method of determining R for various values of these parameters.

TABLE I

CORRECTION FACTOR (R) FOR CHRONOPOTENTIOMETRY WITH CYLINDRICAL ELECTRODES AS A FUNCTION OF DIFFUSION COEFFICIENT, RADIUS OF THE ELECTRODE, AND TRANSITION TIME

$\frac{D^{1/2}}{r_0}$	$\tau^{1/2}$	0.3	0.5	0.7	0.9	1.1	1.4	1.6	2.0	2.5	3.0	3.5	4.0	4.5	5.0	$\tau^{1/2}$	$\frac{D^{1/2}}{r_0}$
	τ	0.09	0.25	0.49	0.81	1.21	1.96	2.56	4.00	6.25	9.00	12.25	16.00	20.25	25.00	τ	
	0.004	1.001	1.001	1.001	1.002	1.002	1.002	1.003	1.004	1.004	1.005	1.006	1.007	1.008	1.009	0.004	
	0.006	1.001	1.001	1.002	1.002	1.003	1.004	1.004	1.005	1.007	1.008	1.009	1.011	1.012	1.013	0.006	
	0.008	1.001	1.002	1.002	1.003	1.004	1.005	1.006	1.007	1.009	1.011	1.012	1.014	1.016	1.018	0.008	
	0.01	1.001	1.002	1.003	1.004	1.005	1.006	1.007	1.009	1.011	1.013	1.015	1.018	1.020	1.022	0.01	
	0.02	1.003	1.004	1.006	1.008	1.010	1.012	1.014	1.018	1.022	1.026	1.031	1.035	1.039	1.044	0.02	
	0.03	1.004	1.007	1.009	1.012	1.015	1.019	1.021	1.026	1.033	1.039	1.046	1.052	1.059	1.065	0.03	
	0.04	1.005	1.009	1.012	1.016	1.019	1.025	1.028	1.035	1.044	1.052	1.061	1.070	1.078	1.087	0.04	
	0.05	1.007	1.011	1.015	1.020	1.024	1.031	1.035	1.044	1.055	1.065	1.076	1.087	1.097	1.108	0.05	
	0.06	1.008	1.013	1.019	1.024	1.029	1.037	1.042	1.052	1.065	1.078	1.091	1.104	1.116	1.129	0.06	
	0.07	1.009	1.015	1.022	1.028	1.034	1.043	1.049	1.061	1.076	1.091	1.106	1.120	1.135	1.150	0.07	
	0.08	1.011	1.018	1.025	1.032	1.039	1.049	1.056	1.070	1.087	1.104	1.120	1.137	1.154	1.171	0.08	
	0.09	1.012	1.020	1.028	1.036	1.043	1.055	1.063	1.078	1.097	1.116	1.135	1.154	1.173	1.192	0.09	
	0.10	1.013	1.022	1.031	1.039	1.048	1.061	1.070	1.087	1.108	1.129	1.150	1.171	1.192	1.213	0.10	
	0.11	1.015	1.024	1.034	1.043	1.053	1.067	1.076	1.095	1.118	1.141	1.164	1.187	1.211	1.235	0.11	
	0.12	1.016	1.026	1.037	1.047	1.058	1.073	1.083	1.104	1.129	1.154	1.179	1.204	1.230	1.257	0.12	
	0.13	1.017	1.029	1.040	1.051	1.062	1.079	1.090	1.112	1.139	1.166	1.194	1.221	1.250	1.281	0.13	
	0.14	1.019	1.031	1.043	1.055	1.067	1.085	1.097	1.120	1.150	1.179	1.209	1.239	1.271	1.306	0.14	
	0.15	1.020	1.033	1.046	1.059	1.072	1.091	1.104	1.129	1.160	1.192	1.224	1.257	1.293	1.333	0.15	
	0.16	1.021	1.035	1.049	1.063	1.076	1.097	1.110	1.137	1.171	1.204	1.239	1.276	1.316	1.364	0.16	
	0.17	1.022	1.037	1.052	1.067	1.081	1.103	1.117	1.146	1.181	1.217	1.255	1.295	1.342	1.398	0.17	
	0.18	1.024	1.039	1.055	1.070	1.086	1.109	1.124	1.154	1.192	1.230	1.271	1.316	1.370	1.439	0.18	
	0.20	1.026	1.044	1.061	1.078	1.095	1.120	1.137	1 171	1.213	1.257	1.306	1.364	1.439	—	0.20	
	0.25	1.033	1.055	1.076	1.097	1.118	1.150	1.171	1.213	1.269	1.333	—	—	—	—	0.25	
	0.30	1.039	1.065	1.091	1.116	1.141	1.179	1.204	1.257	1.333	—	—	—	—	—	0.30	
	0.40	1.052	1.087	1.120	1.154	1.187	1.239	1.276	—	—	—	—	—	—	—	0.40	

The function R was programmed for the IBM 1620 computer with input data for $\tau^{1/2}$ varying over a convenient range (0.3–5.0 $sec^{1/2}$) and $D^{1/2}/r_0$ varying between 0.004 and 0.4 (roughly encompassing diffusion coefficients between 10^{-6} and 10^{-4} cm^2/sec and radii between 0.025 and 0.25 cm). The results are presented in Table I. In Fig. 1, R is plotted as a function of transition time for selected values of $D^{1/2}/r_0$. This form of presentation parallels the method adopted by PETERS AND LINGANE[1,2,3] for comparing experimental data with eqn. (1).

It is apparent from Fig. 1 that R is very close to 1.000 when either τ or D is very small. Under these conditions, the diffusion layer is very thin and the diffusion process is almost linear. R is also very close to 1.000 when r_0 becomes very large, *i.e.*, when the surface becomes more like a plane.

The slope of the R *vs.* transition time curve depends upon the quantity $D^{1/2}/r_0$. For most values of this quantity, the slope is almost constant for transition times between 5–25 seconds, but as $D^{1/2}/r_0$ becomes larger than about 0.2, the slope increases for transition times longer than a few seconds. This tendency was observed by LINGANE[2] in a study of the reduction of hydrogen ion at a cylindrical electrode of radius 0.0252 cm ($D^{1/2}/r_0 = 0.37$ $sec^{-1/2}$). The experimental R *vs.* τ curve showed a constant slope between 3 and 20 sec but the theoretical curve showed deviations similar to Fig. 1. Obviously, eqn. (1) does not adequately represent the facts under these conditions. We conclude that eqn. (1) is not valid in regions of large $D^{1/2}/r_0$ and τ, and we have omitted from Table I those values of R which show an obvious positive deviation. Considerable caution must be exercised in applying eqn. (1) to systems where $D^{1/2}/r_0$ is greater than about 0.2*.

Table I facilitates the calculation of theoretical values of R in chronopotentiometry

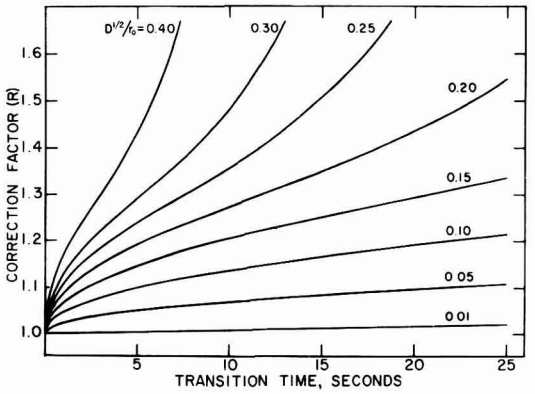

Fig. 1. Correction factor (R) for chronopotentiometry with cylindrical electrodes as a function of transition time for selected values of $D^{1/2}/r_0$.

* These deviations are characteristic of the approximate nature of the Peters and Lingane equation. They arise from the fact that, as $D^{1/2}/r_0$ becomes larger, the last term in the series begins to outweigh the others and the expression rapidly goes toward infinity. A discontinuity occurs when the denominator of R equals zero and at still larger values of τ and/or $D^{1/2}/r_0$, R is negative. Obviously, a somewhat different behavior would occur if the series were terminated with the last term being positive rather than negative. This inadequacy in eqn. (1) is not unexpected since PETERS AND LINGANE used in their derivation an asymptotic expansion of Bessel functions which is not valid for all values of the argument.

with cylindrical electrodes. $D^{1/2}/r_0$ is calculated from the known (or assumed) diffusion coefficient of the species in question and the radius of the electrode. Then R can be determined for up to fourteen values of τ. If $D^{1/2}/r_0$ is identical with any of the twenty-five values listed in Table I, the appropriate values of R can be read directly. Otherwise, one may interpolate between two nearby values. Examination of any vertical column in Table I indicates that R is very nearly a linear function of $D^{1/2}/r_0$ and interpolation is therefore quite accurate.

Furthermore, one may interpolate between adjacent values of $\tau^{1/2}$. R is very nearly a linear function of $\tau^{1/2}$, as can be verified by examining any horizontal row in Table I. In this way, values of R for many different values of D, r_0, and τ can be rapidly and accurately calculated. When these are inserted in eqn. (1) along with $\pi^{1/2}nF/2$ and the appropriate value of $D^{1/2}$, $i\tau^{1/2}/AC^\circ$ is obtained as a function of transition time.

The effect of cylindricity can be made entirely negligible by a judicious choice of r_0 for a given system. The data from Table I indicate that combinations of $D^{1/2}/r_0$ and τ above and to the left of the horizontal line correspond to experimental conditions where the deviation of $i\tau^{1/2}/AC^\circ$ from the Sand value is one per cent or less. Generally, electrode radii must be quite large to reduce the deviation to these levels. For example, for $D = 10^{-5}$ cm^2/sec, r_0 must be greater than 0.7 cm to make R less than 1.01 at a transition time of twenty-five seconds.

The function R also appears in other equations pertinent to chronopotentiometry with cylindrical electrodes. It is a part of the general transition time equation for successive electrochemical reactions[3,4] and it appears in chronopotentiometry with current reversal and "step current impulses"[4]. The function R is also essential for calculating the ratio of transition times in successive electrochemical reactions or stepwise reaction of a single substance[3].

ACKNOWLEDGEMENTS

Appreciation is expressed to Professor J. J. LINGANE who suggested this project. We are also indebted to the National Institutes of Health for a fellowship held by one of us (D.H.E.).

SUMMARY

The properties of the theoretical correction factor for chronopotentiometry with cylindrical electrodes are investigated. A table of correction factors permitting rapid and accurate interpretation of experimental data is presented.

Department of Chemistry,
Harvard University,
Cambridge, Mass. (U.S.A.)
DENNIS H. EVANS
Department of Economics,
Syracuse University,
Syracuse, N.Y. (U.S.A.)
JAMES E. PRICE

1 D. G. PETERS AND J. J. LINGANE, *J. Electroanal. Chem.*, 2 (1961) 1.
2 J. J. LINGANE, *J. Electroanal. Chem.*, 2 (1961) 46.
3 D. G. PETERS AND J. J. LINGANE, *J. Electroanal. Chem.*, 2 (1961) 249.
4 R. W. MURRAY AND C. N. REILLEY, *J. Electroanal. Chem.*, 3 (1962) 182.

Book Reviews

Analyse der Metalle; Betriebsanalysen, 2te Band, Teil I und Teil II, herausgegeben vom Chemikerausschuss der Gesellschaft Deutscher Metallhütten- und Bergleute e.V. Springer Verlag, Berlin–Göttingen–Heidelberg, 1961, 1568 Seiten, D.M. 158.

Der vorliegende zweiteilige zweite Band des Gemeinschaftswerkes *Analyse der Metalle* stellt bereits eine neubearbeitete zweite Auflage dar und umfasst unter dem Titel ,,Betriebsanalysen" eine Sammlung aller derzeit in den Laboratorien der deutschen Metallindustrie angewandten analytischen Verfahren, die notwendig sind, um die Ausgangs- und Endprodukte der Nichteisenmetall erzeugenden Industrie zu überwachen. Er wurde ebenso wie der erste Band, welcher die ausgewählten Methoden der Analyse der Metalle, das sind die ,,Schiedsverfahren" behandelt, vom Chemikerausschuss der Gesellschaft der Metallhütten- und Bergleute herausgegeben. Es ist sehr zu begrüssen, dass dieser zweite Band, der in Wissenschaft und Technik so grossen Anklang gefunden hat und in weniger als sechs Jahren bereits vergriffen war, nach so kurzer Zeit eine zweite Auflage erleben konnte.

Die Metalle sind in alphabetischer Reihenfolge sehr übersichtlich angeordnet. Nach einer kurzen Einleitung über das Vorkommen und den qualitativen Nachweis des jeweiligen Metalles werden dem Gewinnungsgang folgend bei jedem Metall die Analyse seiner wichtigsten Erze und Mineralien, der hauptsächlichsten Hilfsstoffe, der dabei entfallenden Neben-, Zwischen- und Endprodukte sowie nicht zuletzt die Analyse des Roh- und Reinmetalles behandelt. Während im ersten Band dieses Gemeinschaftswerkes die Wertbestimmung der Metall-haltigen Stoffe im Vordergrund steht und somit die Genauigkeit vor dem Zeitbedarf zu stehen kommt, ist es bei der Betriebsanalyse vor allem notwendig, rasche Auskunft über die Richtigkeit der im gegebenen Gewinnungsgang der Metalle eingeschlagenen Wege zu erhalten, wodurch schnelle Analysenverfahren bevorzugt werden. Ausserdem sind noch eine Reihe von Untersuchungen, wie die der metallischen und nicht-metallischen Überzüge von Metallen, des Sauerstoffgehaltes von Metallen, feuerfester Baustoffe, fester und flüssiger Brennstoffe sowie der Industriegase, des Wassers für den Kesselbetrieb und der Beizereiabwässer, wie sie die metallverarbeitende Industrie immer wieder für die eigenen Betriebe braucht oder durch NORMEN festgelegt hat, angeführt. Anschliessend werden allgemeine physikalisch chemische Verfahren beschrieben, die im ersten Band entweder gar nicht oder nur im geringen Umfang angeführt werden. So erfährt man in sehr übersichtlichen und leicht verständlichen Abhandlungen das wichtigste über die Photometrie, Polarographie, Potentiometrie, Konduktometrie sowie in ausgezeichneter Bearbeitung alles notwendige über die Hochfrequenztitration und Spektrochemische Analyse. Eine Übersicht aller benötigten Lösungen und deren genauen Bereitung sowie Einstellung ergänzt diesen zweiten Teil des so umfangreichen Bandes. Schliesslich findet man noch in dankenswerter Weise eine genaue Rezeptur über die wichtigsten Puffergemische und deren pH-Werte, die Anführung aller genormten Metalle und Legierungen sowie ein ausführliches Namen- und Sachverzeichnis.

Auf gutem Papier ist das umfangreiche Werk sehr übersichtlich und verständlich dargestellt. Jedes Analysenverfahren wird in die Punkte: Grundlage, Anwendungsbereich und Bedeutung, Genauigkeit, Dauer, Ausführung, Fehlerquellen und Literatur zergliedert, wodurch die Auswahl der gesuchten Methode sehr erleichtert wird. Besonders hervorzuheben ist der Versuch, die grösstenteils alten, wenn auch sicherlich sehr verlässlichen, Methoden durch modernere zu ersetzen, wodurch vielfach bedeutend Zeit eingespart wird.

Dies kommt zum Beispiel bei der Analyse von Beryllium-Spezialstählen nach R. PŘIBIL oder bei der Nickelgehaltsbestimmung in kobaltführenden Erzen nach F. FEIGL sehr deutlich zum Ausdruck. Ebenso erfreulich ist die Einbeziehung der modernen, wirklich eleganten Methode der Kaliumbestimmung nach G. WITTIG mit dem hervorragenden Reagens: Kalignost, das nach W. RÜDORFF UND H. FLASCHKA sogar eine massanalytische Bestimmung ermöglicht. Sonst is das Werk leider noch in vielen Verfahren viel zu konservativ, so dass bei Benützung modernerer Methodik an Zeit viel eingespart werden könnte. Andrerseits sind wieder so hervorragende Bestimmungsverfahren mitaufgenommen worden, wie sie besonders im Anhang der physikalisch chemischen Methoden ihren erfreulichen Niederschlag gefunden haben, dass man dem wirklich sehr sorgfältig zusammengestellten Werk nur die beste Empfehlung geben kann.

Zusammenfassend bleibt nur zu wünschen, dass dieses wahre ,,Vademekum" des Metallfachmannes auch wirklich überall dort Eingang findet, wo es seiner Natur nach unentbehrlich sein muss.

H. BALLCZO, Wien

Quantitative Analysis, par RAY U. BRUMBLAY, Barnes and Noble Educ., N.Y., et Constable and Co. Ltd., London, 1961, xvii + 235 pages, $ 1.50 or 12 s.

Ce livre, dans la série *College Outline Series* fort bien fait, sans développements inutiles mais renfermant l'essentiel, complété par un ingénieux système de références par matière, aux traités jugés comme fondamentaux par l'auteur.

Beaucoup d'exemples, un grand nombre d'exercices expliqués et corrigés, un plus grand nombre encore, dont les solutions sont données, illustrent les divers exposés. Quelques chapitres remarquablement traités tels que le calcul de l'erreur, l'oxydo-réduction, la solubilité . . .

L'auteur adopte, avec raison, la théorie des acides et des bases de Brönsted, celle qui s'adapte le mieux à la chimie analytique, mais pourquoi y retrouve-t-on les vestiges de la théorie classique, pour quelles raisons par ex. l'auteur introduit-t-il une constante de dissociation des bases alors qu'il est question de couple acide–base? On peut aussi regretter que les méthodes de séparation, qui jouent un rôle fondamental dans l'analyse, n'ont pas été plus développées.

Les principaux chapitres de cet ouvrage sont: L'échantillonnage, le calcul de l'erreur, les analyses gravimétrique et volumétrique, la théorie de l'oxydo-réduction, la neutralisation, les séparations et analyses électrochimiques, les complexes dans l'analyse, etc.

Un livre à recommander à tous ceux qui veulent s'initier à la chimie analytique quantitative et posséder du même coup une bibliographie leur permettant d'approfondir les connaissances acquises.

D. MONNIER, Université de Genève

Handbuch der technischen Elektrochemie, Band 1, Teil 1, Technische Electrolyse wässriger Lösungen, 2nd edn., edited by G. EGER, Akademische Verlagsgesellschaft, Geest and Portig, K.G. Leipzig, 1961, viii + 706 pages, D.M. 78.

Electrochemistry is divided for teaching purposes into two main branches: theoretical electrochemistry, including laboratory applications such as electrochemical analysis, and industrial electrochemistry. These two main branches cannot be sharply separated, and in fact, the development of industrial electrochemistry obviously follows theory. Conversely, scientific electrochemists often receive suggestions and new ideas from industrial electrochemistry. The result of this state of affairs is that, for better understanding and utilization of electrochemical phenomena, it is necessary to have a good knowledge of both theoretical and industrial electrochemistry.

The first and very good edition of this *Handbuch der technischen Elektrochemie* was out of print many years ago, and thus there was an apparent gap in technical chemical literature. The 2nd edition under the direction of the new Editor Dr. Ing. G. EGER is very welcome.

This first part of volume 1 has actually been preceded by some other volumes, not included in the first edition (concerning electrical oven heating and the calcium carbide industry) and by a new edition of the 3rd volume (concerning electrolysis in molten systems).

This volume consists of a theoretical introduction (73 pages) preceding a second chapter which deals with the general technology of industrial electrochemical plants (125 pages). The electrometallurgy of the following metals is then treated in detail (the number of pages for each metal is given in brackets): Fe(53), Mn(47), Cr(15), Ni(34), Co(3), Zn(129), Cd(15), Bi(8), Sb(15), Sn(44), Pb(24), Hg and amalgams(97).

Each chapter has been written by a well known specialist, so that each monograph brings the readers' knowledge really up to date, by means of a very clear text completed by many figures, diagrams, and flowsheets.

Two minor criticisms that can be made are the following. Firstly, a criticism about the structure of the handbook, particularly the theoretical introduction. This is perhaps too short and concise to be really useful for readers who are not acquainted with electrochemistry, but is too long for people who already have some knowledge of the subject. Moreover, no use is made of this theoretical introduction in the practical part of the book. Secondly, no use has been made of the recommendations of the I.U.P.A.C.–C.I.T.C.E. Nomenclature Commission, so that the presentation has, in some ways, an old-fashioned flavour. But these two considerations do not lessen the great usefulness of this book, which can be recommended to every one interested in electrochemistry.

G. MILAZZO, Istituto Superiore di Sanità, Rome

A.S.T.M. Methods for Chemical Analysis of Metals, written and published by the AMERICAN SOCIETY FOR TESTING MATERIALS, Philadelphia, 1961, x + 722 pages, $ 11.

This book contains the current A.S.T.M. methods for the chemical analysis of ferrous and non-ferrous metals and alloys, including methods for spectrochemical analysis. It is essentially a part of the Book of A.S.T.M. Standards. Although this separate publication is complementary to Parts 1 and 2 of the Book of A.S.T.M. Standards, 1958, it can also be used advantageously as a separate volume by analytical chemists.

The first part of the book surveys general methods. Apparatus and preparation of reagents, spectrophotometry and the probability sampling of materials are discussed. In the second part the methods of sampling are described. The sections which follow contain procedures for the chemical analysis of different types of iron and steels and ferro-alloys. Procedures of analysis of nickel, chromium, copper, aluminium, magnesium, titanium, zirconium, molybdenum, lead, tin, antimony, silver, zinc and their alloys are also described. In the last two sections spectrochemical methods for nickel, aluminium, lead, tin and zinc-base alloy analysis and descriptions of some microchemical apparatus are presented.

The methods are partly standard methods already adopted by the American Society for Testing Materials, and partly tentative methods, which have been approved by the originating committee as representing the latest thoughts and practices, and accepted by the Society for use in accordance with established procedures, pending their adoption as standard.

The standard methods are based chiefly on classical methods, although in the recommended and tentative methods photometric, spectrographic, and other modern and rapid methods are also given. Ion exchange methods are recommended for determining aluminium in zirconium, for determining boron in ferroboron, and for determining columbium and tantalum in titanium metal. Chelatometric methods are given for the determination of magnesium, zinc, etc.

The book will be warmly welcomed by analytical chemists. If the promised supplements to the book are issued in succeeding years, the collection will be a good and complete summary of the methods of chemical analysis of metals.

In spite of its fairly wide scope, the book is made easy to handle by its reasonable index and by the fact that it is printed on a fine, thin paper.

J. INCZÉDY, Technical University, Budapest

Gas Chromatography, von D. AMBROSE UND BARBARA A. AMBROSE, George Newnes Ltd., London, 1961, vii + 220 Seiten, 98 Figuren, 40 s.

Vor fünfzehn Jahren wurde erstmalig eine Analyse von Gasen mit Hilfe der Eluierungs-Gas-Chromatographie durchgeführt, und die Eignung dieser Methode zur Schnell- und Mikroanalyse, insbesonders für Kohlenwasserstoffe erkannt. An dem ungeheuren Aufschwung, den die Gas Chromatographie dann erlebte, war hauptsächlich das Interesse der Erdölindustrie Schuld, die in England und Holland grosse Gruppen von Chemikern und Physikern einsetzte, um die neue Methode möglichst rasch zu entwickeln. Eine dieser Gruppen stand unter der Leitung von KEULEMANS, der durch grundlegende Arbeiten und als Verfasser des ersten Standardwerkes für Gas-Chromatographie bekannt wurde, einer zweiten Gruppe entstammt Dr. D. AMBROSE, der gemeinsam mit seiner Frau hier als Autor einer Einführung in die Gas-Chromatographie erscheint. Er ist ausserdem aktives Mitglied des Gas Chromatography Discussion Group und kann also mit Recht zu den ,,well-known authorities" gezählt werden, die laut Angabe des Verlages die Bücher der Serie *Newnes Practical Science Books* bearbeiten deren Ziel es ist praktische Anleitungen für neueste experimentelle Methoden zu geben.

Das Buch ist auch in erster Linie für den Praktiker geschrieben. Es ist eine gute Einführung für jeden, der sich eine gas-chromatographische Apparatur selbst aufbauen will. Sehr wertvoll sind die Hinweise auf mögliche Fehler, die dem Ungeübten leicht unterlaufen. Alle Anweisungen sind durch entsprechende Zeichnungen erklärt. Jeder Teil der gas-chromatographischen Apparatur wird einzeln behandelt. Grosse Sorgfalt wird auch auf eine einheitliche Nomenklatur gelegt. Mathematische Ableitungen werden nur so weit gebracht, als sie unbedingt für das Verständnis der in der Praxis anzuwendenden Formeln notwendig sind. Da allein die Aufzählung der in den letzten zehn Jahren erschienenen gas-chromatographischen Arbeiten den Umfang des Buches benötigen würde, ist es selbstverständlich, dass auf Literaturzitate im Einzelnen verzichtet werden muss. Nur da, wo Originalmessungen gebracht werden, wird auch die Arbeit

zitiert, aus der sie entnommen sind. Anregungen für weiteres Literaturstudium werden am Schluss jedes Kapitels gegeben.

Das Buch behandelt fast ausschliesslich die Eluierungs-Gas-Chromatographie mit Flüssigkeit als stationäre Phase. Ein kurzer Abschnitt ist der Gas–Festkörper-Chromatographie gewidmet, doch wird mit Recht darauf hingewiesen, dass die Abtrennung dieses Gebietes nur formal ist, und dass in allen prinzipiellen Belangen kein Unterschied zwischen der Gas–Flüssigkeits- und der Gas–Festkörper-Chromatographie besteht.

Jedem Chemiker, der die gas-chromatographische Methode von Grund auf erlernen und neue Anwendungen erproben will, kann diese nicht zu umfangreiche und doch eingehende, leicht fassliche Einführung bestens empfohlen werden.

E. CREMER, Universität Innsbruck

J. Electroanal. Chem., 5 (1963) 83–84

Treatise on Analytical Chemistry, by I. M. KOLTHOFF, P. J. ELVING AND E. B. SANDELL, Part II, Vol. 7, Interscience Publishers Inc., N.Y. and London, 1961, xxiii + 567 pages, $ 16.

In preceding volumes of this treatise, various authors collaborated by writing individual chapters. For this volume, devoted to the three somewhat similar elements sulfur, selenium, and tellurium, and to group VII of the periodic system, the authors writing the different sections are: B. J. HEINRICH, M. D. GRIMES AND E. J. PUCKETT (Phillips Petroleum Co.) for sulfur; T. E. GREEN AND M. TURLEY (P. R. Mallory) for selenium and tellurium; C. A. HORTON (Oak Ridge National Laboratory) for fluorine; G. W. ARMSTRONG, H. H. GILL AND R. F. ROLF for the other halogens; M. D. COOPER AND P. K. WINTER (General Motors Corp.) for manganese, and finally C. L. RULFS (University of Michigan) for rhenium.

As is to be expected, the general structure of this volume is similar to that of the preceding ones. Some minor differences result from the special properties of the elements dealt with. A welcome feature of this volume is the greater homogeneity of the treatment of elements in the volume. This facilitates finding analytical methods. Another welcome feature is a brief discussion of the identification and determination of common trace impurities in the elements and compounds whose analytical chemistry is discussed in this book, excepting those of selenium and tellurium.

G. MILAZZO, Istituto Superiore di Sanità, Rome

J. Electroanal. Chem., 5 (1963) 84

Techniques in Flame Photometric Analysis, by N. S. POLUEKTOV, translated from the Russian by C. N. TURTON AND T. I. TURTON, Consultants Bureau, N.Y., 1961, xvi + 230 pages, $ 9.50.

Spectral analysis using a flame as the spectral source is becoming more and more important, as the apparatus used is developed and improved. That this is the case is shown by the fact that many books and monographs on this subject have been published in the last few years.

This monograph is particularly devoted to practical procedures of analysis based on this method, and in this sense it is welcomed because sometimes the practical part is somewhat less fully developed in other more important books.

This book is divided into two parts. The first is a general one, dealing with the basic principles of emission in flames (chapter 1), with descriptions of apparatus, mainly of Russian manufacture (chapter 2), with the factors affecting sensitivity and accuracy (chapter 3), and with photometric measurement procedures, including the elimination of errors, as far as is possible.

The second part deals with the determination of many elements in different systems. The English translation is very clear, and the whole book is worthy of a place on the bookshelves of analysts who are particularly interested in this method of analysis.

J. Electroanal. Chem., 5 (1963) 84

CONTENTS

ELSEVIER PUBLISHING COMPANY, AMSTERDAM

Printed in The Netherlands by

NEDERLANDSE BOEKDRUK INRICHTING N.V., 'S-HERTOGENBOSCH